**ISTANBUL TECHNICAL UNIVERSITY ★ GRADUATE SCHOOL OF SCIENCE ENGINEERING AND TECHNOLOGY**

# BENEFITS OF TUNED MASS DAMPERS IN TERMS OF IMPROVING THE SEISMIC PERFORMANCE OF SUSPENSION BRIDGE TOWERS

**M.Sc. THESIS**

**Oguz BERBER**

**Department of Civil Engineering**

**Structural Engineering Programme**

**September 2015**

**ISTANBUL TECHNICAL UNIVERSITY ★ GRADUATE SCHOOL OF SCIENCE ENGINEERING AND TECHNOLOGY**

# BENEFITS OF TUNED MASS DAMPERS IN TERMS OF IMPROVING THE SEISMIC PERFORMANCE OF SUSPENSION BRIDGE TOWERS

**M.Sc. THESIS**

**Oğuz BERBER**
**(501121062)**

**Department of Civil Engineering**

**Structural Engineering Programme**

**Thesis Advisor: Asst.Prof.Dr. Ufuk YAZGAN**

**September 2015**

**İSTANBUL TEKNİK ÜNİVERSİTESİ ★ FEN BİLİMLERİ ENSTİTÜSÜ**

# ASMA KÖPRÜ KULELERİNİN DİNAMİK DAVRANIŞINDA KÜTLE SÖNÜMLEYİCİ KULLANMANIN FAYDALARININ SİSMİK PERFORMANSLA DEĞERLENDİRİLMESİ

**YÜKSEK LİSANS TEZİ**

**Oğuz BERBER**
**(501121062)**

**İnşaat Mühendisliği Anabilim Dalı**

**Yapı Mühendisliği Programı**

**Tez Danışmanı: Yrd.Doç.Dr. Ufuk YAZGAN**

**Eylül 2015**

Oguz BERBER, a M.Sc. student of ITU Graduate School of Science student ID 501121062, successfully defended the thesis/dissertation entitled "BENEFITS OF TUNED MASS DAMPERS IN TERMS OF IMPROVING THE SEISMIC PERFORMANCE OF SUSPENSION BRIDGE TOWERS", which he prepared after fulfilling the requirements specified in the associated legislations, before the jury whose signatures are below.

| | | |
|---|---|---|
| **Thesis Advisor :** | **Asst. Prof. Dr. Ufuk YAZGAN**<br>Istanbul Technical University | ..... |
| **Jury Members :** | **Assoc. Prof. Dr. Serdar SOYÖZ**<br>Bogazici University | ..... |
| | **Asst. Prof. Dr. Ömer Tuğrul TURAN**<br>Istanbul Technical University | ..... |

**Date of Submission : 27 August 2015**
**Date of Defense : 7 September 2015**

***To my family, I have always considered myself as blessed due to being a part of you, thank you so much for always supporting me.***

***To my friends, although some of you may not understand any single word of this issue, but I feel gratitude to all of you for making my life easier.***

***To Çiğdem Bihter, I believe I could have never completed my master education without your support, thank you so much for your courage and great love.***

FOREWORD

I express my deepest gratitude to my thesis guide Asst.Prof.Dr. Ufuk Yazgan, whose encouragement and guidance from the beginning to the end enabled me to understand deeply this subject.
I will always feel gratitude to Manabu Inoue, who is the General Manager of Design Department at Izmit Bay Suspension Bridge project, that he shared his knowledge, experience and everything I need to develop this article.
I will always be indebted to my all teachers, since I learnt many things from each one you all my education life.
I thank to the all my friends for their supports and sharing their ideas and knowledge with me.
Lastly, I appreciate to my family for their support and love, also I always feel indebted to Cigdem Bihter who encouraged me to the start master education.

September 2015

Oğuz BERBER
(Civil Engineer)

**TABLE OF CONTENTS**

**Page**

## ABBREVIATIONS

**AMD** : Active Mass Damper
**A** : Cross-section area
**c** : Damping of the structure
**$c_d$** : Damping of mass damper
**CL** : Centerline
**e** : eccentricity
**g** : Unit of acceleration
**J14** : Joint 14 at the tower
**k** : Stiffness of the structure
**$k_d$** : Stiffness of the mass damper
**m** : Mass of the structure
**$m_d$** : Mass of the mass damper
**m.d.o.f.** : Multi degree of freedom
**$M_i$** : $i^{th}$ modal mass
**Me** : Bending moment due to ground motion
**MN** : Mega newton
**N** : Newton
**$I_x$** : Moment of inertia on x direction
**$I_y$** : Moment of inertia on y direction
**P** : Axial load at the top of the tower
**s.d.o.f.** : Single degree of freedom
**Sa** : Spectral acceleration
**SSBSZ** : Specification for structures to be built in disaster areas
**TMD** : Tuned Mass Damper
**UDL** : Uniformly Distributed Load
**V** : Vertical Load
**We** : Elastic section modulus on longitudinal direction
**$W_x$** : Section modulus on x direction
**$\sigma_{demand}$** : Demanded stress by ground motion
**$\sigma_{tensile}$** : Tensile stress capacity of the section
**$\sigma_{yield}$** : Yielding stress capacity of the section
**$\zeta_{structure}$** : Damping ratio of the structure
**$\zeta_{opt}$** : Optimum damping ratio of mass damper
**$\alpha_{opt}$** : Optimum tuning ratio for tuned mass damper
**$\mu$** : Mass ratio of tuned mass damper and the structure
**$\Phi$** : Mass participation factor

## LIST OF TABLES

**Page**

**LIST OF FIGURES**

**Page**

.

**BENEFITS OF TUNED MASS DAMPERS IN TERMS OF IMPROVING THE SEISMIC PERFORMANCE OF SUSPENSION BRIDGE TOWERS**

## SUMMARY

This thesis intends to investigate the effects of utilizing tuned mass dampers in mitigating the dynamic response of suspension bridge towers subjected to seismic actions. For this purpose Izmit Bay Suspension Bridge tower, which is located in Izmit Bay, is chosen as the case study bridge. Main span length of the bridge is 1550 meters and the two side spans are 550 meters each.

Dynamic response of the Izmit Bay Bridge Tower structure is investigated considering two models: (1) with mass damper and (2) without mass damper to be able to estimate the impact of utilization of mass damper on the seismic response.

For this purpose, member-based detailed three-dimensional simplified models of the tower are developed in CSI SAP2000 analysis software. Exact tower cross section is created in the analysis software, and for each section of Izmit Bay Bridge tower is reflected to the model with considering as-built geometry of erected tower. Additionally, loads acting on the tower that are coming from the deck and the cable are applied to the model. Also tuned mass damper (TMD) dynamic characteristics are defined according to actual masses of the existing dampers of the Izmit Bay Bridge Tower. At present, active mass dampers are built in the towers. These dampers are setup for mitigating wind and traffic induced vibrations. The existing active dampers are configured to shut down during seismic events. In this thesis, the hypothetical case of utilizing tuned mass dampers for mitigating the seismic vibrations of the towers is investigated. TMD's dynamic characteristic are estimated regarding the Eigen values obtained from the modal analysis result.

Eigen vectors are used to evaluate and understand the modal behavior of each joint of the tower. Twelve ground motions records are applied with direct time integration history using Newmark's constant average method considering the geometrical nonlinearities.

Failure cases are investigated for tower by approximately considering the full-scale bridge effects, accordingly limit state case is defined. Upon obtaining the results of time history analysis, seismic fragility curves are derived comparing the stress demand with the strength capacity at the critical joint sections of the tower.

Finally, fragility curves of two models are compared. As it is expected, failure probability is lower for the model with the tuned mass damper compared to that for the model without damper. In addition, time history analysis results are compared to each model in order to review the effect of mass dampers.

# AYARLI KÜTLE SÖNÜMLEYİCİLERİN ASMA KÖPRÜ KULELERİNİN DEPREM PERFORMANSINA FAYDALARI

## ÖZET

Bu tezin amacı asma köprülerin dinamik davranışında kütle sönümleyicilerin etkilerinin değerlendirilmesidir. Asma köprülerde kütle sönümleycilerin kullanılmasının köprünün deprem etkisi altındaki performansına etkisi incelenmiştir. Konunun gerçekçi bir örnek üzerinden incelenmesi için mevcut çalışmada örnek yapı olarak Izmit Körfez Geçiş Köprüsünün Kuleleri göz önüne alınmıştır. Kulelerin kütle sönümleyicili ve sönümleyicisiz durumları için kırılganlık analizleri yapılmıştır. Elde edilen kırılganlık modelleri temel alınarak, kütle sönümleyiclerinin farklı spektral ivme seviyeleri altında köprünün peformansına olan etkisi değerlendirilmiştir.Izmit Körfez Geçiş Köprüsü Izmit körfezinde bulunmaktadır. Köprünün ana açıklığı 1550 metre uzunluğundadır ve iki kenar açıklık 550 metredir. Tabliyelerin genişlikleri 35 metre olup, ana taşıyıcı kablonun çapı yaklaşık 0.78 metredir. Köprünün kuleleri ise 22 bloktan oluşmaktadır ve blokların yükseklikleri 8 metre ile 13 metre arasında değişmektedir. Kulenin ön panellerinin genişiliği 7 metredir ve kule boyunca sabittir. Kulenin yan panelleri ise eğimlidir, ilk blokta 8 metre olan genişlik, doğrusal olarak azalarak 22'inci blokta 7 metreye düşmektedir. Üst yapının tamamı çelik kullanılarak inşa edilmiştir.

İzmit Körfez Geçiş Köprüsünün kulerinde mevcut durumda aktif kütle sönümleyiciler yerleştirilmiş bulunmaktadır. Bu sönümleyiciler, rüzgar ve trafik yükleri altında çalışıcak, ancak deprem etkisi altında kapanacak şekilde tasarlanmıştır. Bu tez çalışmasında, yapıdaki mevcut sönümleyiciler yerine deprem sırasında çalışacak şekilde tasarlanmış ayarlı kütle sönümleyicilerin bulunması durumu incelenmiştir.

Bu tezde kulelerin dinamik davranışı zaman tanım analizi yöntemiyle, yer hareketi kayıtlarının etkitilmesiyle incelenmiştir. Tezin amacı olan kütle sönümleyicinin etkilerinin görülebilmesi için iki adet model hazırlanmıştır, kütle sönümleyicili kule ve kütle sönümleyici olmadan kule. Tezin literatür araştırma kısmında kütle sönümleyicilerinin tarihsel gelişimi açıklanmıştır.

Modellerde, kulenin her bir bloğu boy ve enkesit olarak ayrı ayrı SAP2000 analiz programında tasarlanmıştır. Daha gerçekçi analiz sonuçları elde edebilmek için çelik blokların imalatında ve sahada montajı sırasında her bir birleşim noktasında oluşan geometrik sapmalar modelde göz önüne alınmıştır. Sonuçta montajı tamamlanan yapıda bu (toleranslar içinde bulunan) üretim kusurları neticesinde eksantrisite vardır ve bu durum yapı modeline aktarılmıştır. Analiz sırasında tanımlanan yüklerin belirlenmesinde, köprünün tamamı (kablo ve tabliyeler) göz önünde bulundurulmuştur. Asma köprülerde, deklere yapı ve konum itibariyle çok fazla yük gelmektedir. Asma köprülerde yapının öz ağırlığı önemli miktardadır, ilave gelen rüzgar yükü ve trafik yükleri de taşınan yükü daha da fazlalaştırır. Tabliyeler kendisine gelen yükleri kablo aracılığıyla kulelere aktarır. Bir döngü misali, açıklık arttıkça tabliyelerden gelen yük artacaktır, tabliyeleri taşıyan kabloların bu yükleri taşıyabilmesi için de kablonun kesiti artacaktır ve sonuç olarak kulelere gelen dikey kuvvet artacaktır.

Izmit Körfez Geçiş Köprüsünde kullanılan kütle sönümleyici ilk olarak ayarlı kütle sönümleyici olarak tasarlanmıştır. Fakat, montaj açısından ayarlı kütle

sönümleyicinin montajının zor olması, aynı dinamik karakteristik özelliklere sahip aktif kütle sönümleyici kullanılmasına sebebiyet vermiştir. Örnek olarak, ayarlı kütle sonümleyicinin ağırlığı 12 tondur, aktif kütle sönümleyici yaklaşık 10 tondur fakat sönümleyicilerin rijitlik ve sönümleme parametreleri yapıya optimum etkiyi sağlamak üzere belirlenmiştir. Izmit Körfez Geçiş Köprüsünün kulelerinde aktif kütle sönümleyiciler, doğu da ve batı'da 2 adet olmak üzere toplam 4 kule ayağı bulunan asma köprüde, her bir kule ayağında 2 adet aktif kütle sönümleyici kullanılmıştır, bu tasarım aşamasında düşünülen ayarlı kütle sönümleyici ile aynı adettir. Titreşim önleyiciler sadece ana açıklık doğrultusunda hareket edecek ve esas olarak kulenin birinci titreşim modunu sönümleyecek şekilde tasarlanmıştır.

Analiz için hazırlanan modelde dizayn aşamasında tasarlanan ayarlı kütle sönümleyicinin parametreleri kullanılırken aslında gerçeğe tamamen uygun bir durumdur zira kullanılan aktif kütle sönümleyicinin dinamik karakteristik özellikleri de aynıdır. Fakat Izmit Körfez Geçiş Köprüsü projesinde kullanılan aktif kütle sönümleyicinin çalışma prensiplerinden biri de yapıya etkiyen yer hareketi ivmeleri karşısında aktif kütle sönümleyici kendisini kapatmasıdır. Zira çalışma prensibi olarak yapıyı titreştiren bir dalgayı sönümlemeye çalışır, oysa yer hareketi sırasında çok sayıda dalga yapıya etkimektedir. Bu durumda bir hareketi engellemeye çalışan aktif kütle sönümleyici belki de diğer bir ivme dalgasına destek olacaktır. Bu da yapıya yer hareketi etkidiğinde yapıda titreşim önleyicilerin çalışmaması, yani bir bakıma kütle sönümleyici yok manasına gelmektedir. Ayarlı kütle sönümleyicileri montaj ve stabilizasyon konusunda dezavantajlı olsa da, hem yer hareketi altında hem de rüzgar yükleri altında çalışır durumdadır. Izmit Körfez Geçiş Köprüsü projesinde kullanılan aktif kütle sönümleyici ise sadece rüzgar dinamik yükü atlında çalışmaktadır.

Modelde kullanılan ayarlı kütle sönümleyicilerin dinamik karakteristik özellikleri belirlenirken Den Hartog'un ayarlı kütle sönümleyici tasarımı metodundan faydalanılmıştır. Kütle sönümleyicinin dinamik karakteristik özellikleri kulenin modal analizi neticesinden elde edilen öz değerler kullanılarak bulunmuştur.

Sismik kırılganlık eğrilerinin oluşturulabilmesi için kulenin limit durumları araştırılmıştır. Sonuç olarak birinci mod şekline (boyuna doğrultu) göre kritik birleşim noktaları belirlenmiştir. Kulenin limit kapasitesi kritik birleşim noktalarında dinamik yüklerin neden olduğu deplasman neticesinde oluşan eksantirik momentin yol açtığı gerilmelerin malzemenin akma dayanımını aşması durumudur. Kırılganlık analizi için seçilen oniki yer hareketi kaydı, belirli katsayılarla arttırılarak yapının limit durumuna kadar analizi yapılmıştır. Yer hareketi kayıtları belli katsayılarla büyütmeden önce Bu veriler altında, yapının kapasitesi ve arttırılmış yer hareketinin talepleri karşılaştırılarak sismik kırılganlık eğrileri oluşturulmuştur.

Analizlerde kullanılan yer hareketi kayıtlarının zemin özelliklerinin ilgili kulenin bulunduğu sahadaki zemin özelliklerine benzer olmasına dikkat edilmiştir. Yer hareketi kayıtları yerin 30m altında dalga hızı 300 m/s civarında olan yerden kayıtlar alınmıştır.
Yapılan zaman tanım alanı hesaplarında Newmark sabit ortalama ivme yöntemi kullanılmıştır. Aynı zamanda hesaplarda geometrik bakımından lineer olmayan davranış göz önünde bulundurulmuştur. Seçilen bu yöntemle gerçeğe daha yakın sonuçlar elde edilmesi amaçlanmıştır. Asma köprülerin kulelerinin sönüm oranı yaklaşık 0.02 civarıdır.

Elde edilen sismik kırılganlık eğrileri karşılaştırılmadan önce, ayarlı kütle sönümleyicinin etkisiyle ilave olarak yapıya etkiyen rijitlik ve sönüm etkileriyle, yapının kritik noktalarında deplasmanların azaldığı, aynı zamanda yer hareketi sona erdikten sonra yapı çok daha hızlı bir şekilde var olan titreşimi sönümleyip ilk konumuna dönmüştür.

# 1. INTRODUCTION

Throughout the long history of suspension bridges, dynamic loads are still one of the biggest challenges for structural engineers. Considering the size of the structure itself and complexity of each joints boundary conditions, to identify the behavior of suspension bridges under dynamic loads it is still one of the major concern. Under these circumstances, mass dampers are widely used to limit the vibration for suspension bridges tower.

## 1.1 Purpose of Thesis

In this thesis, a suspension bridge' tower behavior under seismic loads are investigated. For this purpose, Izmit Bay Suspension Bridge is chosen as the case study structure for the investigation. In order to show the benefits of mass dampers for suspension bridges, Towers of the Izmit Bridge are investigated. Two different models are established for this purpose: one without mass damper, and one with mass damper. Also failure cases are investigated, in order to estimate fragility curves under seismic loads. Main purpose of thesis is to show the benefits of mass dampers based on seismic fragility of the structure. It is expected to observe that, with the additional damping and stiffness coming from mass dampers, relative displacements of the tower would be decreased significantly.

In the model of Izmit Bay Bridge tower, at the beginning, tuned mass dampers (TMD) are considered to control vibration, but then considering the difficulty of TMD installation; instead of TMD, active mass dampers (AMD) are installed. Active mass dampers designed as having the same dynamic characteristics as TMD. AMD is more suitable for installation because of its compact dimension for space inside the tower and more reliable to work from small acceleration range (Inoue et *al.*, 2014). But the working principle of AMD used for Izmit Bay Bridge is that AMD shuts itself down during ground motions exposed to tower, which means the behavior is like there is no mass damper during ground motion. Therefore, when obtain the

seismic fragility curves, the results of both models can be compared. In this case, it is expected to see the advantages of TMD over AMD used for Izmit Bay Bridge.

### 1.2 Literature Review

The Tacoma Narrows Bridge collapse in 1940 forced researchers and engineers to study focused on dynamic behavior of bridges, (Rannie, 1941). In 1950's an approximate method of Rayleigh-Ritz type solution was considered as a reasonably accurate technique to analyze dynamic behavior of suspension bridges. However, according to Shinozuka (2009) "the solution could only be reasonable for the lowest modes due to the great level of complexity and redundancy of higher modes of suspension bridges'' (p.3). For defining the dynamic characteristics of bridges, in 1976 the finite element methods with linearized deflection method was proposed by Abdel-Gaffar. In 1977, Abdel-Gaffar and Housner (1977) has done an analysis for the dynamic characteristics of a suspension bridge. Later (Abdel-Gaffar et al., 1982), conducted additional studies on the behavior of full-scaled suspension bridges under dynamic loads, such as earthquake and wind. Considering the speed of computers become faster day by day, it is now possible to establish and analyze 3-D suspension bridge models.

The first time in 1966 for the Forth Road Bridge in UK, it was considered to use mass damper to control the bridge vibration, (Inoue et al., 2014). A heavy sliding block was used for the Forth Bridge, since the vibration amplitude was around 1 m during 9-10 m/s wind speed.

Sliding block system was also used for Kanmon Bridge in Japan in 1971 which "the tower obtained not only additional mass but also damping by friction between the block and the slope" (Inoue et al., 2014).

In 1980's, tuned mass dampers were become alternative and common solution for suspension bridges. Tuned mass dampers consist of spring, mass and damping; which is quiet effective compared to sliding block system.

In Japan, for the Akashi- Kaikyo Bridge in 1998, which is the word longest suspension bridge, five tuned mass dampers were used for one tower leg to mitigate the vibrations caused by wind and seismic loads.

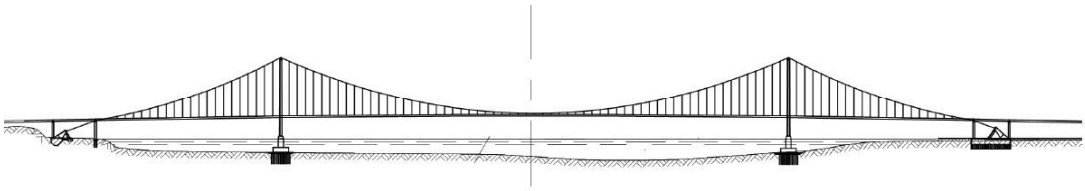

**Figure 1.1 :** Izmit Bay Suspension Bridge general view (Izmit Bay Bridge Detailed Design, 2012a).

### 1.3 Hypothesis

Smaller displacements are expected to be observed under dynamic loading, when tuned mass dampers are installed to any structure. Izmit Bay Bridge has been chosen for modeling, because the author have the necessary information about Izmit Bay Suspension Bridge. A general view in Figure 1.1 is shown for Izmit Bay Suspension Bridge.

The main purpose is to show how to control the vibration for every long and slender structure. The other purpose is the verification of the bridge towers for the energy absorption capacity during vibration. It is highly expected to see that, with the additional damping coming from mass damper, displacement amplitudes shall significantly decrease during ground motions.

Every structure has its own damping characteristics that depend on its structural properties and boundary conditions. It is related to the structure's energy absorption capacity against the vibration caused by dynamic loads. Figure 1.2 presents the effect of damping on the vibration. If a structure has more damping capacity, the vibration energy is absorbed quicker.

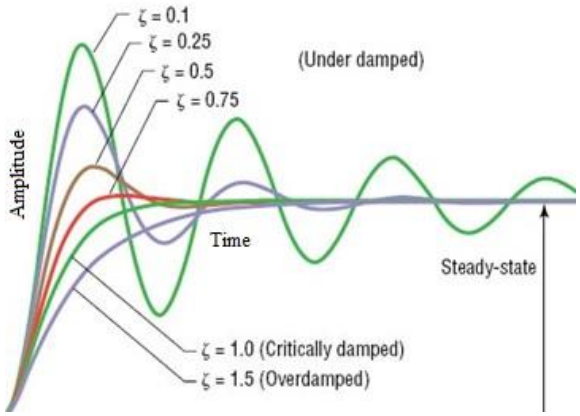


**Figure 1.2 :** Damping effect on vibration.

Response of suspension bridges subjected to ground motion loads has to be analyzed carefully. Especially, for the long period structures located around active seismic fault line, or slender structures are exposed to heavy wind, high vibration amplitudes are expected. Therefore, these amplitudes must be limited considering different solutions. Dynamic displacements should be limited not only for structural health but also for the comfort of the occupants.

Requirements for suspension bridges, such as dynamic behavior against seismic or wind loads etc., are usually defined at the design stage. Necessity for additional damping is with different solutions is evaluated by considering these requirements. Most common solution is to use additional mass dampers for tower, since it has also great benefit to structural health against fatigue. Of course, there are several methods to control the vibrations, like using bearings to limit the displacements of suspension bridge deck laterally or longitudinally, or increasing the section thicknesses and to make the structure more rigid. However, in this latter case when the structure becomes more rigid, the dynamic loads shall also be increased as well. Therefore, the designer should consider the optimal solution. In this thesis, only the tower itself is considered. Izmit Bay Suspension Bridge is supported by four tower legs, and each of them has two dampers to control the vibration.

## 2. IZMIT BAY SUSPENSION BRIDGE TOWER MODEL

### 2.1 Purpose

Izmit Bay Suspension Bridge tower is modelled for two alternative cases; one considering the Tuned Mass Damper (TMD), the other is without TMD. The purpose is to identify the dynamic behavior of tower in each case, considering the full-scaled bridge effect. This means that only the tower is modelled using finite-elements but the effects of full-scaled bridge completion such as the effects of cable on tower considering deck, is also considered. This is achieved by appropriately defining the boundary conditions of the model. In addition, imperfections caused by tower blocks fabrication and during towers erection were considered in the models. Twelve ground motion records are applied to both model to be able to observe the effects of TMD. Subsequently, based on time history analysis results, seismic fragility curves are prepared.

### 2.2 General Information About the Study Bridge

Izmit Bay Suspension Bridge will carry the new Gebze-Orhangazi-Izmir motorway across the Sea of Marmara at the Bay of Izmit (Kawakami et al., 2015). General view and dimension are shown in Figure 2.1. Izmit Bay Bridge consist of one main span and two-side spans. The main span is 1550 m, and side spans are 566 m. The main span of 1550 m will make Izmit Bay Suspension Bridge the $4^{th}$ longest suspension bridge in the world, after the completion of its erection. The suspended deck is an orthotropic stiffened steel box girder with an height of 4.75 m and width is 30.1 m as shown in Figure 2.2. The main cables are designed as pre-fabricated parallel wire strands (PPWS), in which each strand is consist of 127 wire and for main cable has 110 strand between each tower. Between tower and cable anchorage there are 2 additional strands, which results in a total of 112 strands, as shown in Figure 2.3. Each wire has a diameter of 5.91 mm and ultimate strength of wire is 1760 Mpa. Two towers are located in North Side and the other two are located in South Side. Top height of the tower from sea level is 252 m including 10.01 m caisson height

from sea level. The towers are single-cell box steel structures having two cross beam, one is at block 9 and the other is at block 22, tower general view and typical cross section are shown in Figure 2.4. Tower dimensions are 8x7 m at base and it becomes 7x7 meter at top with tapering longitudinally. Two mass dampers are located at 170 m height for each tower leg. Mass dampers locations are determined according to first out of plane bending mode. The point of greatest displacement corresponds to the height of 170 m. This situation will be clarified further based on modal analysis on the next section.

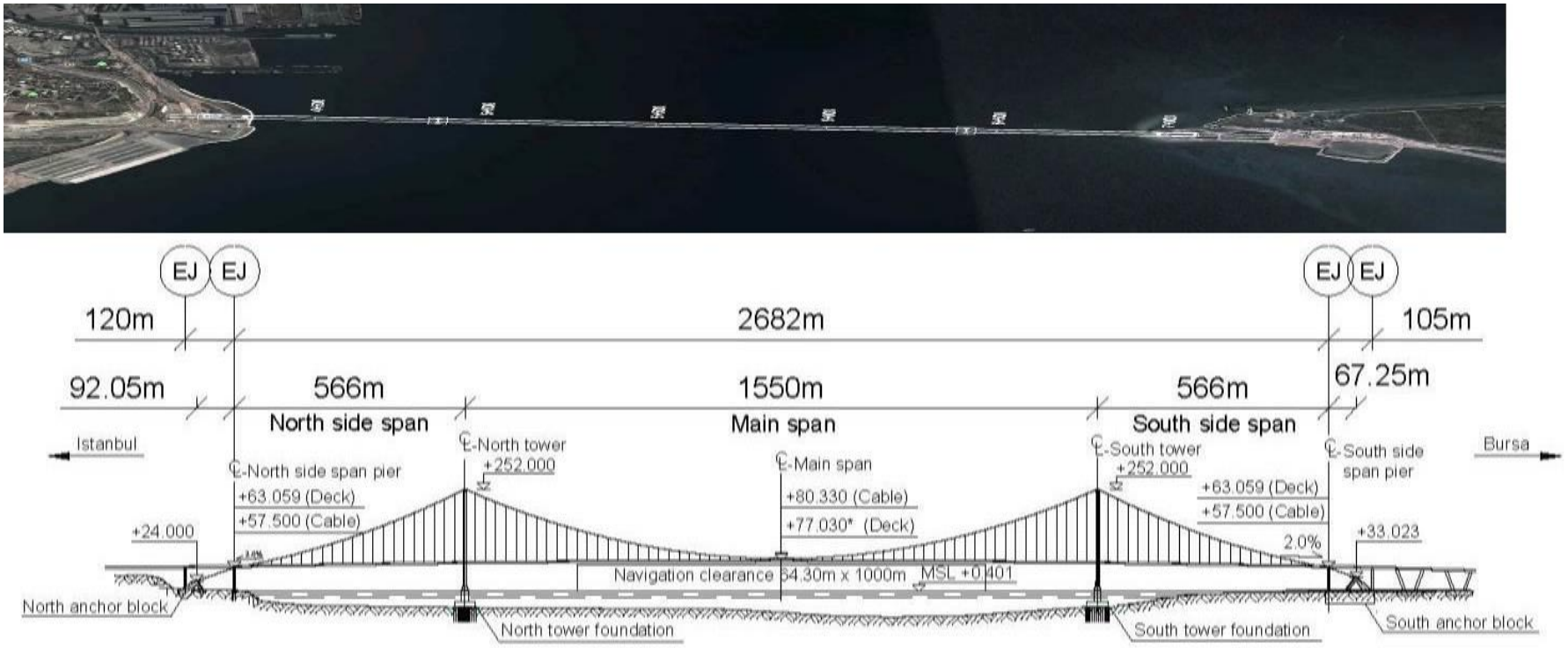


**Figure 2.1:** Izmit Bay Suspension Bridge dimensions (Kawakami *et* al., 2014).

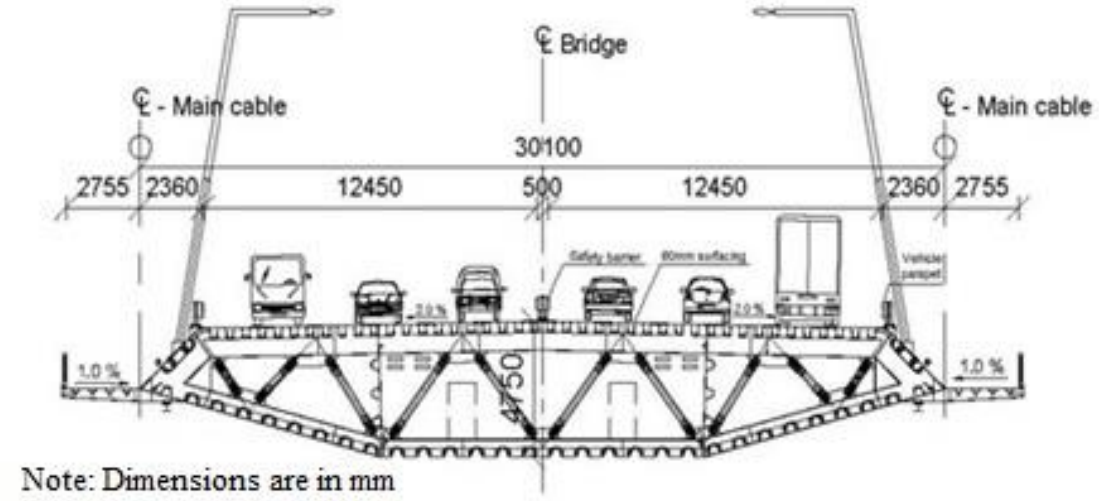


**Figure 2.2 :** Typical orthotropic steel box girder (COWI, 2011a)

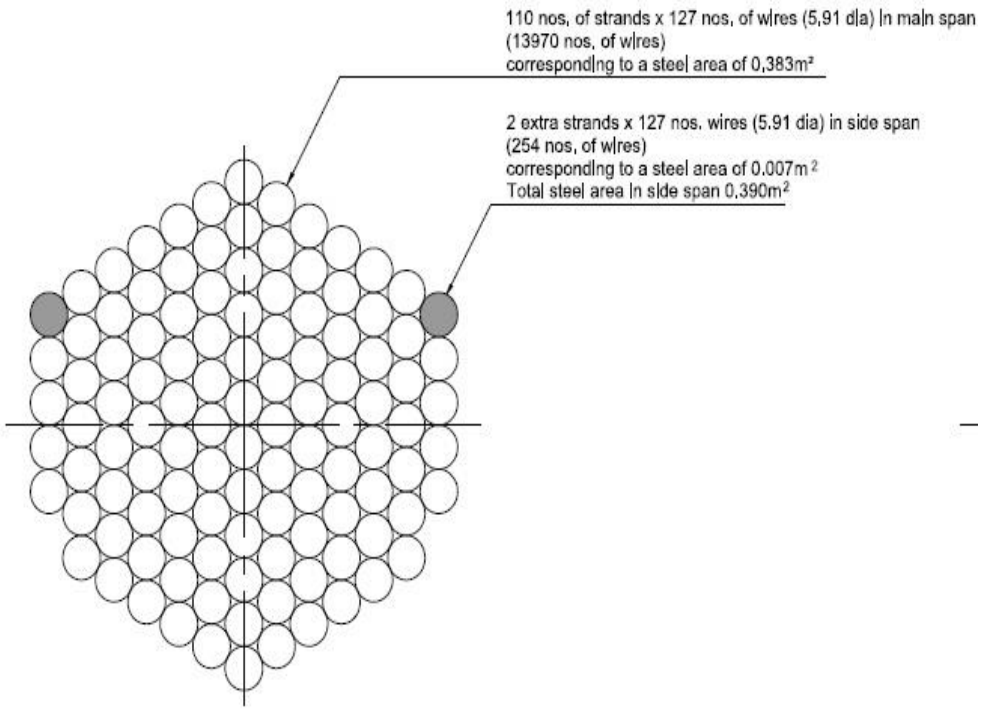


**Figure 2.3 :** Main cable cross-section (COWI, 2011a).

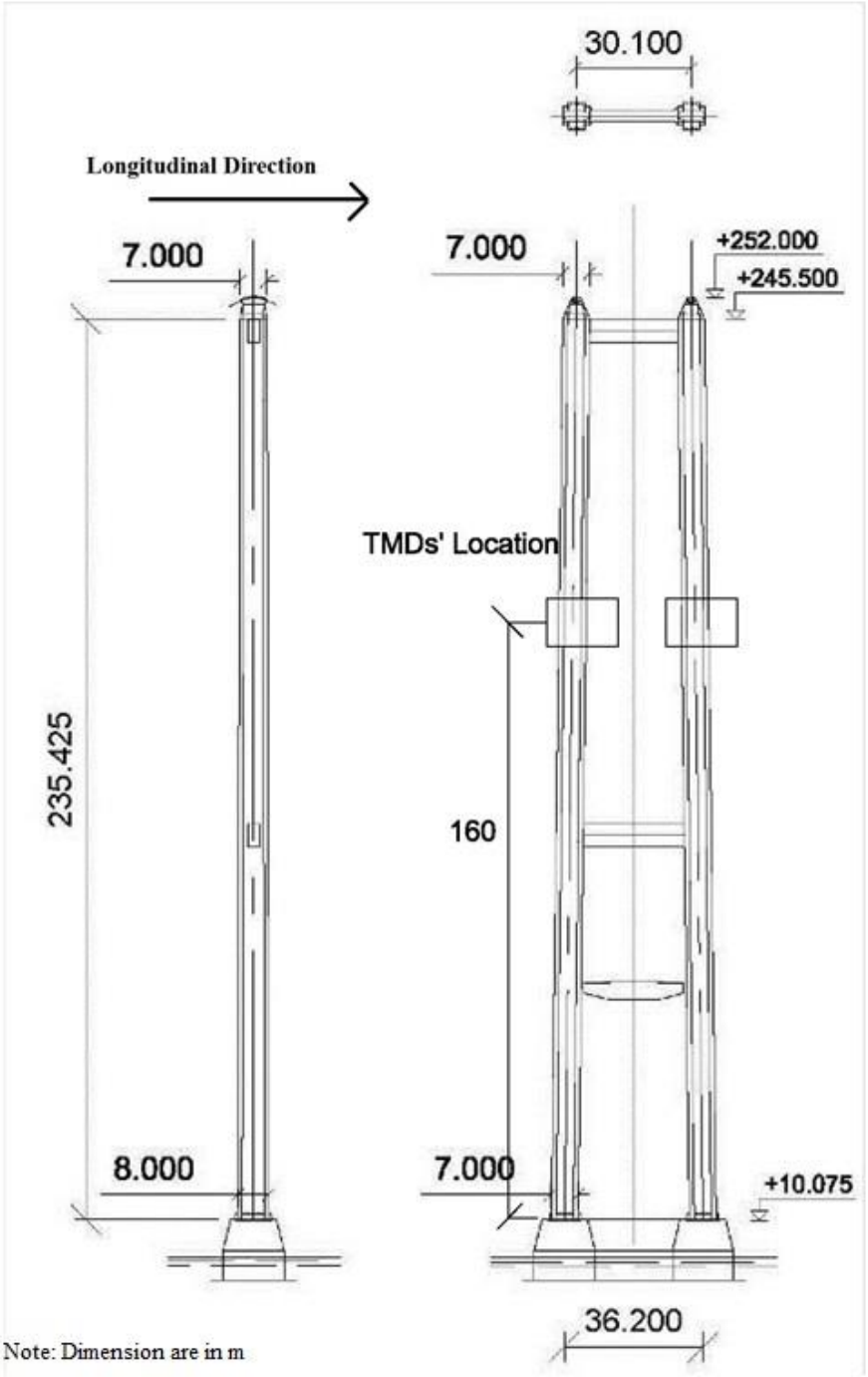


**Figure 2.4 :** Tower general view (COWI, 2011a)

## 2.3 Section Properties of Towers

The section properties of each block are different than the others since the tower blocks are tapered. In Figure 2.5 the general dimensions of tower cross-sections are shown.

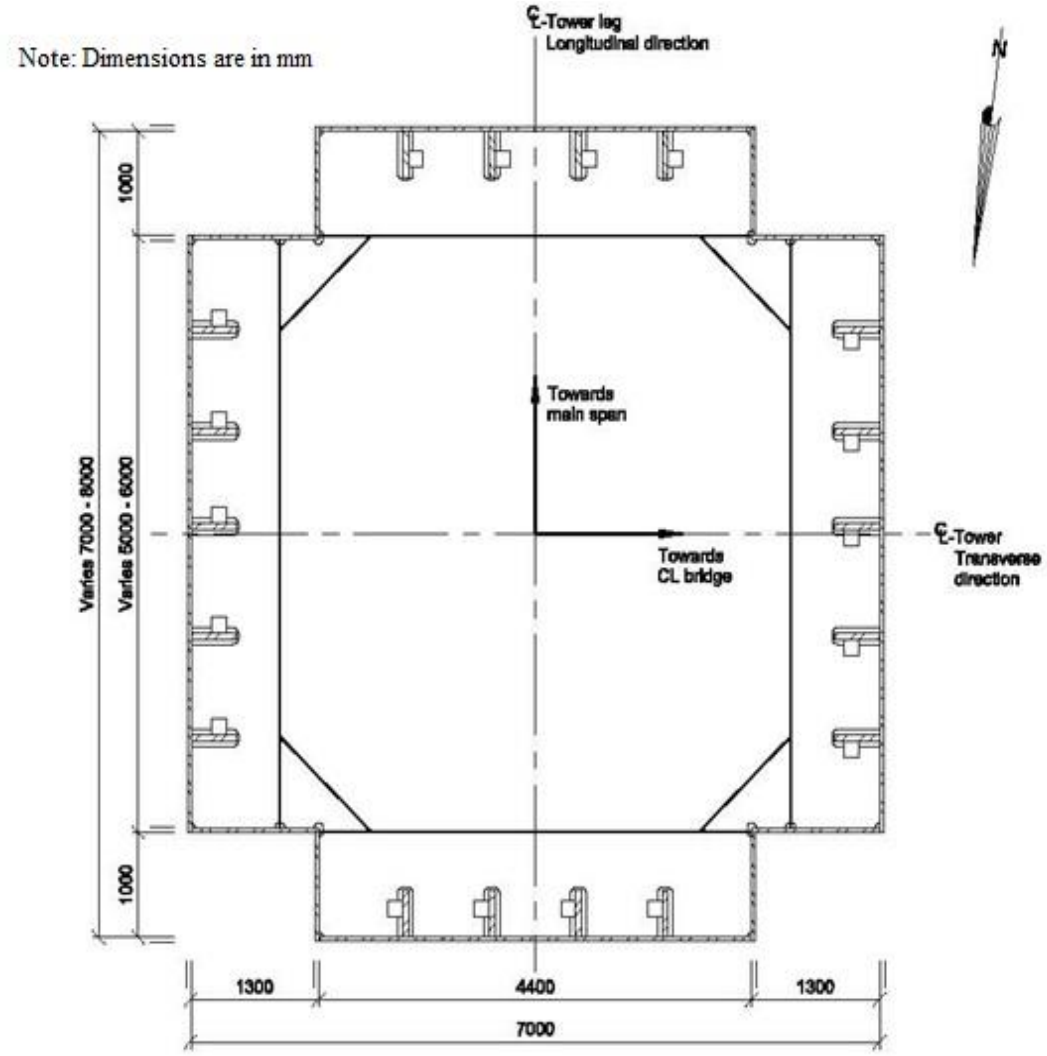


**Figure 2.5 :** Tower typical cross-section (COWI, 2011b)

Before preparing the model of tower, each block's section properties are calculated. Due to tapering of the tower skin plates, each block has different properties, as listed in Table 2.1. Main span direction is defined as the "x direction" and centerline (CL) bridge direction is defined as the "y direction".

**Table 2.1 :** Properties of tower blocks.

Note: Block 9's and Block 22's weights include the cross beams.

| Block | Height (m) | A ($m^2$) | $I_x$ ($m^4$) | $I_y$ ($m^4$) | $W_x$ ($m^3$) | Weight (ton) |
|---|---|---|---|---|---|---|
| 1 | 8 | 2.61 | 22.33 | 18.58 | 5.65 | 352.20 |
| 2 | 10 | 2.60 | 22.08 | 18.51 | 5.61 | 281.76 |
| 3 | 13 | 2.30 | 19.19 | 16.31 | 4.90 | 265.93 |
| 4 | 13 | 2.00 | 16.34 | 14.10 | 4.19 | 237.30 |
| 5 | 13 | 1.75 | 14.27 | 12.05 | 3.69 | 205.55 |
| 6 | 13 | 1.57 | 12.45 | 11.02 | 3.22 | 259.56 |
| 7 | 13 | 1.57 | 12.15 | 5.50 | 3.18 | 188.73 |
| 8 | 13 | 1.64 | 12.50 | 11.58 | 3.37 | 197.43 |
| 9 | 13 | 1.71 | 14.56 | 12.33 | 3.34 | 488.61 |
| 10 | 12 | 1.62 | 11.91 | 5.91 | 3.26 | 180.36 |
| 11 | 12 | 1.62 | 11.91 | 11.21 | 3.21 | 179.87 |
| 12 | 9 | 1.67 | 12.11 | 11.49 | 3.28 | 159.44 |
| 13 | 9 | 1.66 | 11.96 | 11.62 | 3.26 | 159.22 |
| 14 | 9 | 1.66 | 11.82 | 11.58 | 3.24 | 159.44 |
| 15 | 9 | 1.66 | 11.67 | 11.55 | 3.21 | 159.66 |
| 16 | 9 | 1.65 | 11.41 | 11.51 | 3.16 | 157.74 |
| 17 | 9 | 1.57 | 10.58 | 11.29 | 2.94 | 151.17 |
| 18 | 10 | 1.54 | 10.37 | 10.89 | 2.90 | 161.62 |
| 19 | 10 | 1.54 | 10.22 | 10.67 | 2.88 | 161.18 |
| 20 | 11 | 1.45 | 9.54 | 10.31 | 2.70 | 163.07 |
| 21 | 10.455 | 1.43 | 9.18 | 9.89 | 2.62 | 163.34 |
| 22 | 7 | 1.43 | 9.11 | 9.85 | 2.60 | 212.34 |
| Saddle | 5.04 | 1.15 | 6.21 | 5.80 | 1.80 | 81.80 |

In Table 2.1, where 'Height' shows each blocks' length. 'A' is the cross section area of each block, '$I_x$' is the moment of inertia in the longitudinal direction, 'Iy' is the moment of inertia in the lateral direction, '$W_x$' represents the section modulus of each block, 'Weight' shows each blocks' weight. Considering the tower inclination, A $I_x$, $I_y$, $W_y$ are the mean values of bottom and top sections of each blocks. The data are calculated manually using the related design drawings in COWI (2011b) in order to verify the cross-sections created in SAP2000

Tower legs are connected to each other (north and south tower) with cross beams at block 9 and block 22, cross beam at block 22 level as shown in Figure 2.6.

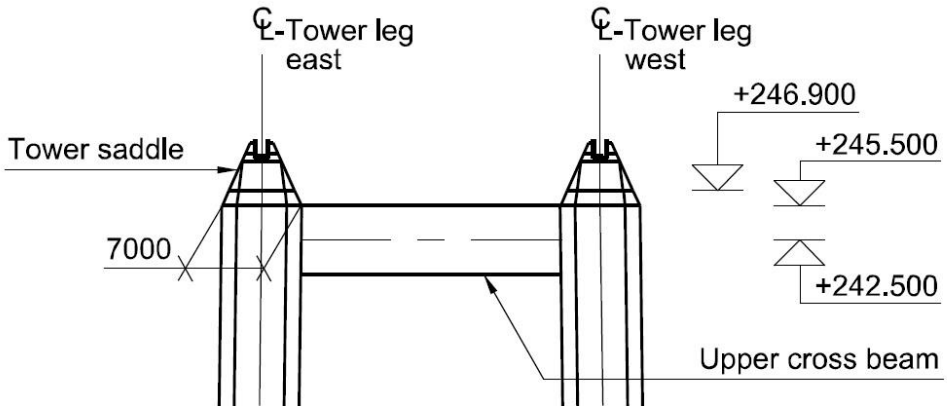


**Figure 2.6 :** Upper cross beam connecting two tower legs.(COWI, 2011b)

## 2.4 Tower Dynamic Characteristics

Tower foundation is made of concrete and the bottom of tower foundation has no fixation except the friction between the tower foundation bottom and soil layer. According to Christensen (2013), " The towers are allowed to slide on top of the friction layers when the horizontal shear exceed 70% of the vertical reaction, which is defined for gravel with friction angle of 35 deg''. Thus, based on this information, the tower bottom sliding behavior can be defined without considering tower caisson. Figure 2.8 shows the friction model of tower bottom sliding.

In this investigation, it is assumed that for the dynamic behavior of the tower, bottom side behavior is defined by a friction model. A spring is attached to tower top in order to catch the resistance against movement at that point due the cable. Figure 2.7 simply shows the model of the tower.

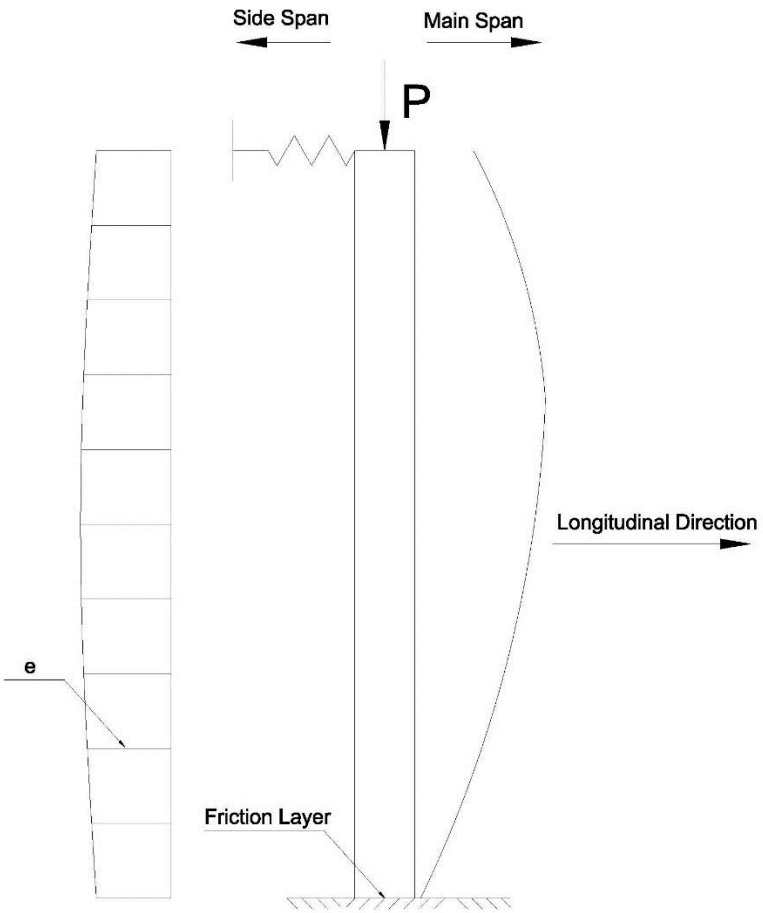


**Figure 2.7 :** Tower model.

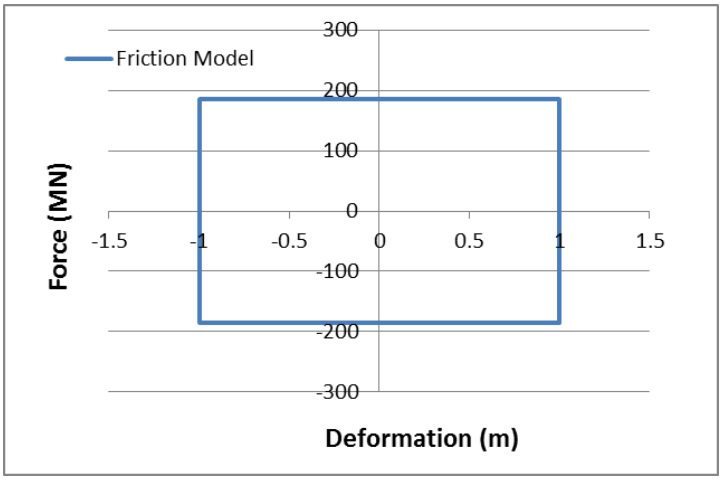


**Figure 2.8 :** Tower bottom sliding model.

The friction model can be modelled in SAP2000 with using the friction isolator link considering the coulomb friction model (Figure 2.8). According to Christensen (2013), the friction coefficient between soil layer and tower bottom is equal to 0.7. In

SAP2000 software, friction isolator link parameters are defined according to CSI Analysis Reference Manual (2013). In the finite-element model, tower caisson was not included but the friction capacity at the base was estimated by taking the weight of the caisson into consideration.

**Table 2.2:** Friction isolator link properties for tower foundation.

| Axial stiffenes (k1) | | | Shear Stiffenes (k2) | | Friction coefficient | Poisson ratio |
|---|---|---|---|---|---|---|
| E ($kN/m^2$) | A /L ($m^2/m$) | EA /L (kN/m) | G ($kN/m^2$) | GA/ L (kN/m) | - | - |
| 3.60E+07 | 3685 | 1.33E+11 | 15000000 | 5.53E+10 | 0.7 | 0.2 |

Table 2.2 shows the values for the k1 and k2 stiffnesses of friction model of tower foundation. E and G represents the modulus elasticity and shear modulus of concrete, A is the square sliding surface at the caisson bottom and L represents the height. L was taken 1 m in order to obtain a sufficiently large stiffness value before the initiation sliding.

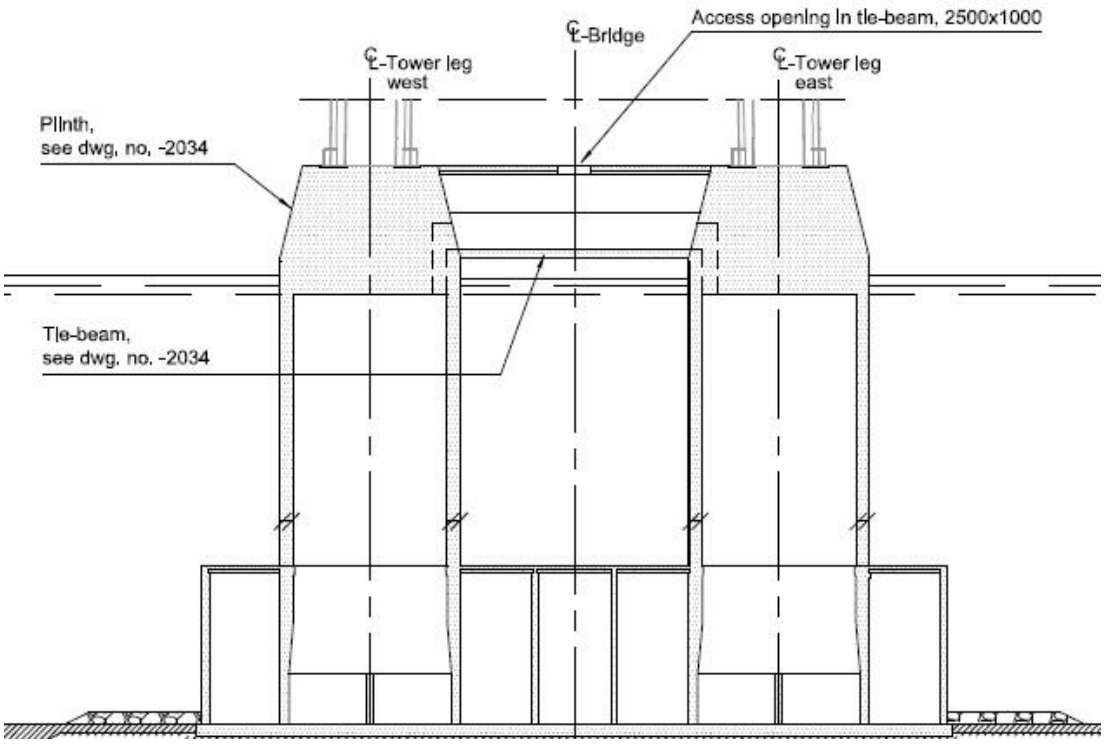


**Figure 2.9 :** Tower foundation, Caisson (Izmit Bay Bridge Detailed Design, 2012b).

The tower top side is modelled by a spring representing the cable effect. Figure 2.9 shows the horizontal component of the total force exerted on the tower top by the cables, at different levels of top point displacement as reported by Inoue (2015a).

Using this figure, the contribution of the cables to the stiffness of the top point against lateral movement can be identified. After obtaining the stiffness from the Figure 2.10, a spring is used in SAP2000 software with defining the spring stiffness.

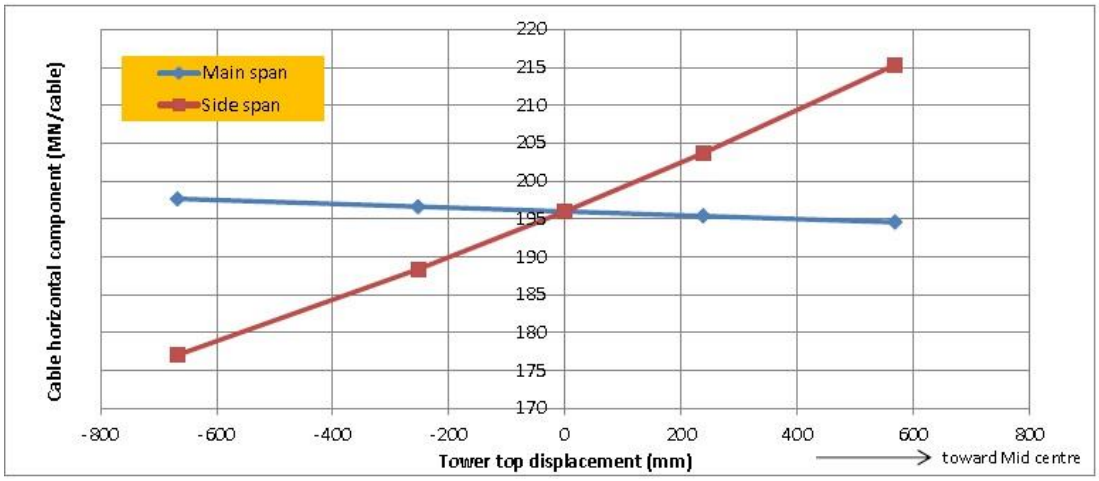


**Figure 2.10 :** Tower top characteristic (Inoue,2015a).

Additionally according to Inoue (2015), "The tower can be designed by simplifying the tower as a beam with a hinged supported at the top since the longitudinal displacement at the tower is mostly restricted by the main cable''. At the design stage, the tower top side can be modelled with a hinged supported, since the tower top stiffness is huge. Nevertheless, to make the analysis closer to the actual response, spring is the solution to identify the dynamic character. At the top side, spring is attached only for longitudinal direction, because mass dampers effect are investigated, and mass damper working through longitudinal direction.

After modelling tower considering the restraints, also misalignments during fabrication and erection of tower is considered. As built construction of Izmit Bay Bridge tower (2015) shows the misalignments for the north as listed in Table 2.3.

**Table 2.3 :** Misalignments at joints in longitudinal direction for north tower.

| Joint No. | North East (m) | North West (m) |
|---|---|---|
| Joint 1 | -0.0013 | 0.0048 |
| Joint 2 | 0.006 | 0.0074 |
| Joint 3 | -0.0018 | -0.0086 |
| Joint 4 | 0.0029 | -0.0077 |
| Joint 5 | 0.0185 | -0.0059 |
| Joint 6 | 0.009 | 0.0083 |
| Joint 7 | 0.0022 | 0.0096 |

| Joint No. | North East | North West |
|---|---|---|
| Joint 8 | -0.0002 | 0.0004 |
| Joint 9 | -0.0075 | 0.0012 |
| Joint 10 | -0.0203 | -0.0145 |
| Joint 11 | -0.0117 | -0.0045 |
| Joint 12 | -0.021 | -0.0179 |
| Joint 13 | -0.0193 | 0.0044 |
| Joint 14 | -0.0213 | 0.0044 |
| Joint 15 | -0.0303 | 0.0024 |
| Joint 16 | -0.0176 | 0.0057 |
| Joint 17 | -0.0027 | 0.0101 |
| Joint 18 | -0.0334 | -0.0208 |
| Joint 19 | -0.0324 | -0.035 |
| Joint 20 | -0.039 | -0.0376 |
| Joint 21 | -0.0444 | -0.0416 |
| Joint 22 | -0.0553 | -0.0475 |
| Saddle | -0.0588 | -0.0368 |

First mode shape of the tower corresponds to the 36$^{th}$ mode shape of the full-scaled bridge, and the biggest displacements are observed in this mode shape for the tower itself. Figure 2.7 shows the 36$^{th}$ mode shape of full-scaled bridge.

**Figure 2.11 :** 36$^{th}$ mode shape of full scaled bridge (Izmit Bay Bridge Detailed Design, 2012b).

According to this information, tower is modelled, fixed at the bottom and hinged supported at the top in SAP2000 and modal analysis is performed in order to identify the dynamic characteristics of tower.

Tower has been modelled in software SAP2000, and modal analysis has been executed. In Table 2.4, frequencies of the modes are listed.

**Table 2.4 :** Modal analysis result.

| Mode | Period (Sec) | Frequency (Cycle/sec) |
|---|---|---|
| 1 | 2.64429 | 0.37817 |
| 2 | 1.93849 | 0.51587 |
| 3 | 1.75575 | 0.56956 |
| 4 | 1.07022 | 0.93439 |
| 5 | 1.02447 | 0.97611 |
| 6 | 0.76141 | 1.3134 |
| 7 | 0.73853 | 1.354 |
| 8 | 0.59932 | 1.6686 |
| 9 | 0.54767 | 1.8259 |
| 10 | 0.47777 | 2.0931 |
| 11 | 0.33146 | 3.0169 |
| 12 | 0.33135 | 3.018 |

First out of bending mode shape (on longitudinal direction) is shown at Figure 2.12, it is the modal analysis results obtained from CSI SAP2000 software. The maximum modal displacement is at joint 14 (J14), which is located at height of 160 m height from tower base. It is obvious that, J14 is one of the critical points, since the biggest displacement shall be observed.

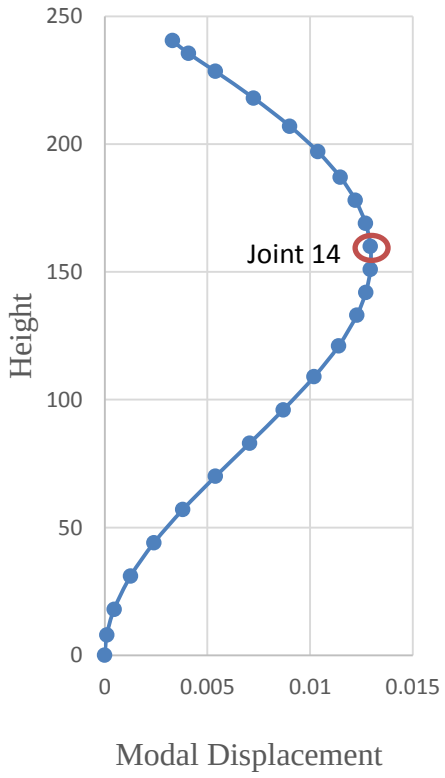


**Figure 2.12 :** 1st longitudinal bending mode shape.

TMDs' are useful to decrease the displacements during vibration. In order to increase TMD's damping efficiency, mass dampers should be located at the point where maximum displacements are observed. For example, for a 50 storey building maximum displacements are observed at the top for the first mode, therefore TMD works most efficiently if it is located at the top. There are some other parameters, to find a proper place to locate mass dampers for stabilization, so designer should consider other parameters which may cause other problems. For suspension bridge towers, considering the restraint conditions of top and base, maximum modal displacement is seen at joint 14. As a result, two mass dampers are located at joint 14 for Izmit Bay Suspension Bridge.

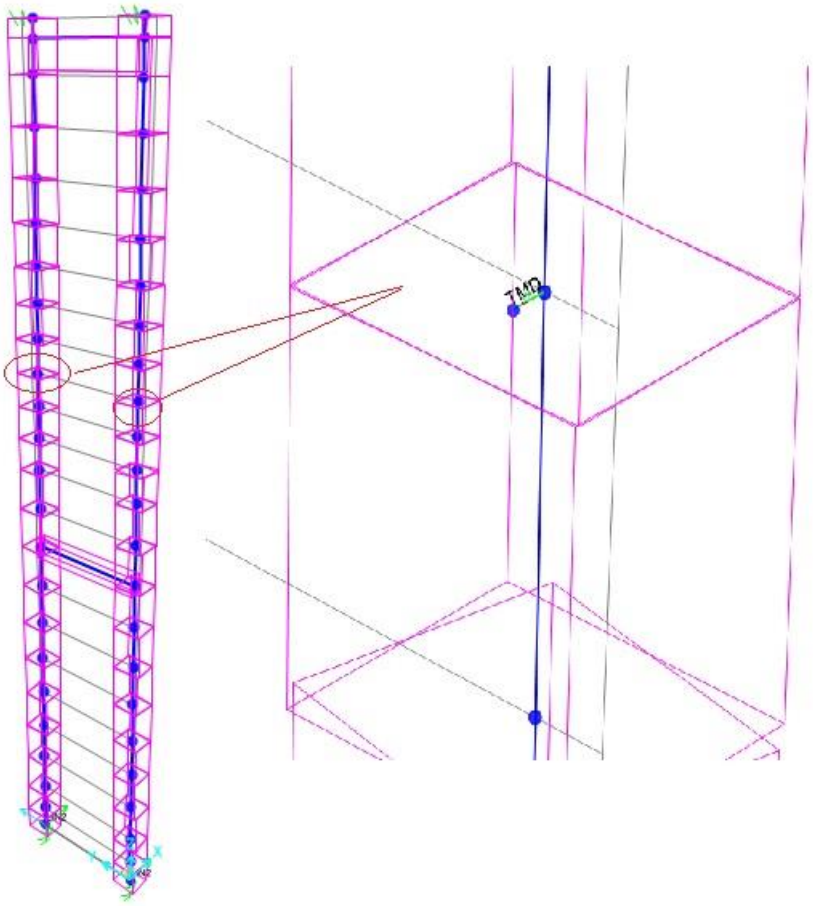

**Figure 2.13 :** Tower model in SAP2000.

## 2.5 TMD's Dynamic Characteristics

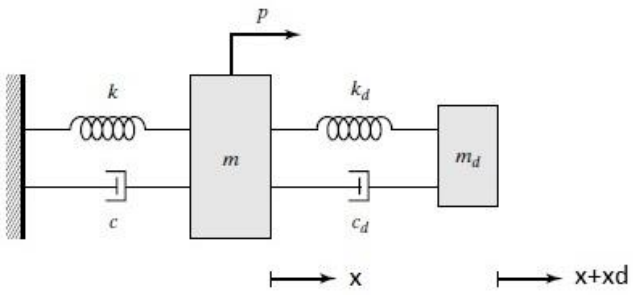


**Figure 2.14 :** TMD mounted on main structure.

In the Figure 2.14, k is the stiffness of main structure, c is the damping of main structure and m is the mass of structure. Moreover, $k_d$, $m_d$, $c_d$ represent the stiffness, mass and damping of TMD. Figure 2.14 shows the working mechanism of TMD. Stiffness and damping properties of the mass damper are tuned based on the dynamic characteristics of the main structure.

It is important to determine which mode's vibration will be targeted to be mitigated by mass dampers. For Izmit Bay Bridge, mass damper mitigates the vibrations in the 1st out of plane bending mode shape. Two tuned mass dampers are used for one tower leg, in total four mass dampers are used to control the vibration of one tower. Each TMD has a mass of 12 tons, so for one tower leg there are 24 tons of TMDs.

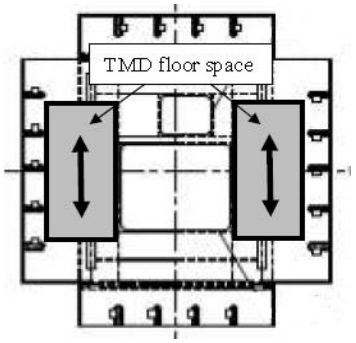


**Figure 2.15:** TMDs are located at joint 14 (Izmit Bay Bridge Detailed Design, 2012c).

There are several methods for determining the optimal values for TMD's stiffness and damping. Working mechanism and efficiency of TMD has been studied and formulated by Den Hartog (1947). In this research, Den Hartog's (1947) method is applied since Den Hartog's approach is one of the most common ones today.

Mass ratio, $\mu$ of the structure and TMD has significant effect to define the TMD characteristics, where μ is the mass ratio as expressed in Equation 2.2,

$$\mu = \frac{m_d}{m} \tag{2.2}$$

where $m_d$ is the mass of TMD and m represents the structural mass.

For multi-degree-of-freedom (m.d.o.f.) structure, M is defined as the modal mass, which is calculated as shown in Equation 2.3,

$$M_i = \varphi_i{}^T m \varphi_i \tag{2. 3}$$

where M is the mass matrix of m.d.o.f. structure, $\varphi_i$ is the modal matrix, and $M_i$ is the modal mass of the $i^{th}$ mode. And $\varphi_i$ shall be scaled as unit 1 at the location of TMD.

According to Den Hartog's method the optimal tuning frequency ratio ($f=\omega_d/\omega_i$) for the TMD system is obtained using Equation 2.4,

$$f = \frac{1}{1+\mu} \tag{2.4}$$

and the optimum damping ratio, $\zeta_{opt}$ of the damper can be obtained as follows:

$$\zeta_{opt} = \sqrt{\frac{3\mu}{8(1+\mu)^3}} \tag{2.5}$$

$$\omega_i{}^2 = k_i / M_i \tag{2.6}$$

Where $\omega_i$ is the frequency of structure, i represents the mode shape number, k is the modal stiffness, and $M_i$ is the modal mass.

After obtaining the optimum tuned frequencies and damping ratios of TMD, dynamic characteristics of TMD as calculates in equation 2.7, 2.8, 2.9 and 2.10. Here, the subscript “d” refers to the TMD.

$$\omega_d = f\,\omega_i \tag{2.7}$$

$$k_d = m_d\omega_d^2 \tag{2.8}$$

$$c_c = 2m_d\omega_d \tag{2.9}$$

$$\frac{c_d}{c_c} = \zeta_{opt} \tag{2.10}$$

Where,

f is the optimum tuning ratio calculated according to each method

$\omega_d$ represents the frequency of TMD

$k_d$ shows the stiffenes of TMD

$c_d$ is the damping of TMD

$c_c$ is the critical damping,

and $\zeta_d$ is taken as the $\zeta_{opt}$ from each calculation methods.

The optimal TMD parameter values obtained using Den Hartog's method for the Izmit Bridge Tower are shown in Table 2.5.

**Table 2.5 :** TMD dynamic characteristics for each tower leg.

| Method | $m_d$ $kNs^2/m$ | μ - | $\alpha_{opt}$ - | $\omega_{tower}$ rad/sec | $\omega_d$ rad/sec | $k_d$ kN/m | $c_c$ kN/m.s | $c_d/c_c$ - | $c_d$ kN/m.s |
|---|---|---|---|---|---|---|---|---|---|
| J.P.Den Hartog | 24 | 0.0074 | 0.993 | 2.362 | 2.35 | 131.99 | 112.57 | 0.052 | 5.86 |

In SAP2000, linear link is used to define TMD in the model and with two joint link draw command. One joint is attached to the structure on desired TMD location and the other joint is free. The TMD mass is attached for the free joint to catch the tuning. In order to assess the suitability of this modeling strategy in capturing the effects of TMDs a simple single degree of freedom (s.d.o.f.) system was modelled as

a trial system. The frequency response curve for this s.d.o.f. model was derived as follows:

1. Define the mass, and the frequency of the s.d.of. system.

2. Define TMD's mass and then use Den Hartog's formulas to define TMD's stiffness and damping to catch the optimum tuning.

3. Make steady-state analyses with different forcing frequency ratios in SAP2000 and get the results for displacement amplitudes at each frequency level. Then graph the amplitude ratios using static deflection.

4. Compute the amplitudes analytically using Equation 2.11 below and graph the amplitude ratios using static deflection.

5. Compare the amplitude ratios

The frequency response curves obtained from the results of SAP2000 analyses is compared with the curve that is obtained using the following analytical relationship proposed for TMDs by Den Hartog (1947):

$$\frac{\chi_1}{\chi_{st}} = \sqrt{\frac{(2\frac{c}{c_c}gf)^2 + (g^2 - f^2)^2}{(2\frac{c}{c_c}gf)^2(g^2 - 1 + \mu g^2)^2 + \left[\mu f^2 g^2 - (g^2 - 1)(g^2 - f^2)\right]^2}} \qquad \textbf{(2.11)}$$

Where;

$\chi_1$ is the displacement of main mass

$\chi_{st}$ is the static deflection of the system

$c_d$ is the damping of TMD

$c_c$ is the critical damping,

g is forced frequency ratio,

f is the optimum frequency ratio.

**Table 2.6 :** Parameters for frequency response curve.

| M | $m_d$ | μ | f | $\omega_m$ | $\omega_d$ | $k_d$ | $c_c$ | $c_d/c_c$ | $c_d$ |
|---|---|---|---|---|---|---|---|---|---|
| $kNs^2/m$ | $kNs^2/m$ | - | - | rad/sec | rad/sec | kN/m | kNm/s | - | kN/m.s |
| 15 | 3.75 | 0.250 | 0.8000 | 69.0000 | 55.2 | 11426 | 414.3 | 0.219 | 90.73 |

In order to investigate the suitability of the utilized TMD modeling stragety, a simple single degree of freedom (SDOF) model was modelled in SAP2000 as an initial trial application. Using the given parameters listed in Table 2.6, the results presented Figure 2.15 are obtained for the simple SDOF model. The good agreement in between the finite-element model results and the analytically calculated values confirms that the utilized modeling strategy is properly representing the effects of TMD on the dynamic response. In Figure 2.15 and Figure 2.16 ω is the frequency of the harmonic force and $\omega_m$ is frequency of the main structure.

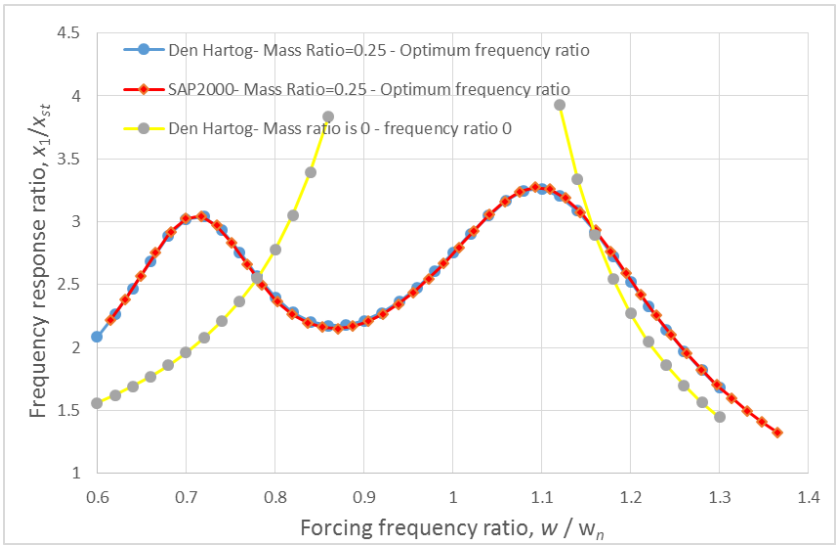


**Figure 2.16:** Frequency response curves comparison for s.d.o.f. model

Figure 2.15 proves that TMD modeling approach adopted for the SAP2000 model is properly capturing the expected behavior. Blue series in Figure 2.16 was obtained using Equation 2.11 proposed by Den Hartog (1947) and the red series was obtained using SAP2000 by exciting the s.d.o.f. model with harmonic loading. Yellow series represent the case with no TMD. This series is obtained using the analytical expression by Den Hartog (1947).

Equation 2.11 is an efficient way to check the TMDs effect in mitigation vibrations of the structure under harmonic loading. In addition, it is useful in assessing whether

the damper modeling approach implemented in the software is reproducing the expected behavior or not.

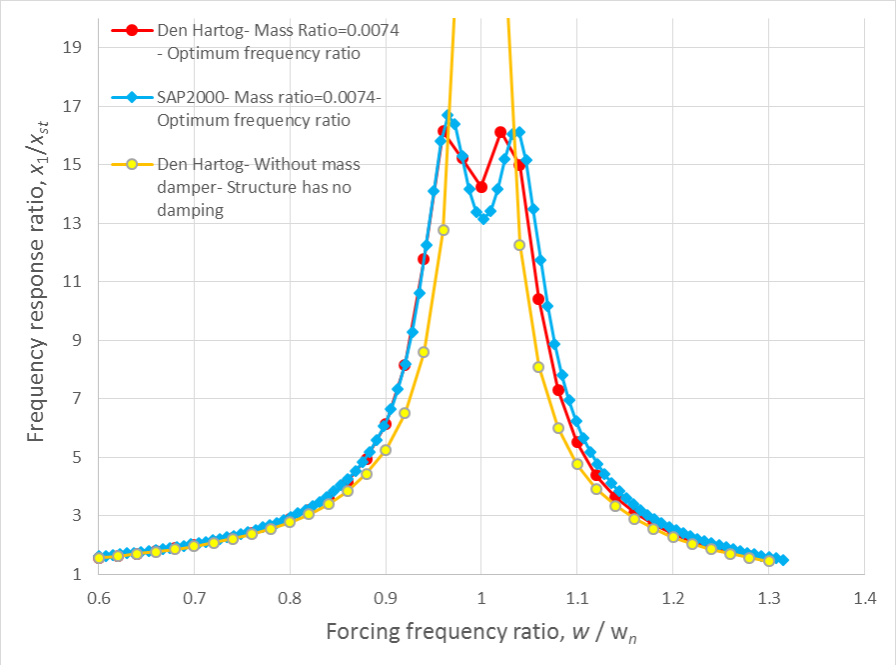


**Figure 2.17:** Frequency response curves comparison for tower.

In Figure 2.16 frequency response curves of tower is presented. As it is seen that, yellow series represent the case with no TMD, which the resonance condition is seen when the forcing frequency ratio is 1. The red line was obtained using Equation 2.11 by substituting the optimal dynamic characteristics of TMDs calculated for the Izmit Bridge Tower. The blue series was derived by using the SAP2000 software.

## 3. SEISMIC FRAGILITY CURVES

According to Nielson and DesRoches (2007), " Seismic fragility curves for highway bridges are conditional probability statements about the vulnerability a bridge possesses to seismic loading'' (p.1). In typical expressions, vulnerability means the function of the reparability the damage of the bridge (Nielson and DesRoches, 2007).

For a given ground motion and dynamic structural analysis result, the occurrence or nonoccurrence of collapse can be defined in a number of ways (Zareian and Krawinkler 2007). In this study, non-linear time history analysis is performed considering second order effect, in order to determine the demand imposed on the structure by each ground motion. Twelve ground motion records are chosen for the analysis. For each ground motion, spectral acceleration at the period corresponding to first mode of vibration, is increased with a factor till the demand becomes greater than capacity of the tower.

Fragility curve is defined using Equation 3.1.

$$P(C \mid Sa = x) = \varphi\left(\frac{\ln x - \eta}{\beta}\right) \qquad \textbf{(3.1)}$$

P(C\Sa=x) is the probability of collapse for the case when the spectral acceleration, *Sa* of the ground motion is equal to $x$ . In the equation above, φ( ) is the normal cumulative distribution function, η and β are the mean and standard deviation of ln Sa (Baker J.W., 2015).

### 3.1 Nonlinear Time History Analysis

In this study, Newmark's average acceleration method is chosen for nonlinear time history analysis. For any given ground motion record, according to time-displacement, time- velocity, time- acceleration graphs can be obtained. There are two Newmark's Methods that most commonly used one is constant average acceleration method, and the other is the linear acceleration method (Chopra, 2012).

The assumptions regarding time variation of acceleration is the key difference between the two methods. For the constant average acceleration method, constants are $\boldsymbol{\gamma = \frac{1}{2}, \theta = \frac{1}{4}}$ and for the linear acceleration method $\boldsymbol{\gamma = \frac{1}{2}, \theta = \frac{1}{6}}$. Although both methods are having accurate results, linear acceleration method is not stable if the time interval is less than 0.551 of governed period. Therefore, average acceleration method is applied since it is more reliable for all periods.

Average constant Newmark method formulas are shown in Chopra (2012, p.690)

### 3.2 Load Combinations for Analysis

In this study, the North tower of Izmit Bay Suspension Bridge is analyzed. Since the tower is effected by main span side cable and side span side cable, both loads must be considered accordingly. Cable axial loads for load combinations are calculated for the points are shown in Figure 3.1.

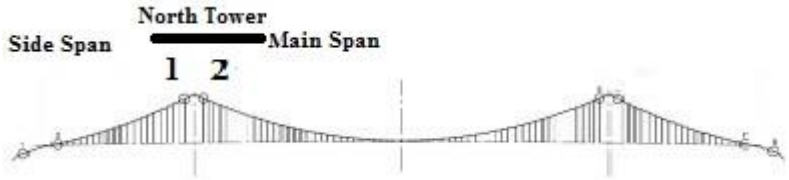


**Figure 3.1:** Key points for loading.

Non-linear analysis considers the large displacements, therefore vertical load coming from the cables should be carefully estimated. Table 3.1 shows the normal force on the points shown Figure 3.1

**Table 3.1 :** Normal forces for cable on key point 1 and 2.

| | Load Participation Factor | 1 MN | 2 MN |
|---|---|---|---|
| Dead Load | 1 | 154.07 | 150.27 |
| Super imposed dead load | 1 | 37.04 | 36.17 |
| Traffic-tandem system | 1 | 0.93 | 0.99 |
| Traffic-UDL | 1 | 62.86 | 62.56 |
| Wind-static mean wind | 1 | 1.71 | 1.72 |
| Load | - | 256.61 | 251.70 |

When estimating the load case, the important thing is to identify the most realistic scenario for the loads during ground motion. Therefore, load participation factors are set as 1. Figure 3.2 shows the forces at north tower top by cable.

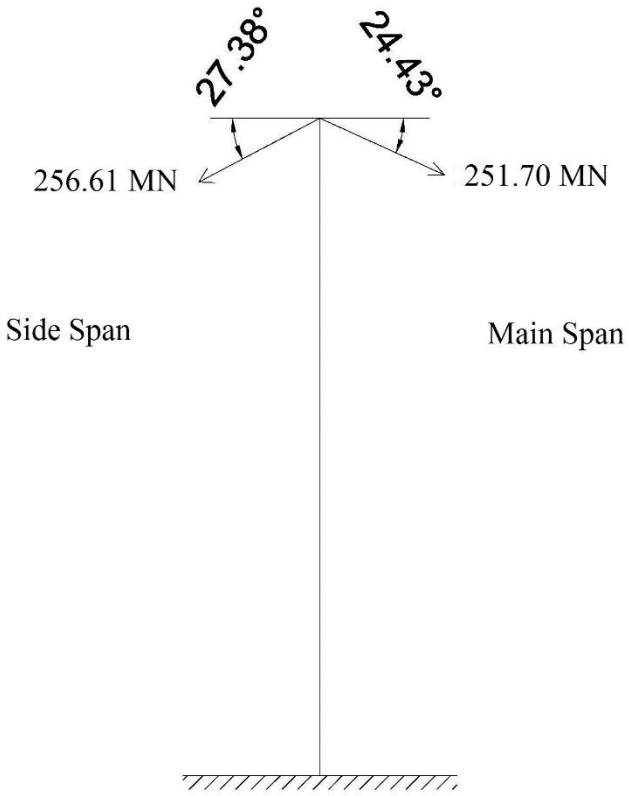


**Figure 3.2:** Cable loads on tower top.

Cable forces are taken from full-scale bridge analysis performed by the designer of Izmit Bay Suspension Bridge (Izmit Bay Bridge Detailed Design, 2012b). Cable forces are investigated in detail, because for the large displacements there will be great stress impact due to bending moment caused by eccentricity. Considering the slenderness of the tower, the additional moment due to eccentricity may cause failures. Also according to modal analysis, J14 makes the biggest modal displacement, therefore one of the critical joint due to moment caused by eccentricity is joint 14. This situation is taken care by using second order effect during analysis in the software. Figure 3.3 shows the 1$^{st}$ out of plane bending mode shape under vertical component of cable load.

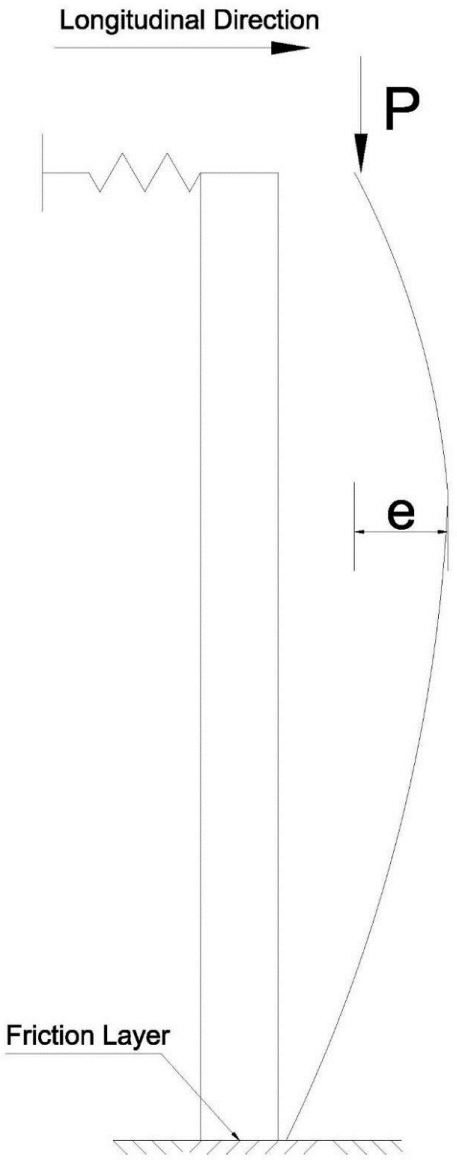


**Figure 3.3:** 1st out of plane bending mode shape under vertical load.

Vertical forces come from the cable are easily calculated using the cable angle. Table 3.2 shows the cable forces at the tower top.

**Table 3.2 :** Cable loads at the top of the tower.

| Points | Angle Degree | Axial Force(N) (MN) | Horizontal Force(H) (MN) | Vertical Force(V) (MN) |
|---|---|---|---|---|
| 1 | 27.38° | 256.61 | 227.87 | 118.01 |
| 2 | 24.43° | 251.70 | 223.50 | 115.75 |

Points of the positions are defined in figure 3.1.

### 3.3 Ground Motion Records

Twelve ground motion records are used in the non-linear time history analysis. Ground motion records are chosen according to soil condition of the site. The average shear-wave velocity in the first 30 m of subsoil in the site area is around 250 m/s. Since it has a great effect whether the soil is rock or clay, the recorded acceleration caused by this earthquake shall be different in those areas. Large magnitude earthquakes' data are used in condition that, these data are recorded in a similar soil around the bridge tower foundation. Thus, the target is to perform the analysis under seismic loads, which is estimated to be likely to be excited the bridge during its service life.

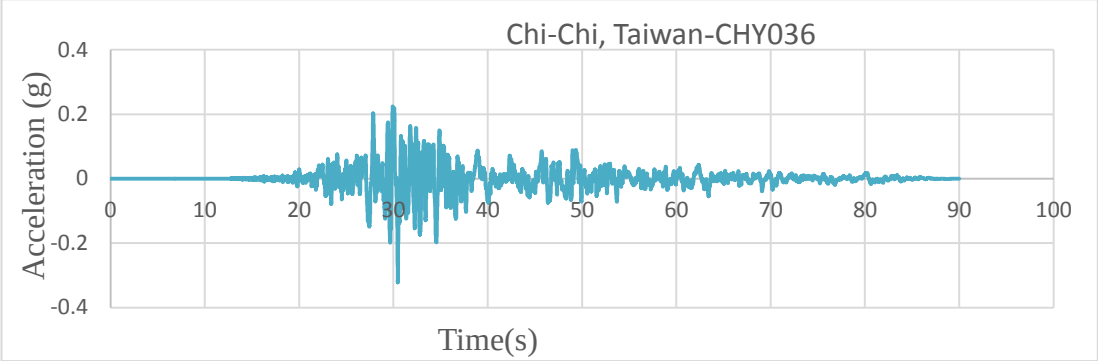


**Figure 3.4a:** Ground motion record 1.

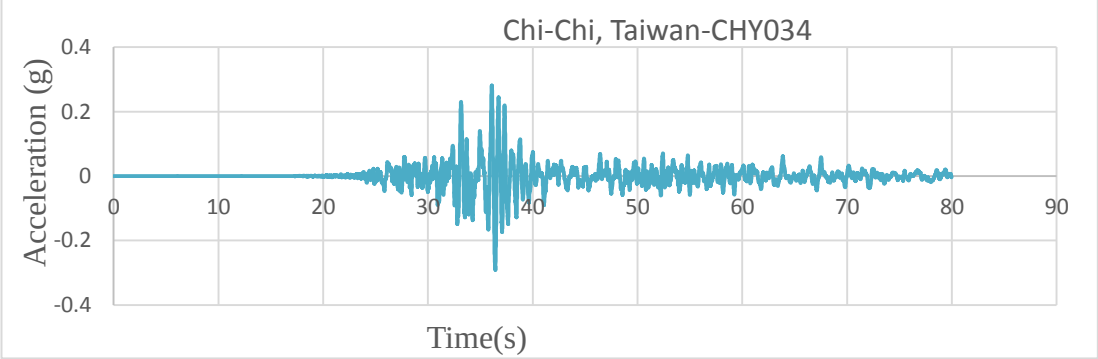


**Figure 3.4b:** Ground motion record 2.

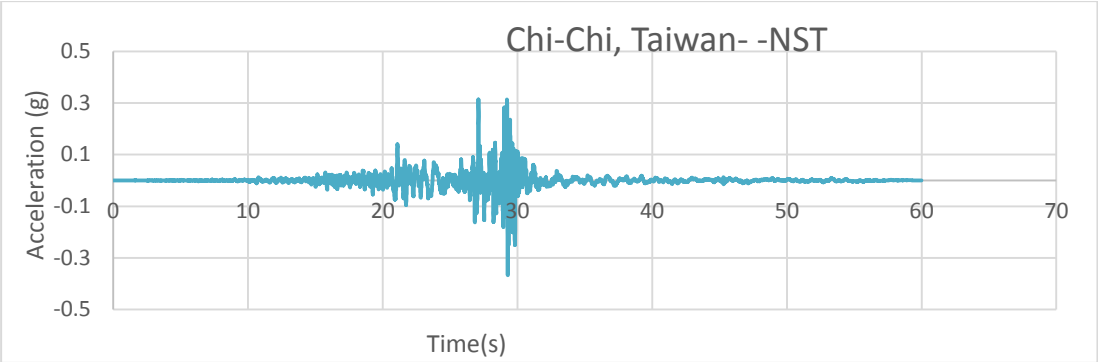


**Figure 3.4c:** Ground motion record 3.

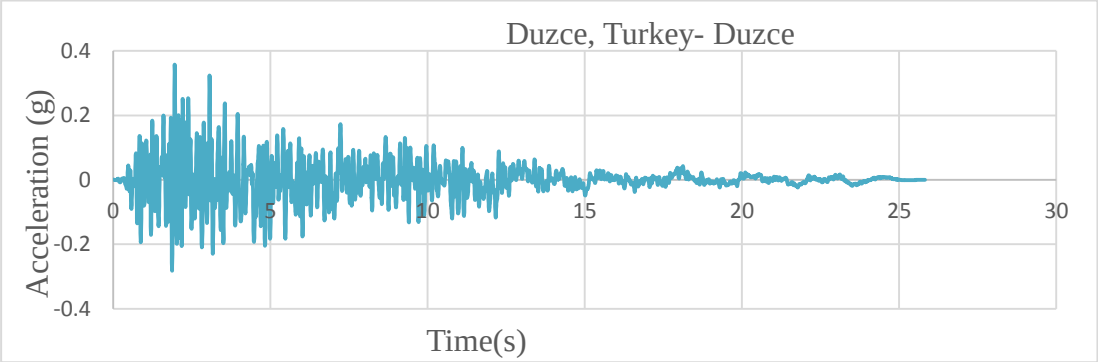


**Figure 3.4d:** Ground motion record 4.

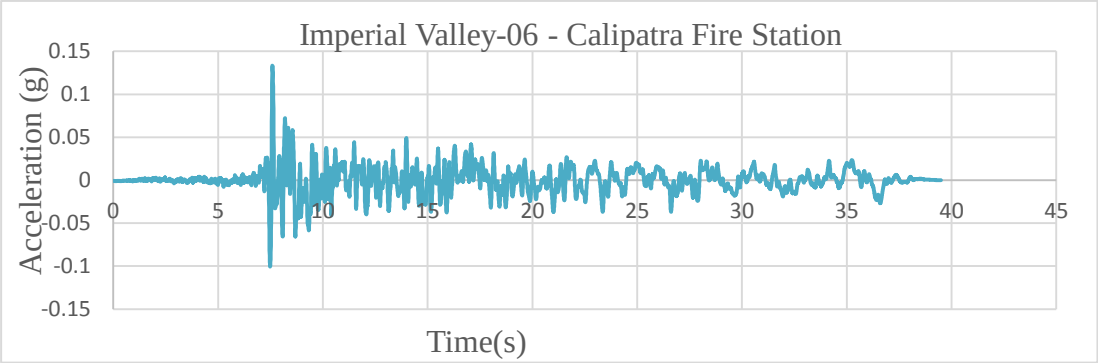


**Figure 3.4e:** Ground motion record 5.

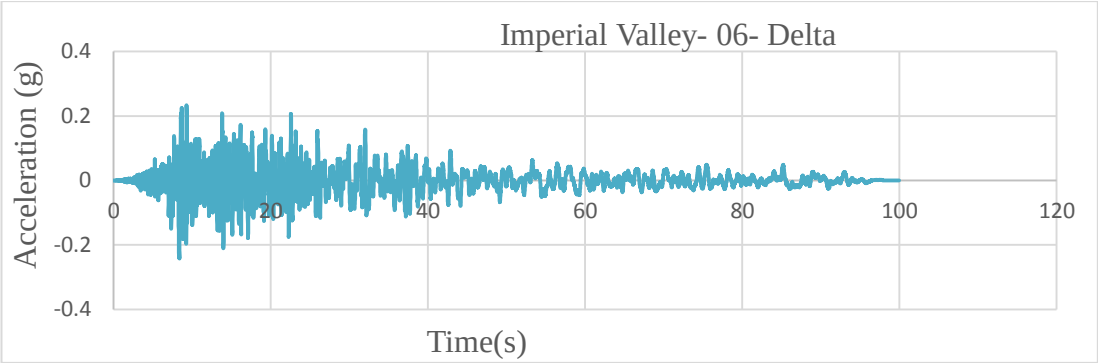


**Figure 3.4f:** Ground motion record 6.

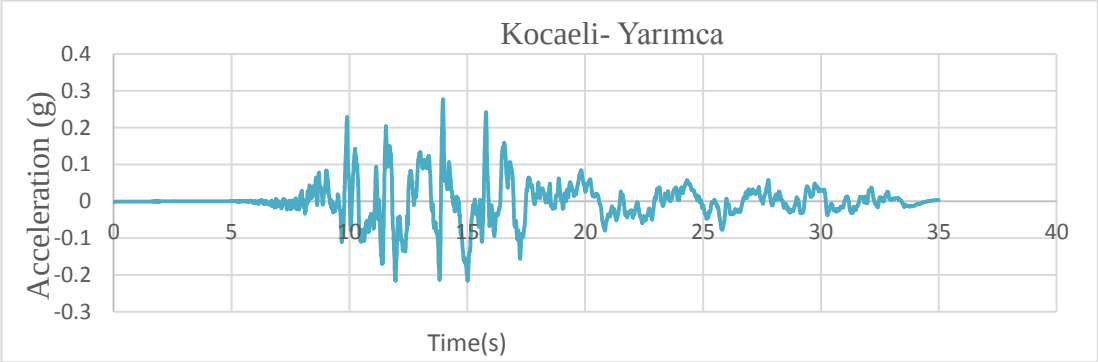


**Figure 3.4g:** Ground motion record 7.

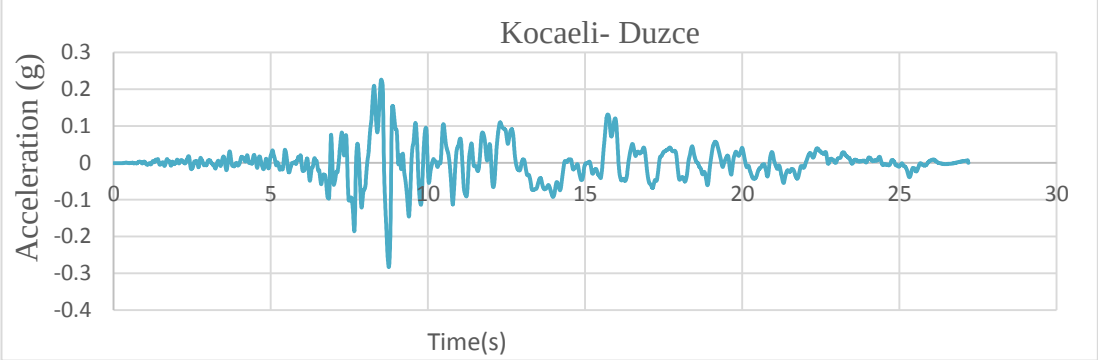


**Figure 3.4h:** Ground motion record 8.

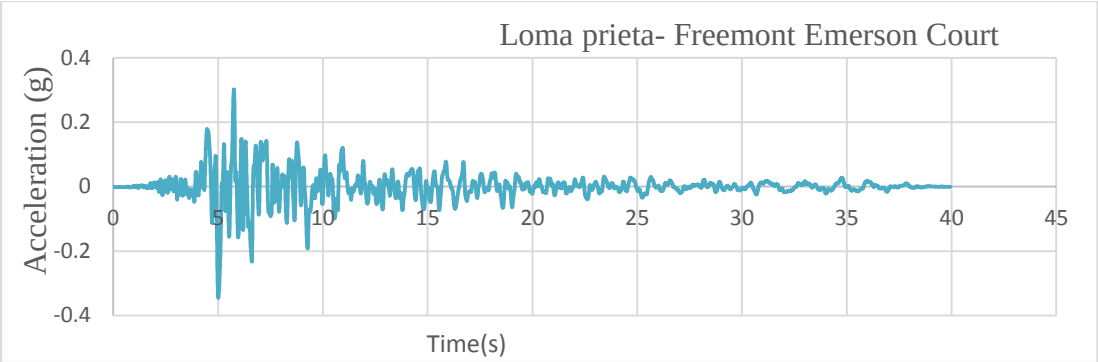


**Figure 3.4i:** Ground motion record 9.

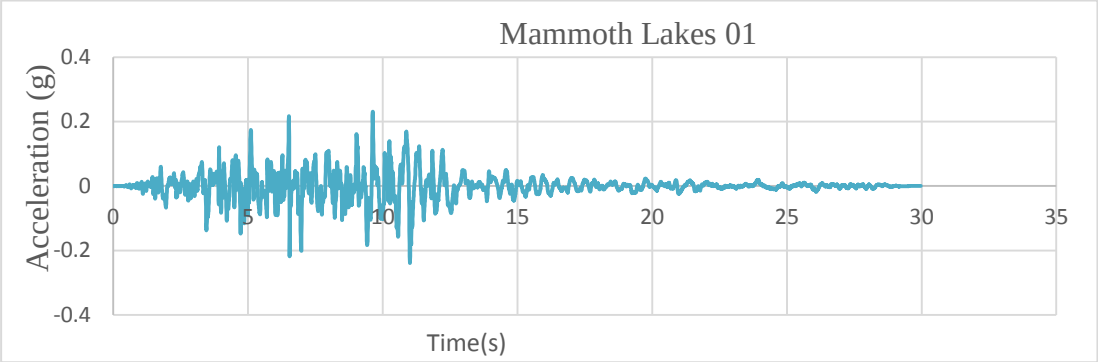


**Figure 3.4j:** Ground motion record 10.

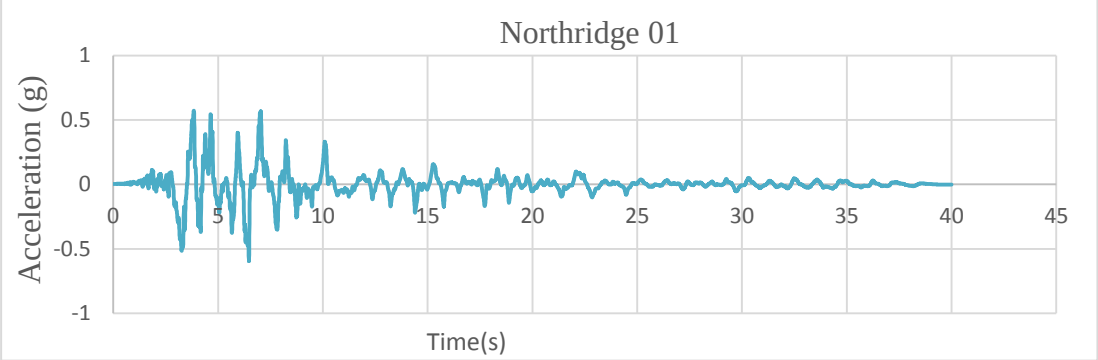


**Figure 3.4k:** Ground motion record 11.

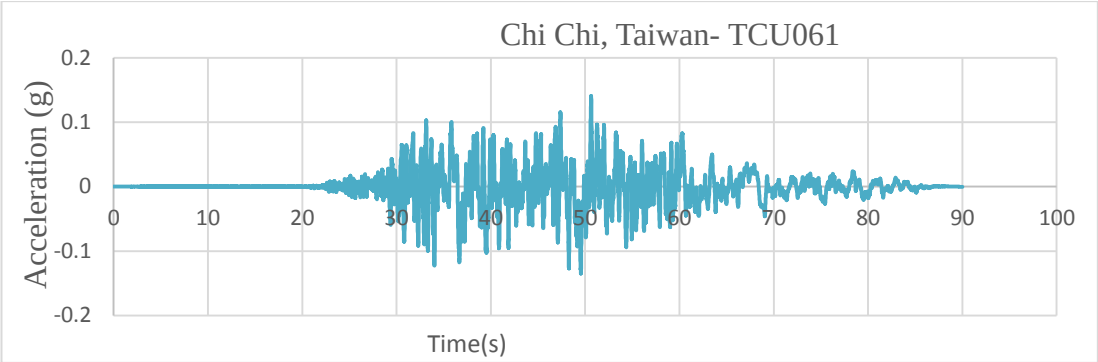


**Figure 3.4l:** Ground motion record 12.

Figure 3.3a to Figure 3.3l show the twelve ground motion records, which are used for non-linear seismic analysis (Baker et. al, 2015). The summary data for the selected ground motion records are listed in Table 3.3.

**Table 3.3 :** Basic summary data for chosen ground motion records (Baker et. al, 2015).

| Record Number | Earthquake Name | Year | Station | Magnitude | Closest Distance | Preferred Vs30(m/s) |
|---|---|---|---|---|---|---|
| 1 | Chi-Chi,Taiwan | 1999 | CHY036 | 7.6 | 16.1 | 233 |
| 2 | Chi-Chi, Taiwan | 1999 | CHY034 | 7.6 | 14.8 | 379 |
| 3 | Chi-Chi, Taiwan | 1999 | NST | 7.6 | 38.4 | 375 |
| 4 | Duzce, Turkey | 1999 | Duzce | 7.1 | 6.6 | 276 |
| 5 | Imperial Valley-06 | 1979 | Calipatria Fire Station | 6.5 | 24.6 | 206 |
| 6 | Imperial Valley-06 | 1979 | Delta | 6.5 | 22 | 275 |
| 7 | Kocaeli, Turkey | 1999 | Yarimca | 7.5 | 4.8 | 297 |
| 8 | Kocaeli, Turkey | 1999 | Duzce | 7.5 | 15.4 | 276 |
| 9 | Loma Prieta | 1989 | Fremont- Emerson Court | 6.9 | 39.9 | 285 |
| 10 | Mammoth, Lakes-01 | 1980 | Long Valley Dam(Upr L Abut) | 6.1 | 15.5 | 345 |
| 11 | Northridge-01 | 1994 | Sylmar Converter Sta | 6.7 | 5.4 | 251 |
| 12 | Chi-Chi, Taiwan | 1999 | TCU061 | 7.6 | 17.2 | 273 |

**Table 3.4 :** Spectral accelerations.

| | $Sa(T_1=2.64\ s)$ $m/s^2$ | $\alpha_1$ - | $\alpha_1 Sa\ (T_1=2.64\ s)$ $m/s^2$ |
|---|---|---|---|
| G. Motion 1 | 1.10 | 5.45 | 6 |
| G. Motion 2 | 0.85 | 7.04 | 6 |
| G. Motion 3 | 1.55 | 3.87 | 6 |
| G. Motion 4 | 2.36 | 2.54 | 6 |
| G. Motion 5 | 0.54 | 11.11 | 6 |
| G. Motion 6 | 2.04 | 2.94 | 6 |
| G. Motion 7 | 2.74 | 2.19 | 6 |
| G. Motion 8 | 1.39 | 4.32 | 6 |
| G. Motion 9 | 0.95 | 6.32 | 6 |
| G. Motion 10 | 0.79 | 7.58 | 6 |
| G. Motion 11 | 7.94 | 0.76 | 6 |
| G. Motion 12 | 1.26 | 4.77 | 6 |

Table 3.4 shows the spectral acceleration values for the 1st longitudinal mode shape period. Spectral acceleration graphs are shown in Appendix A-3.

On the second column of Table 3.4, the spectral acceleration of each ground motion, are listed. Our aim is to set all the spectral accelerations as equal. 6 $m/s^2$ is just a symbolic one, 8 $m/s^2$ or 10 $m/s^2$ can also be choosen. The purpose is after setting equal all the spectral accelerations, another magnification factor is used to check the structures fragility under some spectral acceleration range. The critical point is, it is not easy to define the spectral acceleration range at the first step. In order to handle this problem, some trials might be done considering the limit cases, because it is not a solution that if all the results are fail in the range or if there is no fail in the range.

### 3.4 Limit Cases

Failure cases of the tower were investigated in order to obtain seismic fragility curves. The largest displacements for the tower are observed at the first longitudinal mode shape of tower, since tower acts like a beam, fixed at the bottom and hinged supported at the top. The failure of the tower is assumed to take place when the steel starts yielding.

According to Gimsing and Georgakis (2012), " The seismic design loads for large cable supported bridges will differ from those of ordinary structures, as they should not only avoid collapse, but also continue to serve as vital transportation links after a

large earthquake''. Since suspension bridges are special structures, no collapse earthquake mean return period is defined as 2475 years.

Fragility curve is a probabilistic method to define vulnerability of the structure; therefore elastic section modulus is used in order not to increase the capacity of the section but to make it close to actual behavior. Figure 3.5 shows the failure case of the tower under vertical load during vibration caused by ground motion.

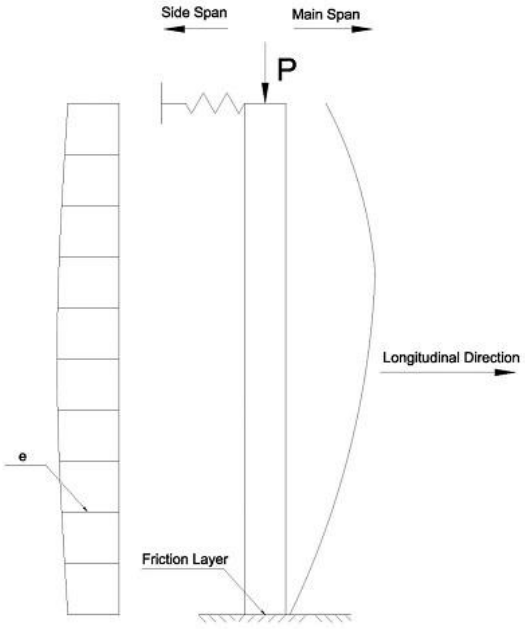


**Figure 3.5:** Eccentricity caused by ground motions.

$$\sigma_{demand} \geq \sigma_{capacity} \qquad \textbf{(3.2)}$$

Equation 3.2 defines the normal stress demand caused by the ground motion. When the demanded stress becomes greater than the stress capacity of the section, failure shall be observed. Where P is the axial load that comes from cable, e is the eccentricity caused by ground motion, Me is the moment caused by ground motion, $W_e$ is the elastic section modulus and A is the cross-sectional area.

In this study it is assumed that greatest stress demands occur in the direction normal to the section. Slenderness of the tower supports this assumption. In reality, the yielding would be controlled by the principal stresses. Depending on the level of shear force acting on the component, direction and magnitude of the principal stresses may deviate from the direction of the normal stress. However, evaluation of

principal stresses would not be feasible with the frame element based FE model considered in this study. Shell or solid finite element based models would be needed instead.

To define the capacity of tower, test results for S460 material used for Izmit Bay Suspension Bridge towers. Figure 3.6 shows the results for 50 randomly selected material tests from the tower's steel. According to test results, $\sigma_{y,mean}$=448 Mpa and $\sigma_{u,mean}$=573 Mpa are identified for the S460 material.

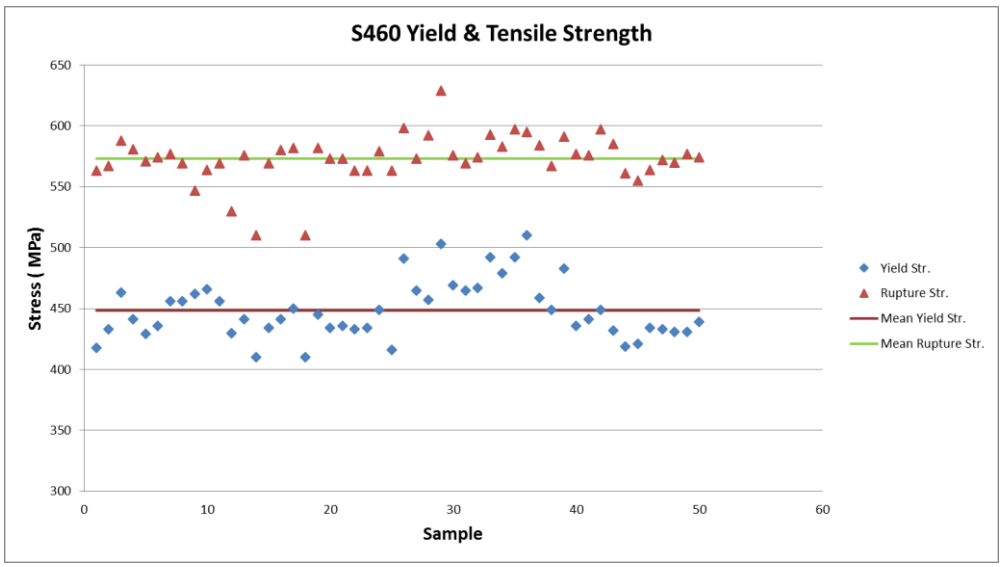


**Figure 3.6:** Test results for S460 materials used for Izmit Bay Bridge Tower.

Table 3.5 shows the minimum yielding stresses for S460 steel regarding the material thickness, these data are taken from EN 100025.3 (2004). The tower steel material thickness are between the 36 mm to 110 mm, therefore σy,mean=448 Mpa is a suitable value. The minimum yielding stress shown in the Figure 3.6 is belonged to 110 mm thickness S460 steel.

**Table 3.5 :** Minimum yielding stress of S460 steel according to EN 10025:3 (2004).

| Thickness | σy (Mpa) |
|---|---|
| up to 16 mm | 460 min |
| 16 to 40 mm | 440 min |
| over 40 to 63 mm | 430 min |
| over 63 to 80 mm | 410 min |
| over 80 to 100 mm | 400 min |
| over 100 to 150 mm | 380 min |
| over 150 to 200 mm | 370 min |

### 3.5 Seismic Fragility Curves

Seismic fragility curves are derived considering the stress demands imposed at all levels of the tower. For this purpose, stress level versus height graphs are prepared. As explained before, it is expected to see the failure due to large displacements. To derive the seismic fragility curves, non-linear time history analyses were performed. The resulting stress graphs are shown in Figure 3.7 and 3.8 for all ground motion records. In order to make a comparison, there are two graphs to compare, Figure 3.7 represent the stresses considering the TMD, Figure 3.8 represent the condition without TMD, and also the results are taken from the scaled ground motion records, spectral acceleration is adjusted to 9m/s$^2$.

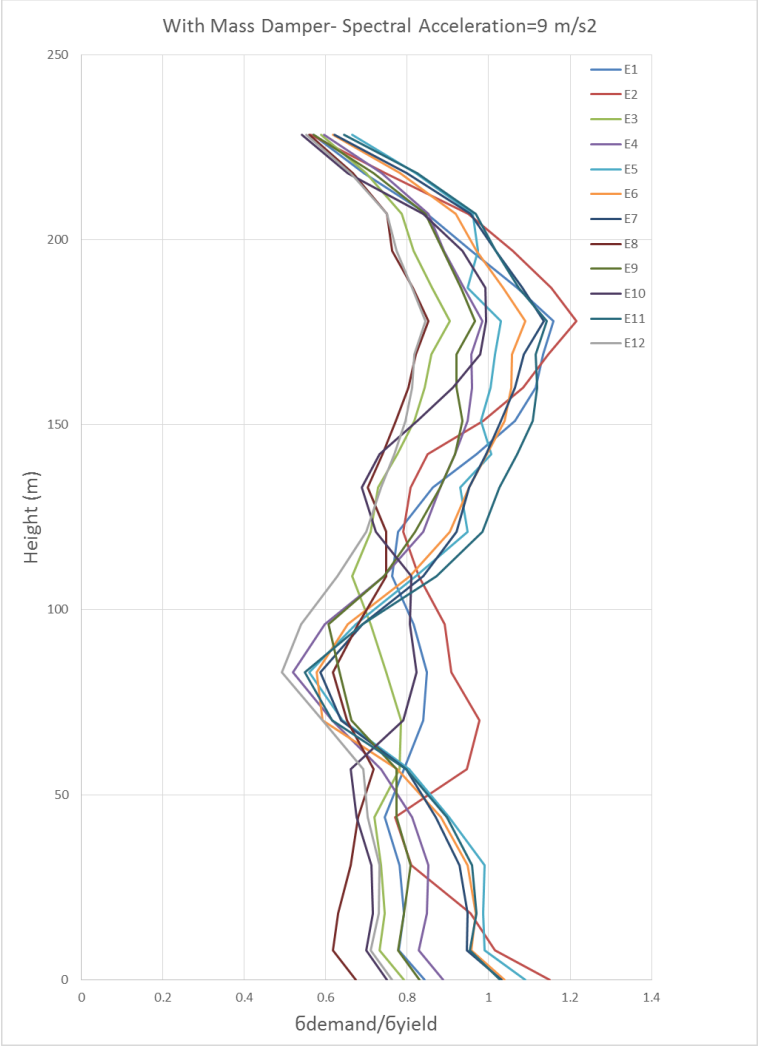


**Figure 3.7:** Stress graph for spectral acceleration 9 m/s$^2$ - with TMD- $\sigma_{y,mean}$=448 Mpa.

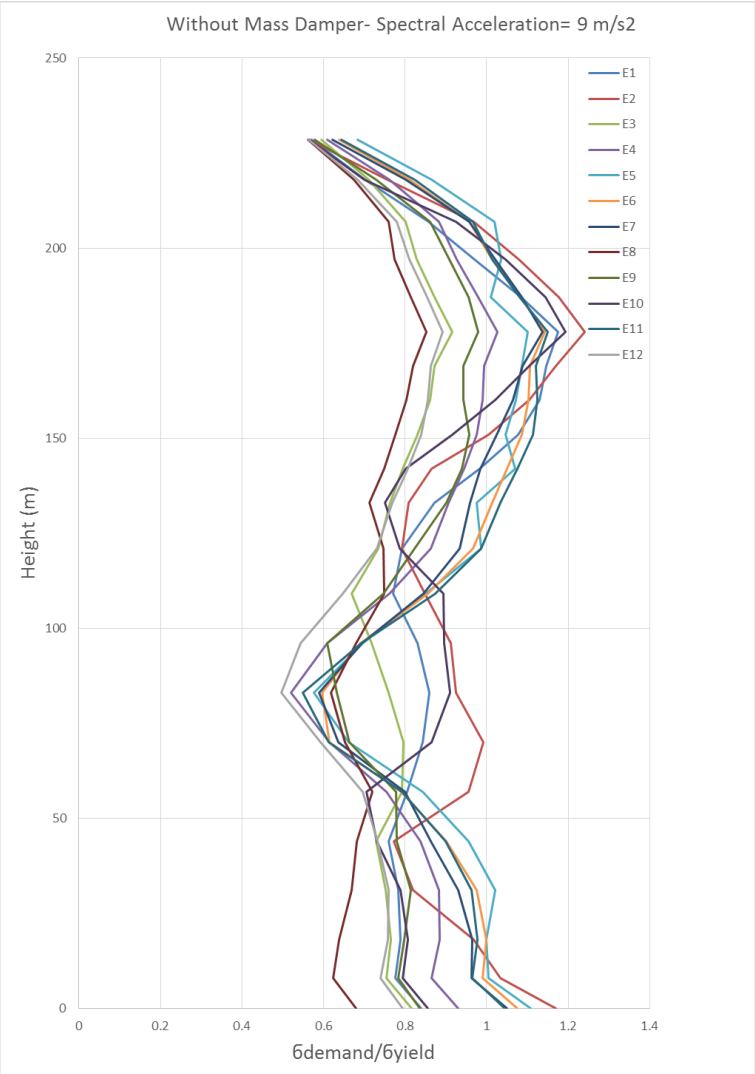


**Figure 3.8:** Stress graph for spectral acceleration 9 m/s$^2$ - without TMD- $\sigma_{y,mean}$=448 Mpa.

Stress graphs are prepared for spectral accelerations between 6 m/s$^2$ to 15 m/s$^2$. As explained before, the limit case is the yielding of steel material. The stress graphs are compared with $\sigma_{y,mean}$=448 Mpa, if any point of the structure starts yielding, we assume that structure fails. It is not suitable to compare the results with $\sigma_{u,mean}$=573 Mpa, because material nonlinearity is disregarded during the analysis. The other stress graphs are shown in Appendix A-1.

A comparison of the seismic fragility curve graphs for the two models is shown in Figure 3.9.

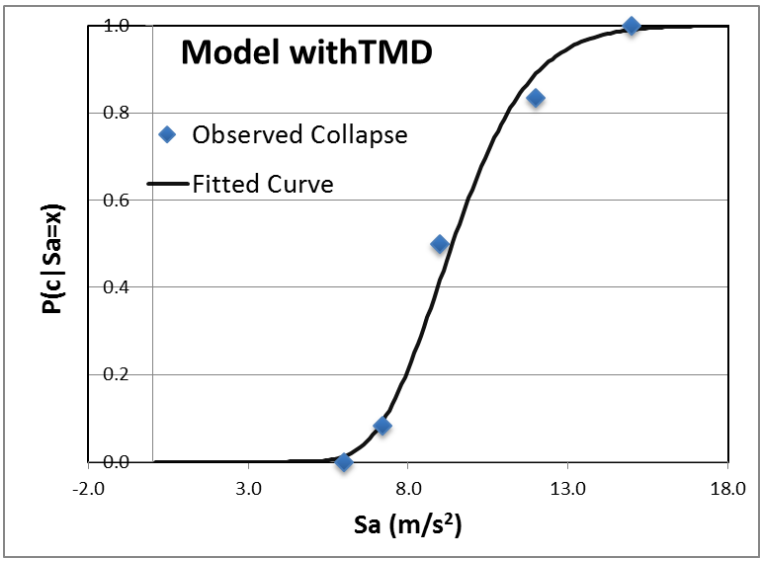


**Figure 3.9:** Seismic fragility curve for the model with TMD.

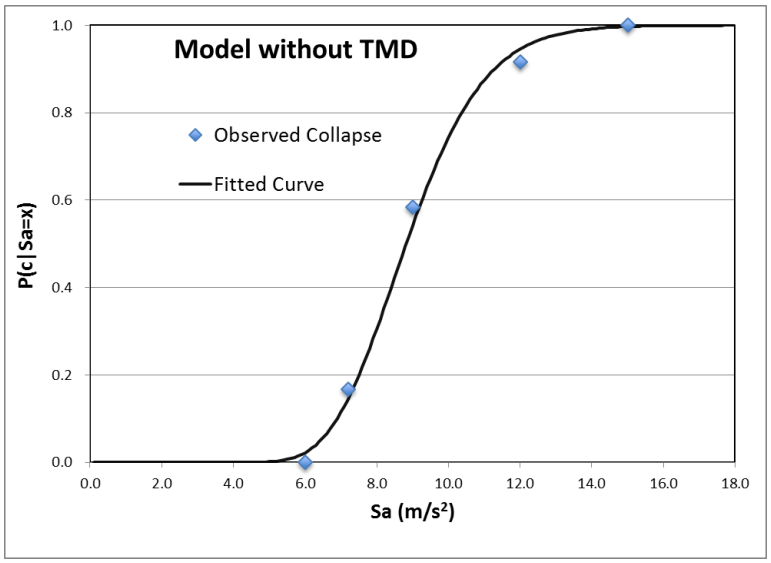


**Figure 3.10:** Seismic fragility curve for the model without TMD.

# 4. CONCLUSIONS AND RECOMMENDATIONS

In this study, seismic performance of suspension bridge towers is investigated by comparing the seismic fragility curves obtained for the cases with TMD and without TMD. It is observed from the analysis results that, TMDs' are quiet effective for controlling the structure vibration, and TMDs' are quiet effective to increase the structure damping. Also despite modelling the tower bottom as friction, no sliding is observed before tower starts yielding for the finite-element model utilized in this thesis and at the considered acceleration levels, no sliding was observed in the friction isolator at the base of the tower.

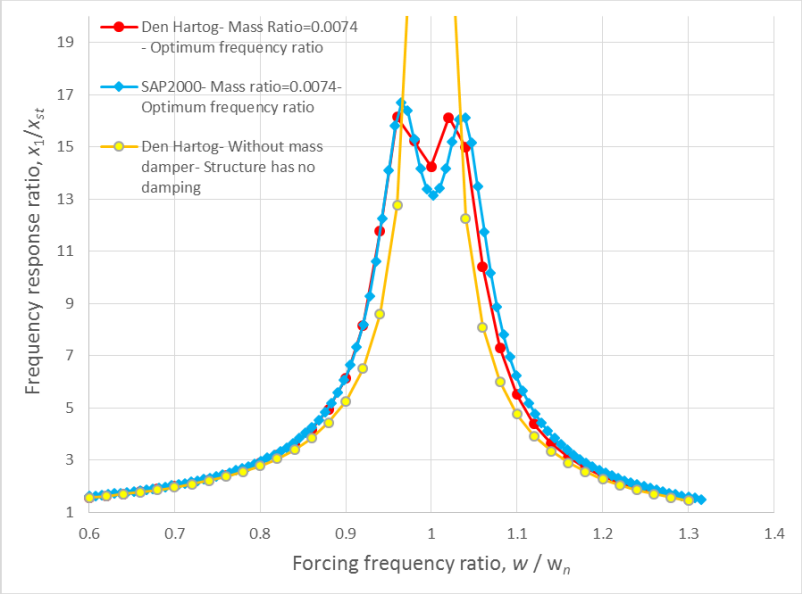


**Figure 4.1:** Frequency response curves comparison for tower.

Figure 4.1 shows the tower frequency response graph and Figure 4.2 shows the non-linear time history analysis results for the ground motion 1, both for the model with TMD and for the model without TMD. The displacements are shown in Figure 4.2 belong to J14, which mass dampers are located and where the biggest modal displacements is observed, and this graphs shows the results for non-scaled ground motion records. Also in Figure 4.2, it is seen that J14 displacement is not starting from zero, the initial deformation caused by dead loads. For the other non-linear time history analysis result graphs, Appendix-A2 can be seen. In Figure 4.3, seismic

fragility comparison is shown to understand the probability of failure with two conditions, one with TMD, one without TMD.

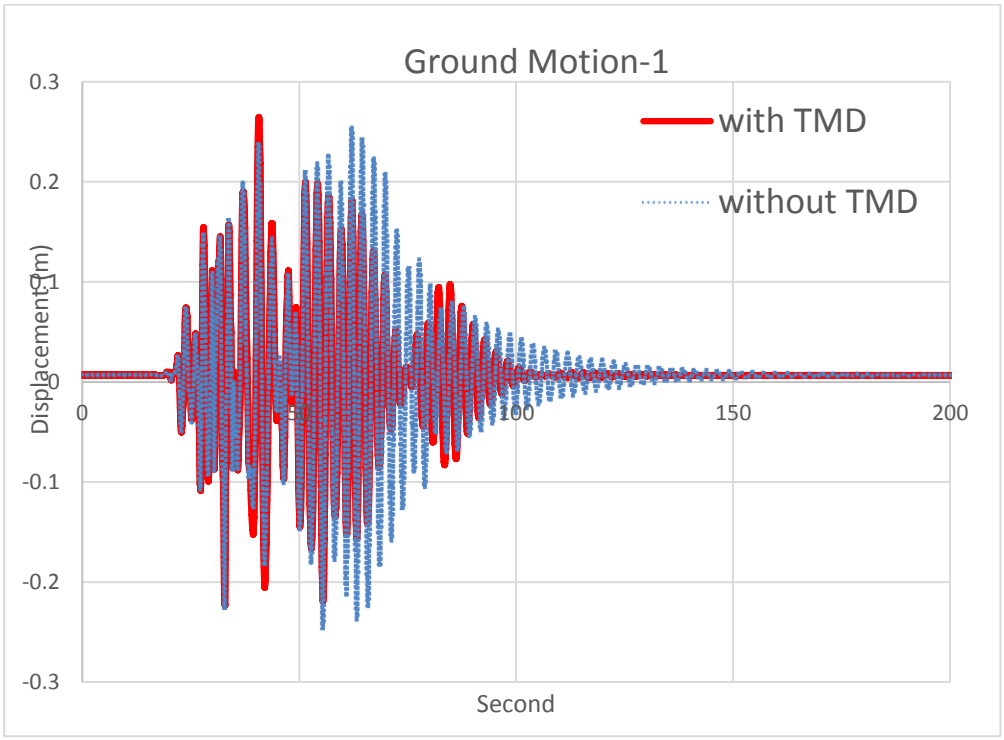


**Figure 4.2:** Time history results comparison for ground motion-1.

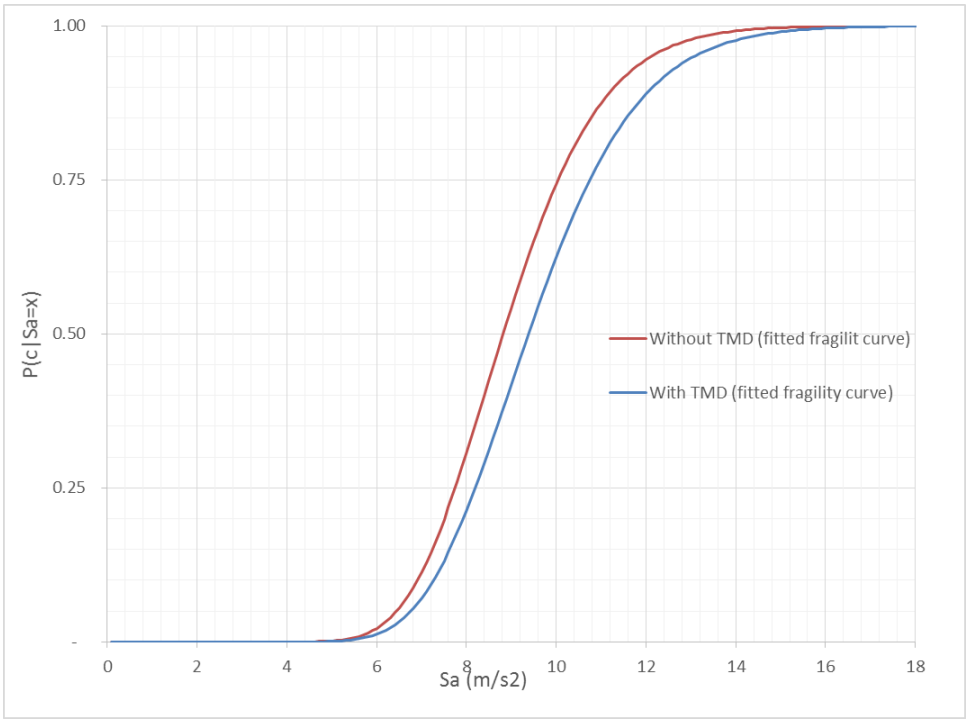


**Figure 4.3:** Seismic fragility curves comparison graph.

The benefits of TMD is listed below after evaluating the Figure 4.1, Figure 4.2 and Figure 4.3,

- Maximum displacements are reduced,
- Structure mitigates the vibration much faster,

As explained, instead of TMD, AMD is used in the actual Izmit Bay Suspension Bridge, and AMD is designed not to work during seismic events. Since the ground motions are consist of many seismic waves, AMD cannot perform damping, because while AMD is trying to mitigate the one seismic wave, it shall support the other seismic waves of ground motion, therefore it shuts itself down during ground motion. The same situation can be observed also for the TMD as well. After ground motion ends, AMD starts working again to mitigate the vibration.

Analysis results of the model without TMD can be considered a close approximation to the actual tower behavior, since AMD will not work during earthquake. Which means, this study also investigates a case similar to the actual behavior of Izmit Bay Bridge during ground motion (with the locked AMD except with the additional mass of AMD).

Seismic design requirements for the Izmit Bay Suspension Bridge are listed below (Izmit Bay Bridge Detailed Design, 2012b);

- No damage shall be observed for the ground motion return period of 150 years,
- Repairable damage shall be observed for the ground motion return period of 1000 years,
- No collapse shall be seen for the ground motion return period of 2475 years.

In Figure 4.4, annual hazard curves at different structural periods at north tower location is shown. According to Figure 4.4, spectral acceleration corresponding to period of 3 seconds for 1000 year return period earthquake is 0.5g, 4.9 $m/s^2$. Using the fragility curves developed within this thesis study, the likelihood of yielding for

the model with TMD, at the spectral acceleration of 0.5g is found to be equal to 0.031%. On the other hand, for the model without TMD the corresponding likelihood is equal to 0.049%. This indicates that the likelihood of yielding for the 1000 mean return period seismic event is decreased by a factor of 1.58 due to TMD effect.

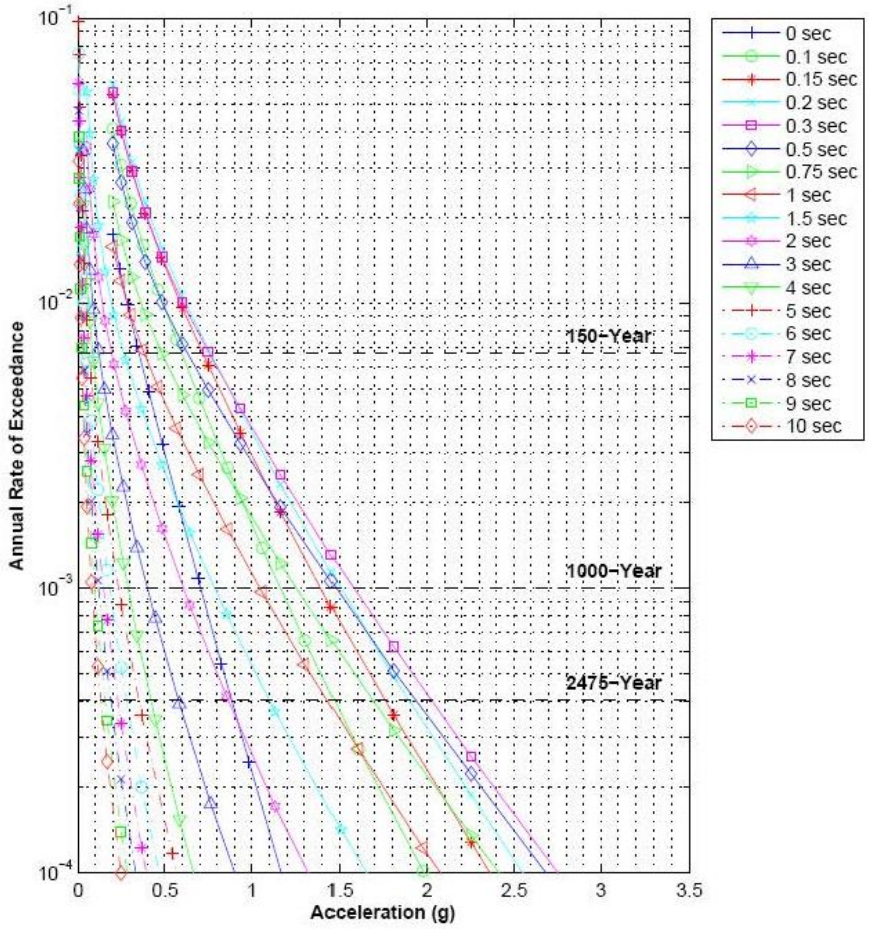


**Figure 4.4:** Annual hazard curves (Fugro, 2011).

Median capacity at yielding limit is 0.96g for the model with TMD and for the model without TMD corresponding capacity is 0.9g. Based on these results, it can be concluded that the median capacity against yielding is 7% higher for the model with TMD compared to that without TMD.

As a result of this study, tuned mass dampers are necessary and practical solutions to control the vibration of structure imposed by ground motion and wind. In addition, they are effective for large and for small displacements. In this study, benefits of mass dampers at various ground motion levels are investigated.

Designer should identify the optimal and suitable solution, since especially for suspension bridge towers, the location of mass dampers are very important. It may not be possible to use mass damper with high mass ratio. But, despite such low mass ratio between main structure and mass dampers, the benefits of mass dampers can be observed again.

## REFERENCES


**Abdel-Ghaffar, A.M.**(1976). Dynamic analysis of suspension bridge structures. Technical Report 76-01, California Institute of Technology, Earthquake Engineering Research Laboratory, College of Engineering, Passadena, CA.

**Abdel-Ghaffar, A.M., and Housner, G.W.** (1977). An analysis of the dynamic characteristics of a suspension bridge by ambient vibration measurements. Technical Report 77-01, California Institute of Technology, Earthquake Engineering Research Laboratory, College of Engineering, Passadena, CA.

**Abdel-Ghaffar, A.M. and G. W. Housner.** (1978), Ambient Vibration Tests of a Suspension Bridge. Journal of Engineering Mechanics, ASCE, 104(EM5):983 999, October 1978.

**Abdel-Ghaffar, A.M., Scanlan, R.H., and Rubin, L.I.** (1983). Earthquake response of long-span suspension bridges. Technical Report 83-SM-13, Princeton University, Civil Engineering Department, Princeton, NJ.

**As Built Construction of Izmit Bay Bridge Tower**. (2015). IHI.

**Bryant G. Nielson and Reginald DesRoches.** (2006), Seismic fragility methodology for highway bridges using a component level approach. Earthquake Engng Struct. Dyn. 2007; 36:823–839.

**Baker, J.W.** (2015). "Efficient analytical fragility function fitting using dynamic structural analysis." Earthquake Spectra, 31(1), 579-599.

**Baker Jack, Nirmal Jayaram, and Shrey Shahi.** Ground Motion Studies for Transportation Systems. Transportation Systems Research Program. Pacific Earthquake Engineering Research Center. Web. 2 Apr. 2015. <http://peer.berkeley.edu/transportation/projects/ground-motion-studies-for-transportation-systems/>.

**Chopra, A.** (2012). Dynamics of Strucures (4th ed.). Prentice Hall.

**Christensen, S.** (2013). Izmit Bay Suspension Bridge, Global Analyses Incorporating Local Sub Models. In IABSE 2013.

**COWI.** General Design Drawings-IZMIT BAY SUSPENSION BRIDGE IZMIT-COW-DD-DWG-TWR (2011a).

**COWI.** Tower Design Drawings-IZMIT BAY SUSPENSION BRIDGE IZMIT-COW-DD-DWG-TWR (2011b).

**Den Hartog, J.P.** (1947), Mechanical vibrations. McGraw-Hill, New York, 3rd ed.

**Ed. Niels J. Gimsing, Georgakis, Christos T.** (2012), Cable Supported Bridges. WILEY, 569. Print.

**EN 10025:3** (2004), Hot rolled products of structural steels.

**Fugro** (2011). Earthquake Engineering Report. Izmit Bay Bridge Crossing.

**Inoue, Manabu.** (2015a). Izmit Bay Suspension Bridge, Cable Characteristics at Tower Top.

**Inoue, Manabu.** (2015b). Design Principles of Suspension Bridge Towers against Dynamics Loads. Personal correspondance.

**Inoue,Manabu, Yamasaki, Yasutsugu, Yamamoto, Syuuji, Kazama, Mitsuhiro, Imazeki, Masanori, Koike, Yuuji**. Izmit Bay Suspension Bridge-Vibration control of Steel tower. IABSE Symposium Madrid 2014 37 (2014).

**Izmit Bay Bridge Detailed Design.** Towers- Design Report IZMIT-COW-REP-DD-SUP-3100 (2012a). COWI.

**Izmit Bay Bridge Detailed Design.** IBDAS Global Analysis Model- Design Report IZMIT-COW-REP-DD-ANA-1001 (2012b). COWI.

**Izmit Bay Bridge Detailed Design.**Tower TMD specification- Design Report IZMIT-COW-REP-DD-ANA-1001 (2012c). COWI.

**Kawakami Takeshi, Masahiro Yanagihara, Yamasaki Yasutsugu, A. Nebil Ozturk, and Fatih Zeybek.** Izmit Bay Suspension Bridge- Over View of the Project. IABSE Symposium Madrid 2014 37 (2014).

**Masanobu Shinozuka, D. Karmakar, S.R. Chaudhuri and H. Lee.** (2009), Verification of Computer Analysis Models for Suspension Bridges, California Department of Transportation, pp. 3 -5, 2009.

**Nielson, B. G., & DesRoches, R.** (2007), Analytical seismic fragility curves for typical bridges in the central and southeastern United States. *Earthquake Spectra, 23*(3), 615-633.

**Rannie, W.D.** (1941). The Failure of the Tacoma Narrows Bridge. Board of Engineers, O.H. Amman, T. von Karman, G.B. Woodruff, eds., Federal Works Agency, Appendix VI, March 28.

**Sadek F., Mohraz B., Taylor A.W., Chung R.** (1997), A method of estimating the parameters of tuned mass dampers for seismic applications. Earthq Eng and Structl Dyn; 26:617-35.

**Salomos, G., Pinto, A., & Dimova, S**. (2008). A REVIEW OF THE SEISMIC HAZARD ZONATION IN NATIONAL BUILDING CODES IN THE CONTEXT OF EUROCODE 8. European Comission, (EUR 23563 EN - 2008).

**SSBSZ**, Specification for Structures to be built in Disaster Areas. (2007). Ministry of Public Works and Settlement.

**Warburton G.B., Ayorinde E.O.** (1980), Optimum absorber parameters for simple systems. Earthq Eng and Structl Dyn; 8: 197-217

**Y. Arfiadi & M.N.S. Hadi.** (2011). Optimum Placement and Properties of Tuned Mass Dampers Using Hybrid Genetic Algorithms. International Journal of Optimization in Civil Engineering, 1:167-187, 2011.

**Zareian, F., & Krawinkler, H.** (2007), Assessment of probability of collapse and design for collapse safety. *Earthquake Engineering & Structural Dynamics, 36*(13), 1901-1914.

**APPENDICES**

**APPENDIX A-1:** Stress graphs
**APPENDIX A-2:** Non-linear time history analysis results graphs
**APPENDIX A-3**: Spectral Acceleration graphs

**APPENDIX A-1**

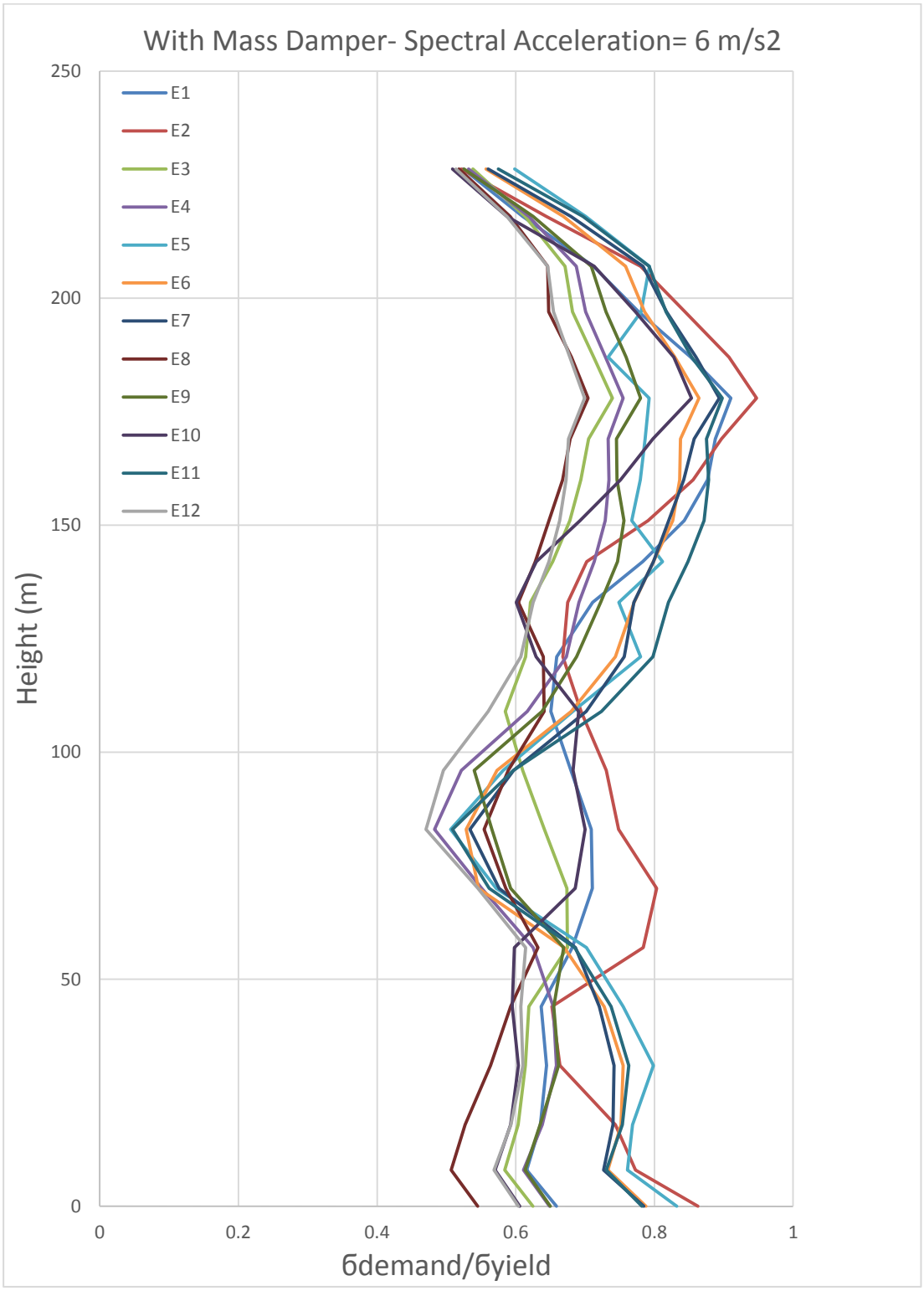
With Mass Damper- Spectral Acceleration= 6 m/s2
250
200
150
100
50
0
Height (m)
E1
E2
E3
E4
E5
E6
E7
E8
E9
E10
E11
E12
0
0.2
0.4
0.6
0.8
1
δdemand/δyield

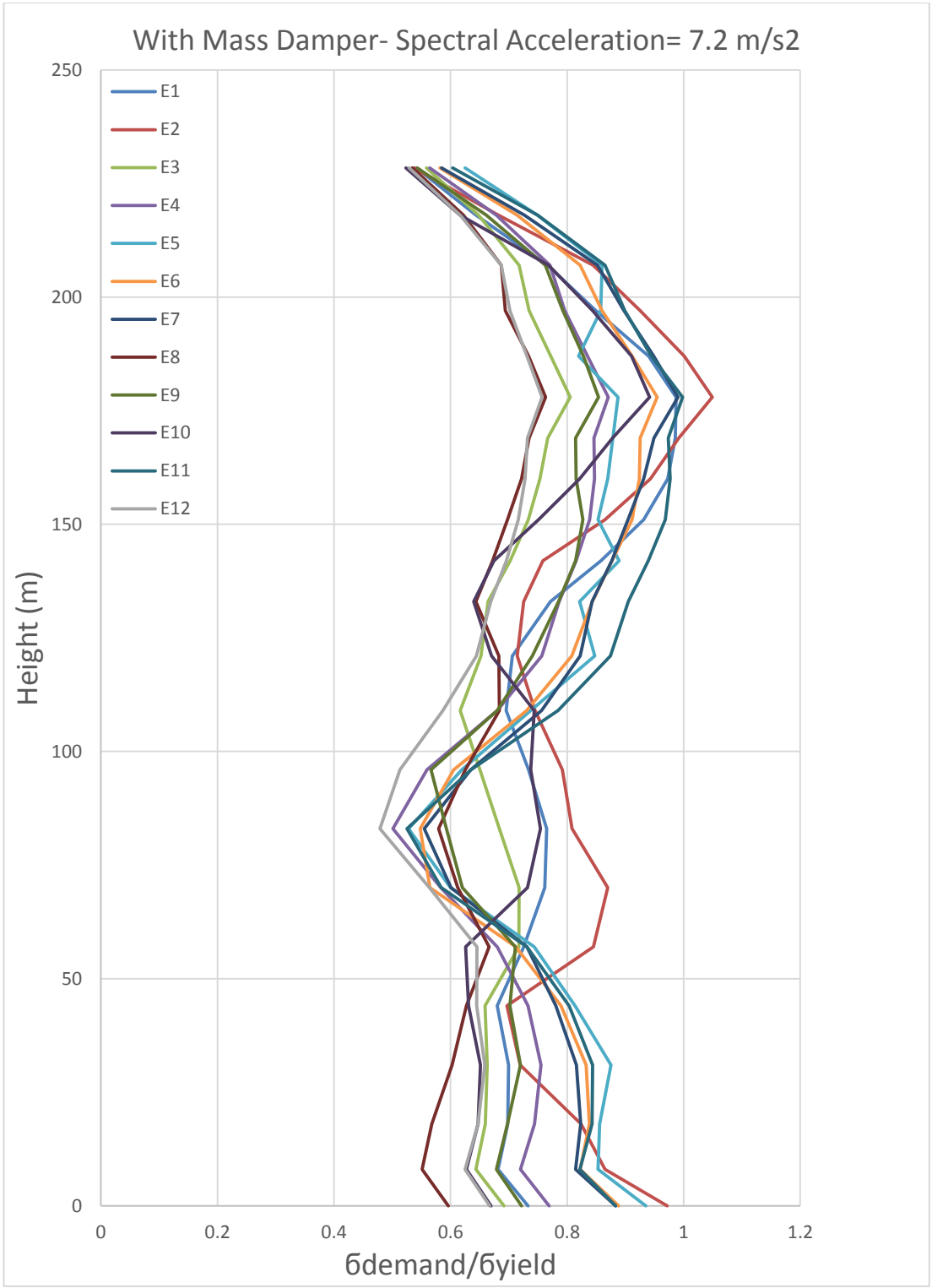
With Mass Damper- Spectral Acceleration= 7.2 m/s2
250
200
150
100
50
0
Height (m)
E1
E2
E3
E4
E5
E6
E7
E8
E9
E10
E11
E12
0
0.2
0.4
0.6
0.8
1
1.2
бdemand/бyield

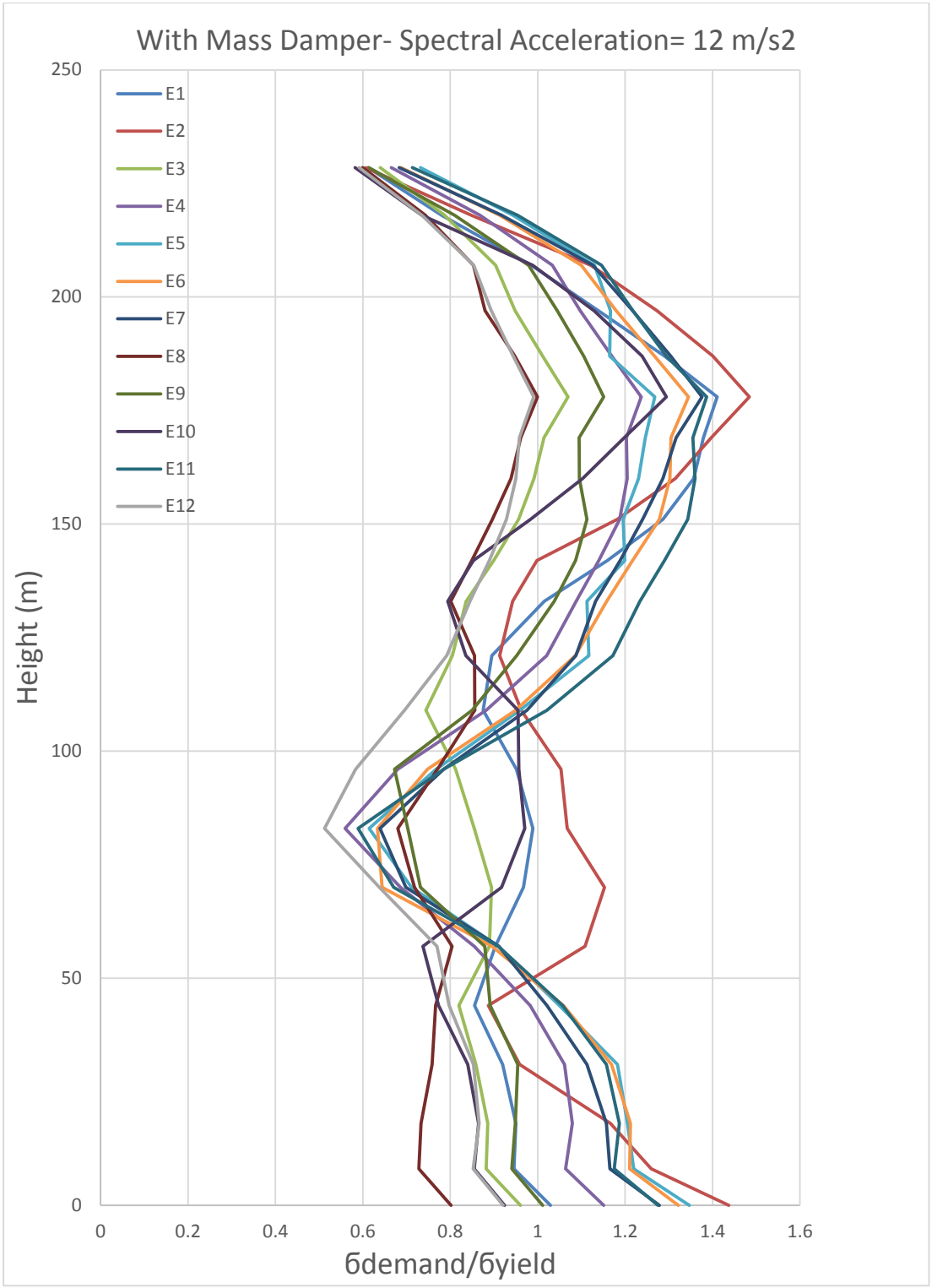
With Mass Damper- Spectral Acceleration= 12 m/s2
250
200
150
100
50
0
Height (m)
E1
E2
E3
E4
E5
E6
E7
E8
E9
E10
E11
E12
0
0.2
0.4
0.6
0.8
1
1.2
1.4
1.6
бdemand/бyield

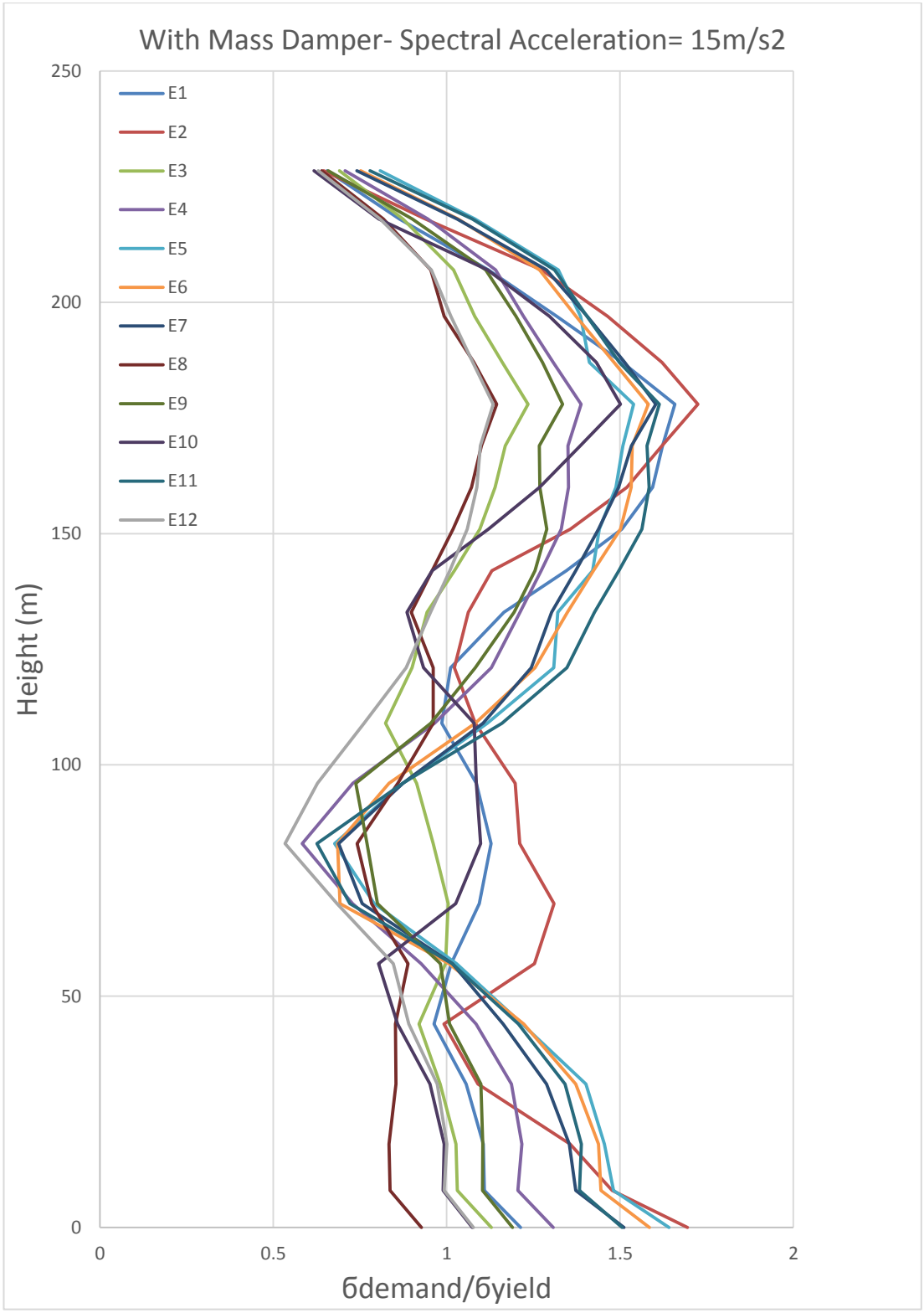
With Mass Damper- Spectral Acceleration= 15m/s2
250
200
150
100
50
0
Height (m)
E1
E2
E3
E4
E5
E6
E7
E8
E9
E10
E11
E12
0
0.5
1
1.5
2
бdemand/бyield

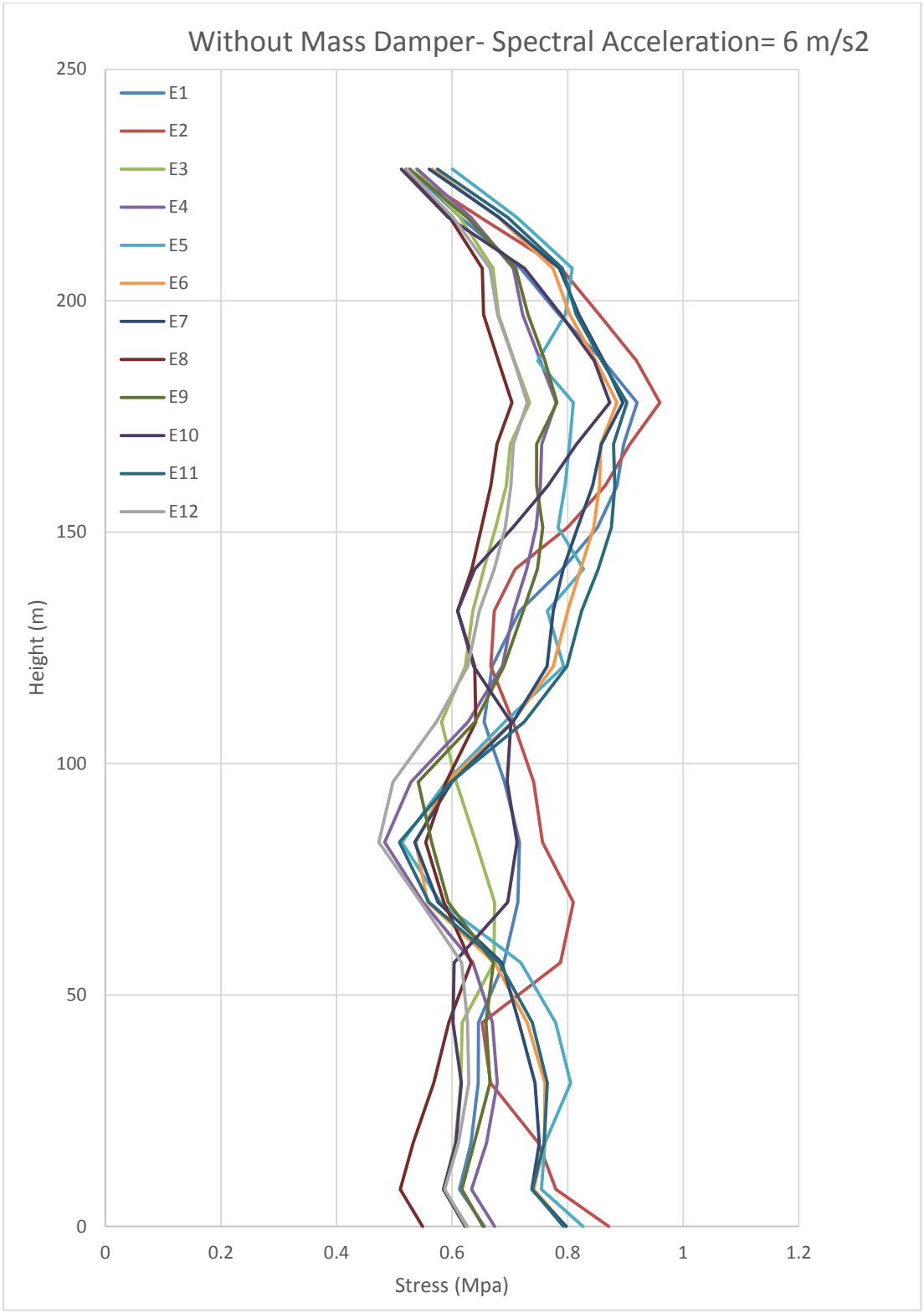
Without Mass Damper- Spectral Acceleration= 6 m/s2
250
200
150
100
50
0
Height (m)
E1
E2
E3
E4
E5
E6
E7
E8
E9
E10
E11
E12
0
0.2
0.4
0.6
0.8
1
1.2
Stress (Mpa)

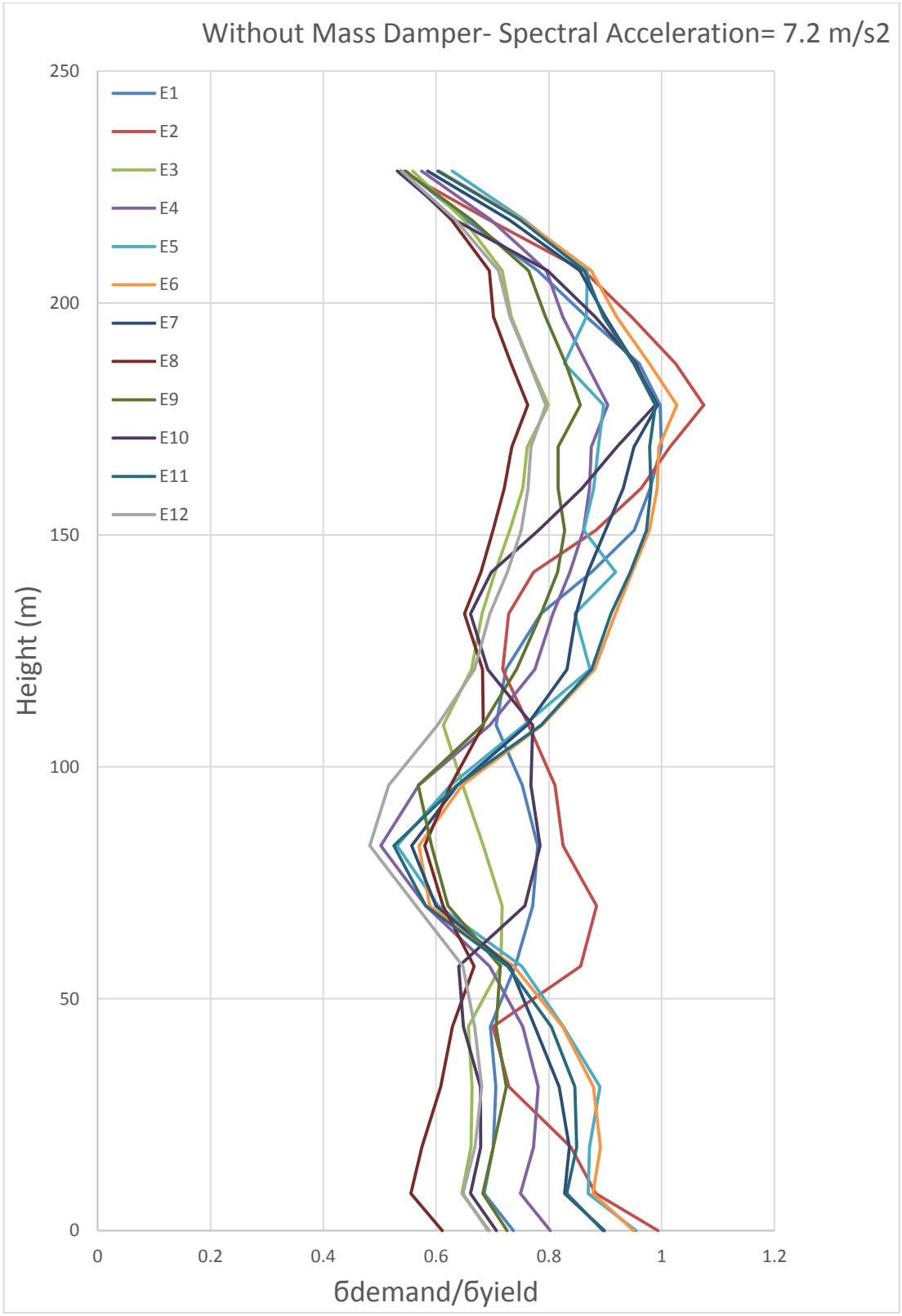
Without Mass Damper- Spectral Acceleration= 7.2 m/s2
250
200
150
100
50
0
Height (m)
E1
E2
E3
E4
E5
E6
E7
E8
E9
E10
E11
E12
0
0.2
0.4
0.6
0.8
1
1.2
бdemand/бyield

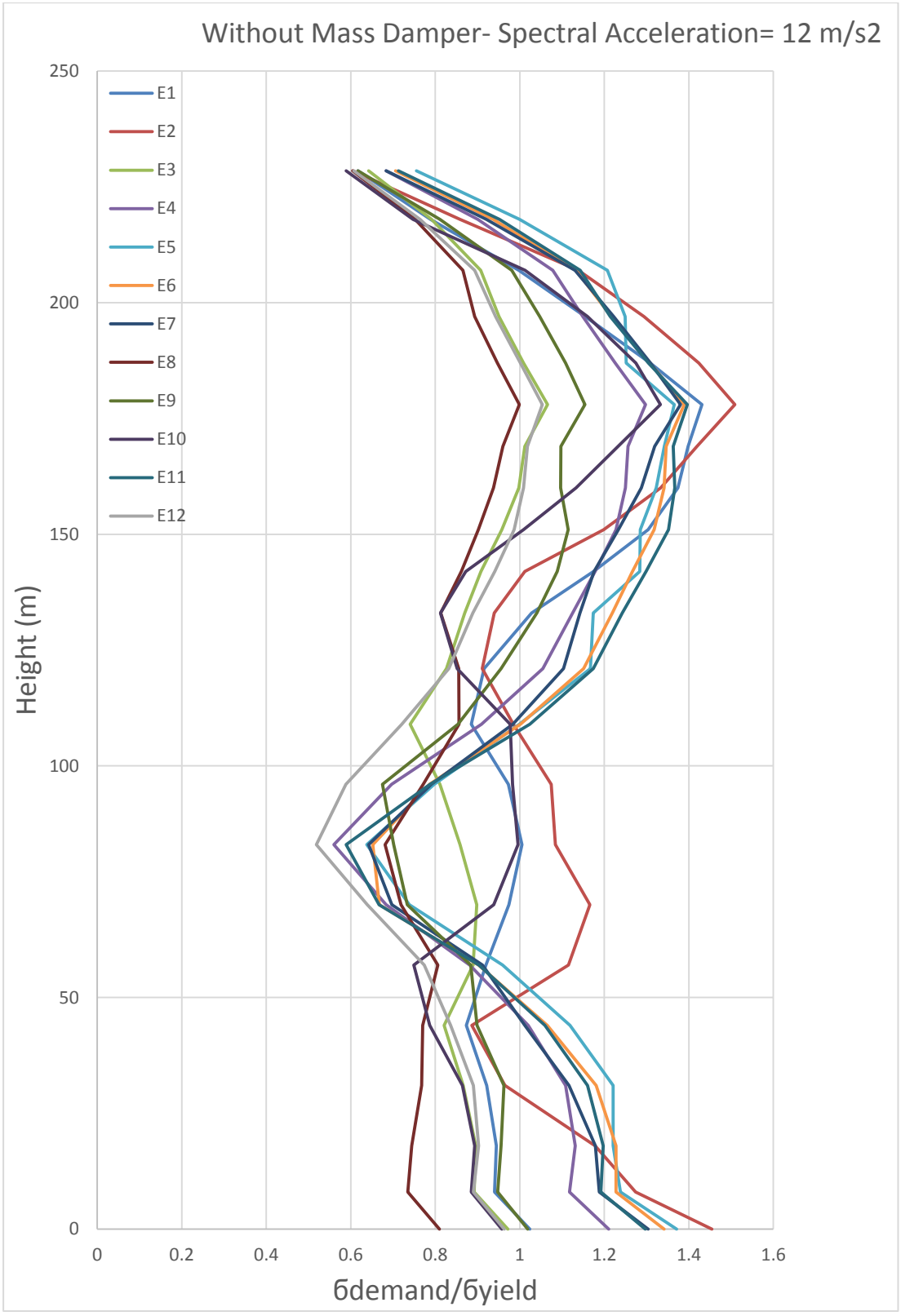
Without Mass Damper- Spectral Acceleration= 12 m/s2
250
200
150
100
50
0
Height (m)
E1
E2
E3
E4
E5
E6
E7
E8
E9
E10
E11
E12
0
0.2
0.4
0.6
0.8
1
1.2
1.4
1.6
бdemand/бyield

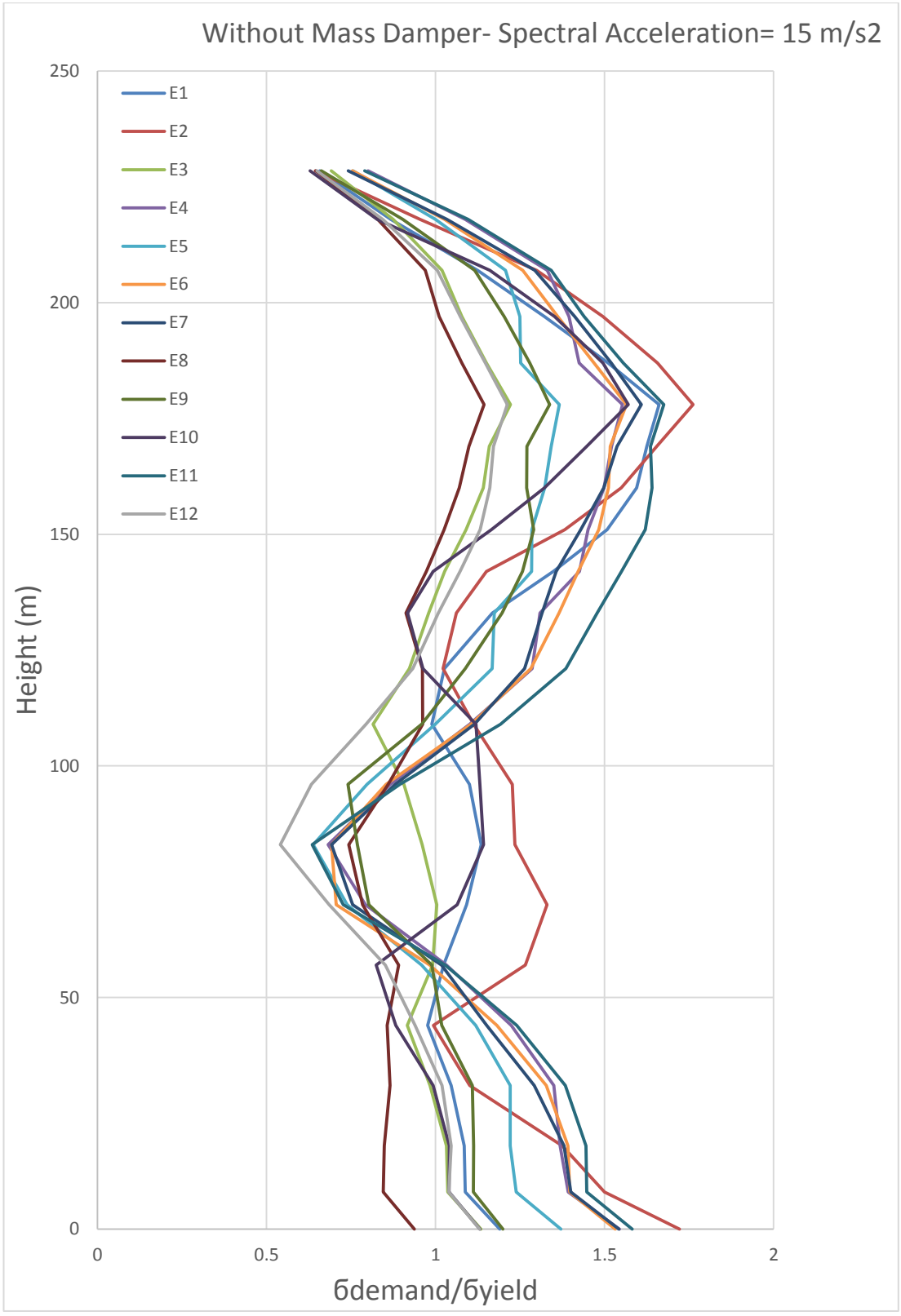
Without Mass Damper- Spectral Acceleration= 15 m/s2
250
200
150
100
50
0
Height (m)
E1
E2
E3
E4
E5
E6
E7
E8
E9
E10
E11
E12
0
0.5
1
1.5
2
δdemand/δyield

**APPENDIX A-2**

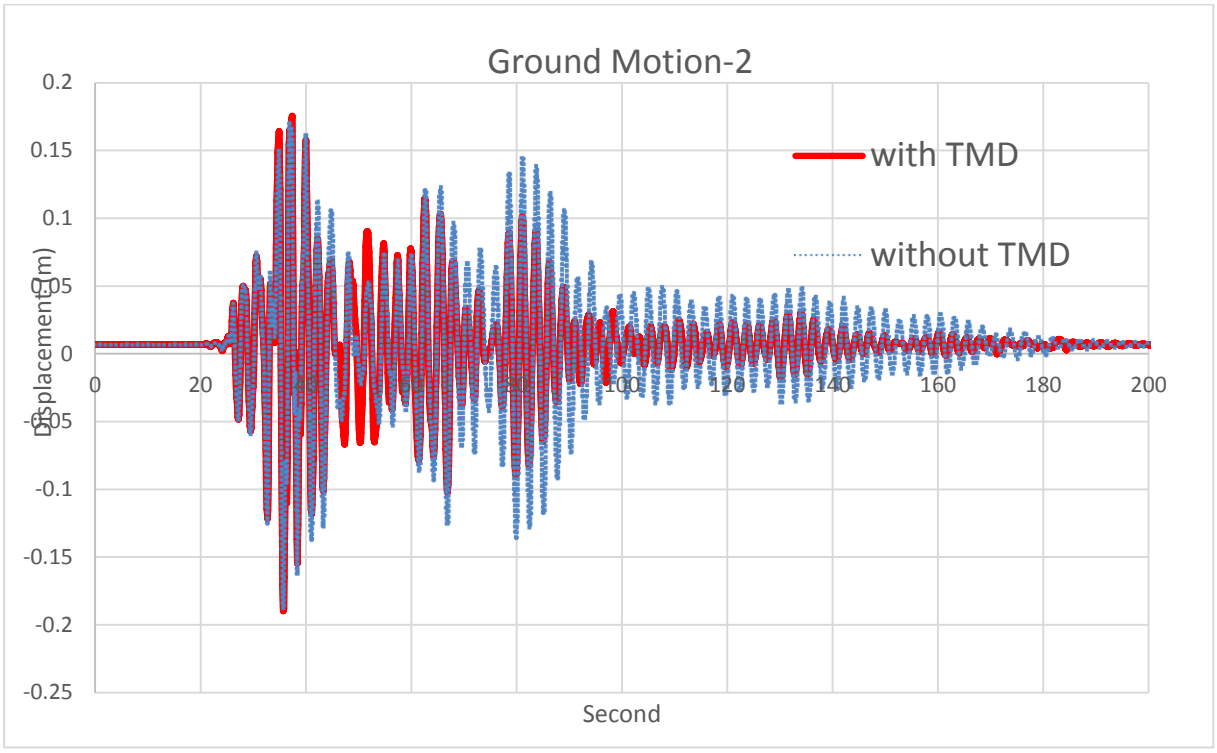
Ground Motion-2
with TMD
without TMD
Displacement (m)
Second
0.2
0.15
0.1
0.05
0
-0.05
-0.1
-0.15
-0.2
-0.25
0
20
100
120
140
160
180
200

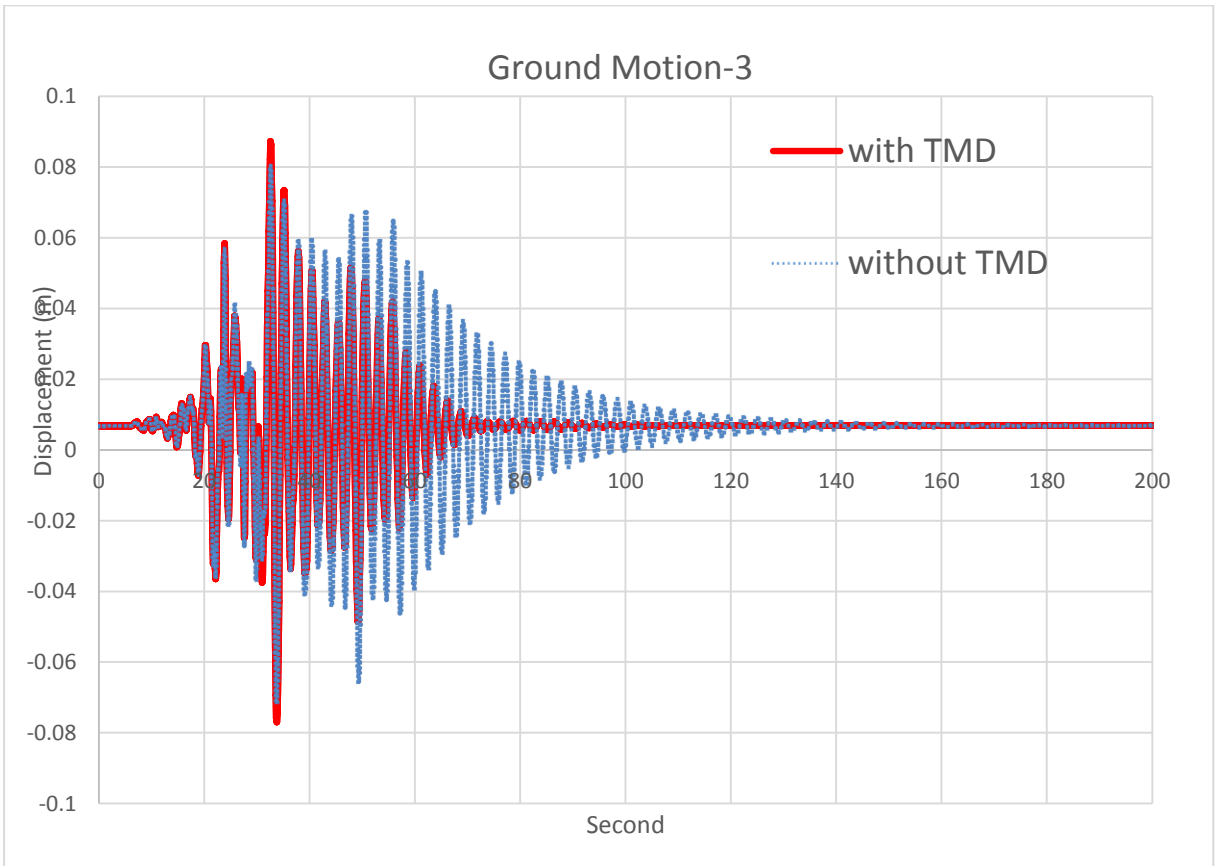
Ground Motion-3
with TMD
without TMD
Displacement (m)
Second
0.1
0.08
0.06
0.04
0.02
0
-0.02
-0.04
-0.06
-0.08
-0.1
0
100
120
140
160
180
200

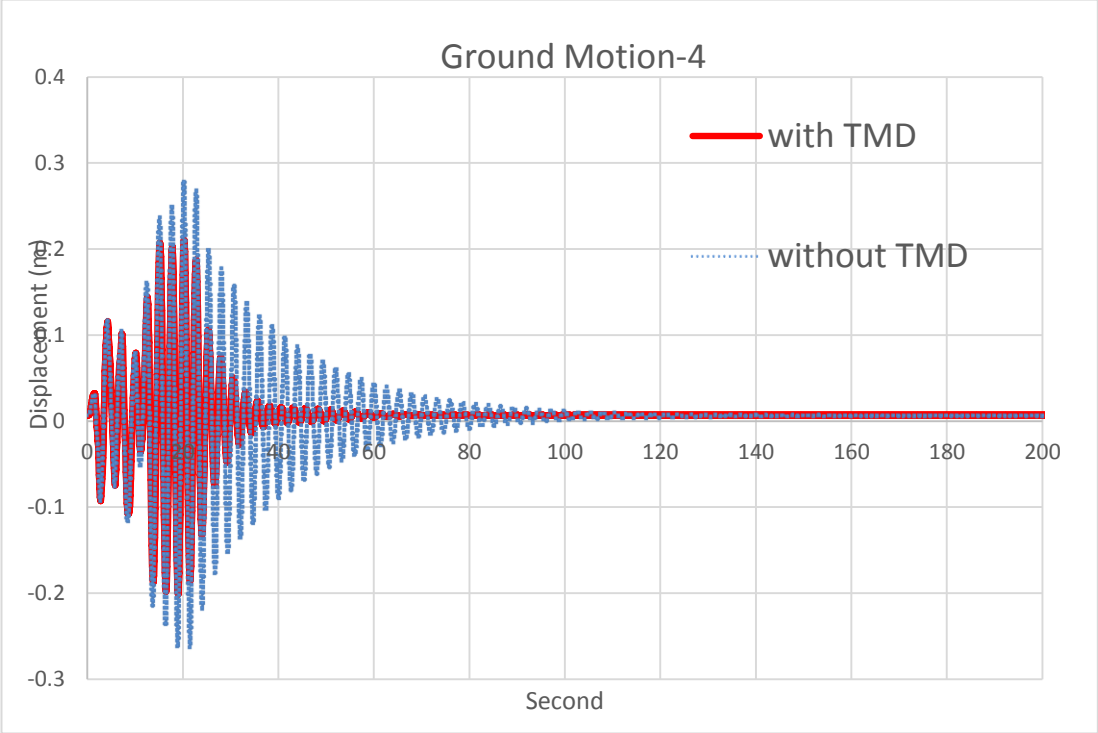
Ground Motion-4
with TMD
without TMD
Displacement (m)
Second
0.4
0.3
0.2
0.1
0
-0.1
-0.2
-0.3
0
20
40
60
80
100
120
140
160
180
200

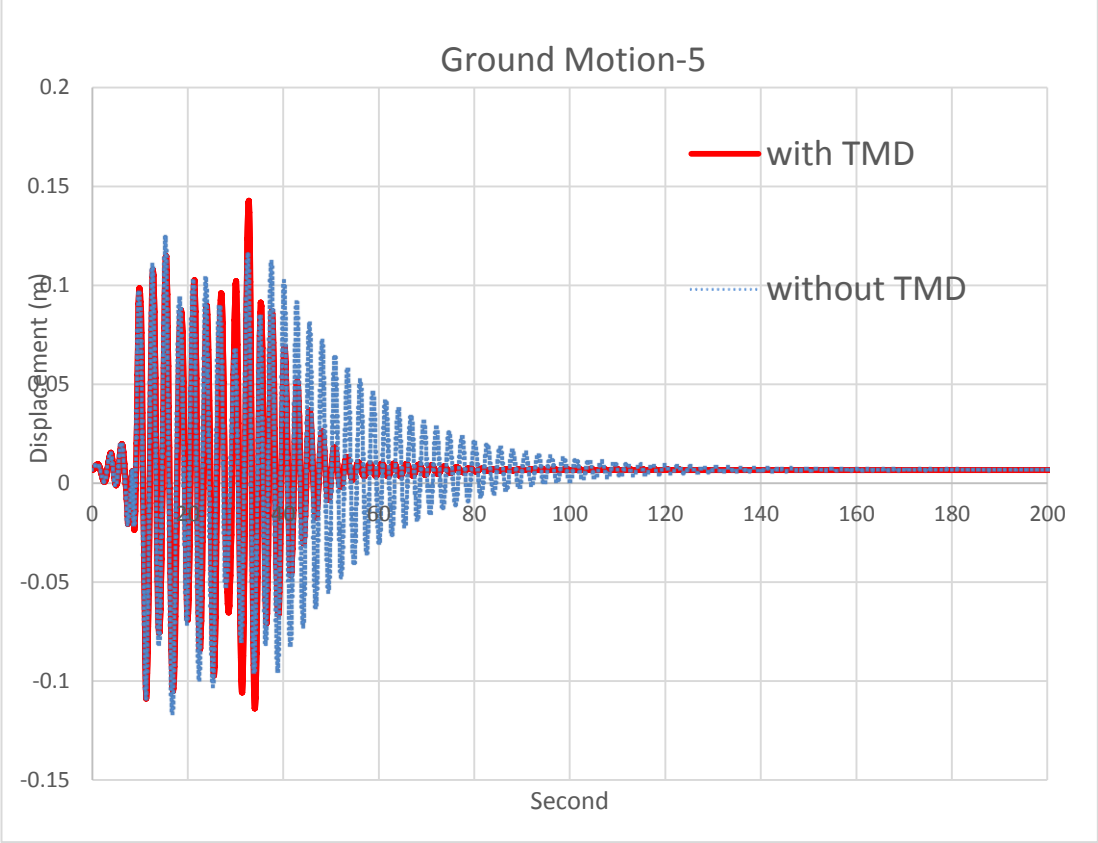
Ground Motion-5
with TMD
without TMD
Displacement (m)
Second
0.2
0.15
0.1
0.05
0
-0.05
-0.1
-0.15
0
20
40
60
80
100
120
140
160
180
200

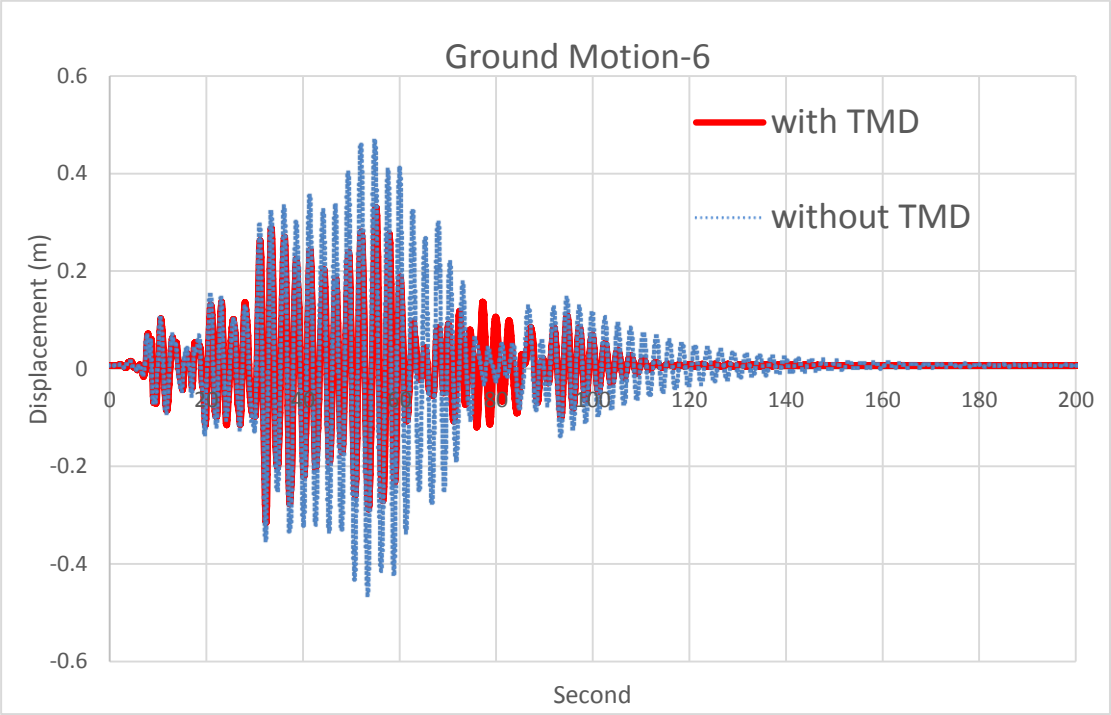
Ground Motion-6
with TMD
without TMD
Displacement (m)
Second
0.6
0.4
0.2
0
-0.2
-0.4
-0.6
0
120
140
160
180
200

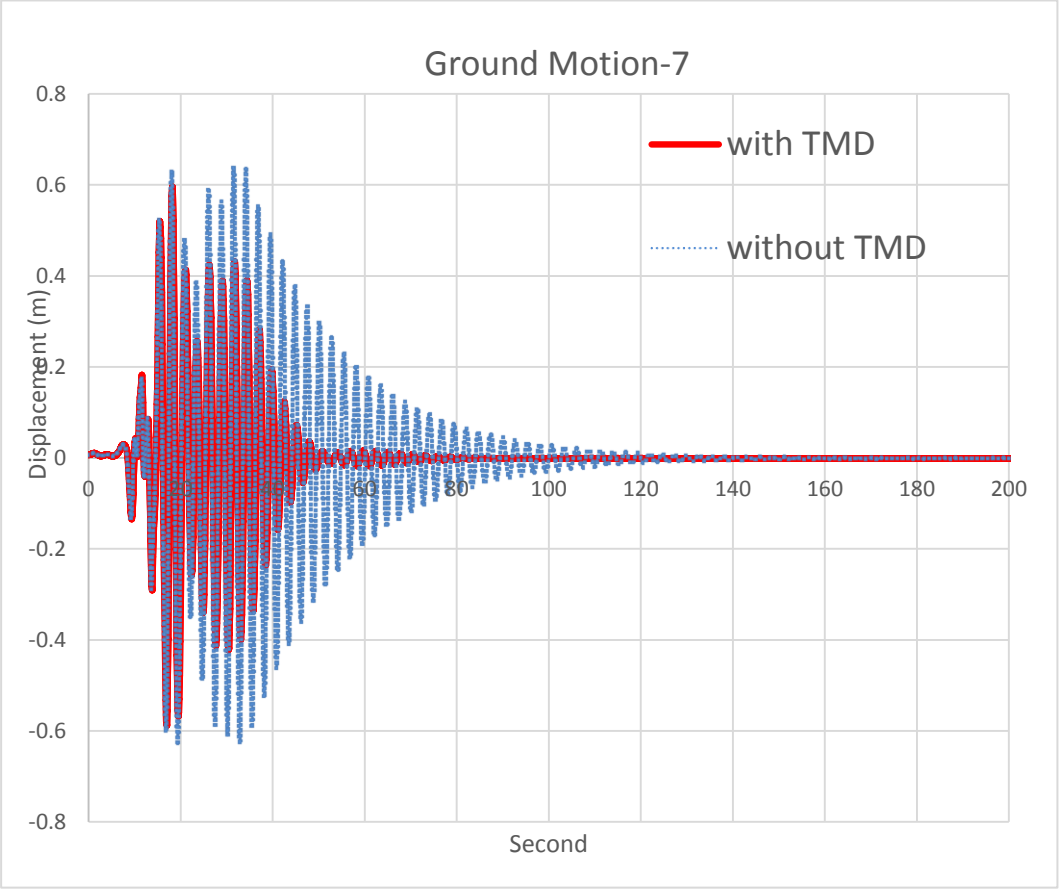
Ground Motion-7
with TMD
without TMD
Displacement (m)
Second
0.8
0.6
0.4
0
-0.2
-0.4
-0.6
-0.8
0
100
120
140
160
180
200

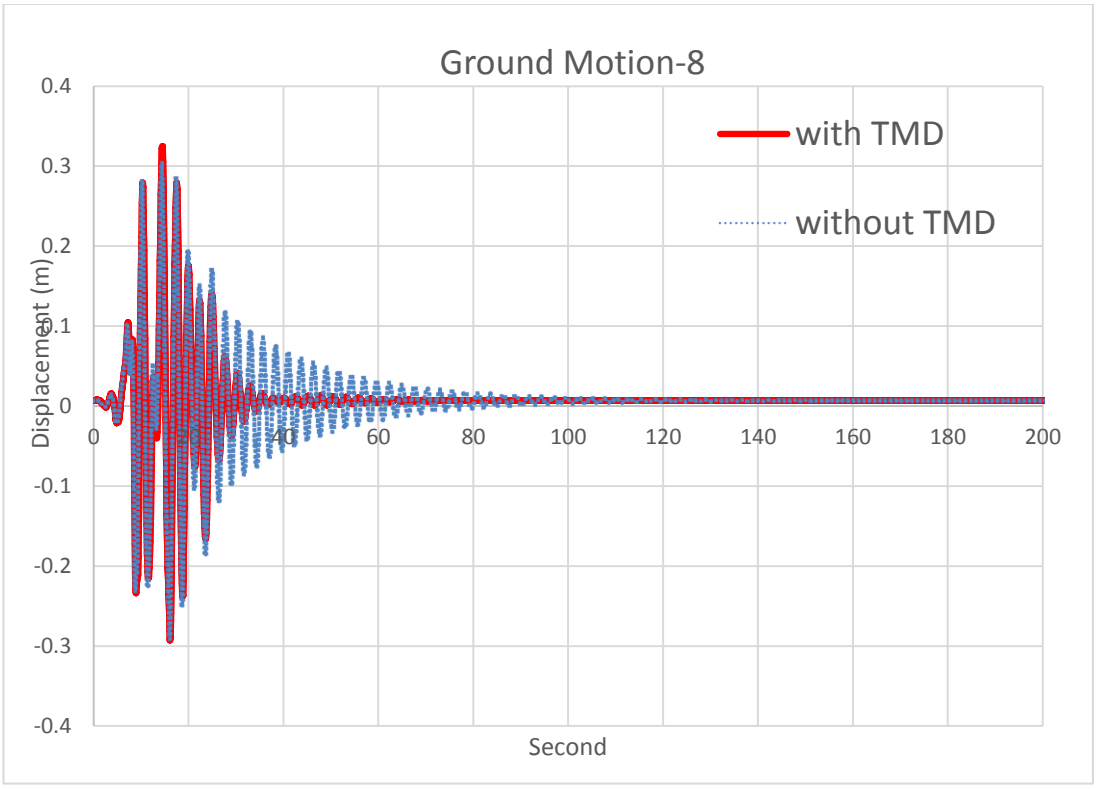
Ground Motion-8
with TMD
without TMD
Displacement (m)
Second
0.4
0.3
0.2
0.1
0
-0.1
-0.2
-0.3
-0.4
0
20
40
60
80
100
120
140
160
180
200

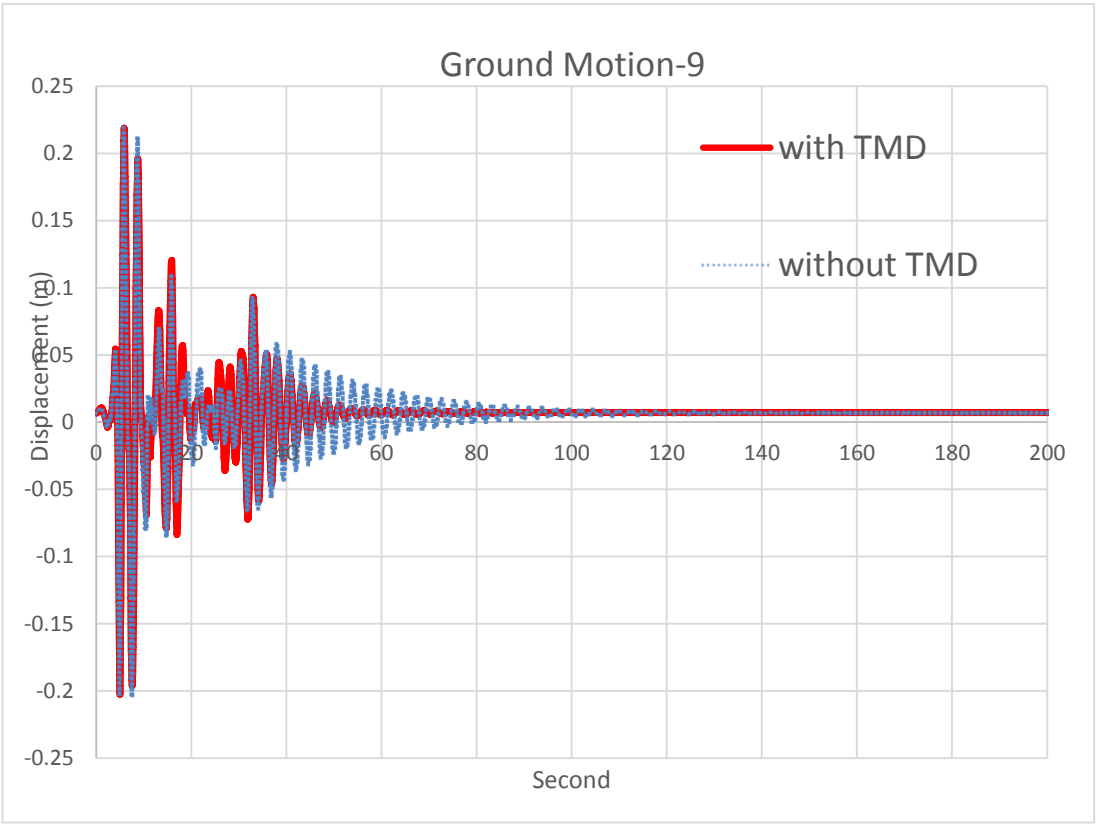
Ground Motion-9
with TMD
without TMD
Displacement (m)
Second
0.25
0.2
0.15
0.1
0.05
0
-0.05
-0.1
-0.15
-0.2
-0.25
0
20
40
60
80
100
120
140
160
180
200

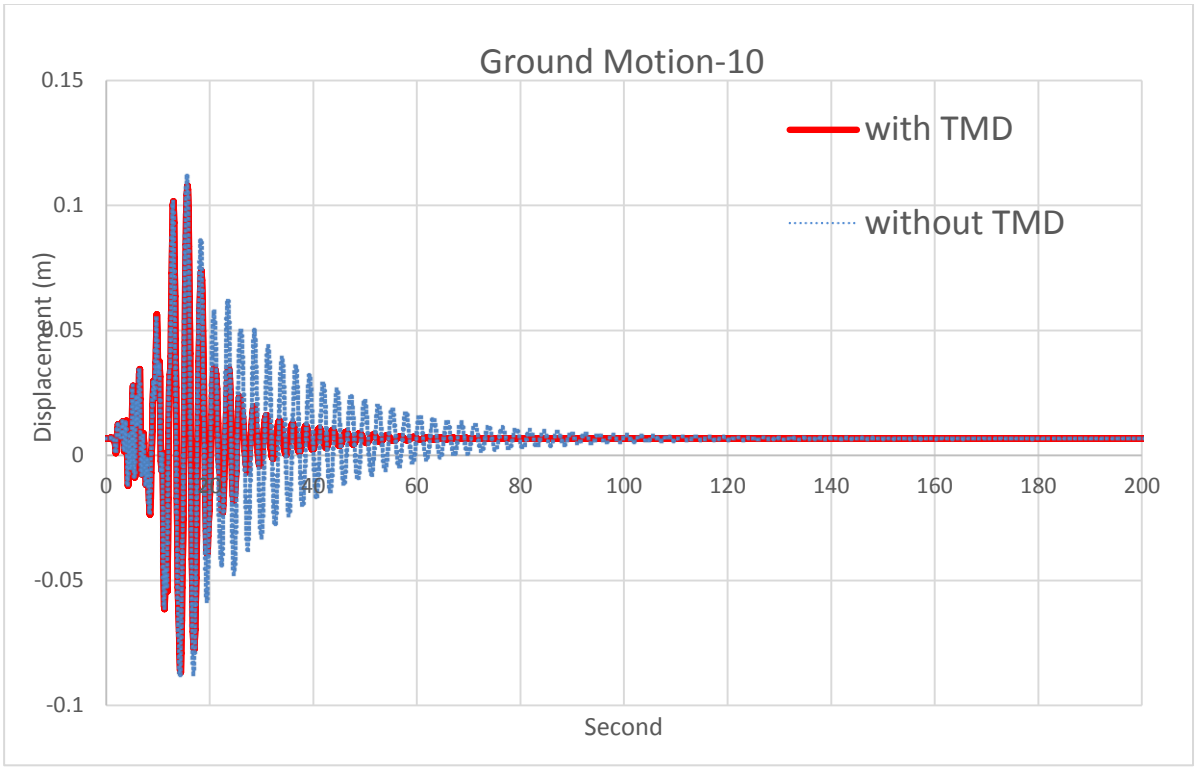
Ground Motion-10
with TMD
without TMD
Displacement (m)
Second
0.15
0.1
0.05
0
-0.05
-0.1
0
20
40
60
80
100
120
140
160
180
200

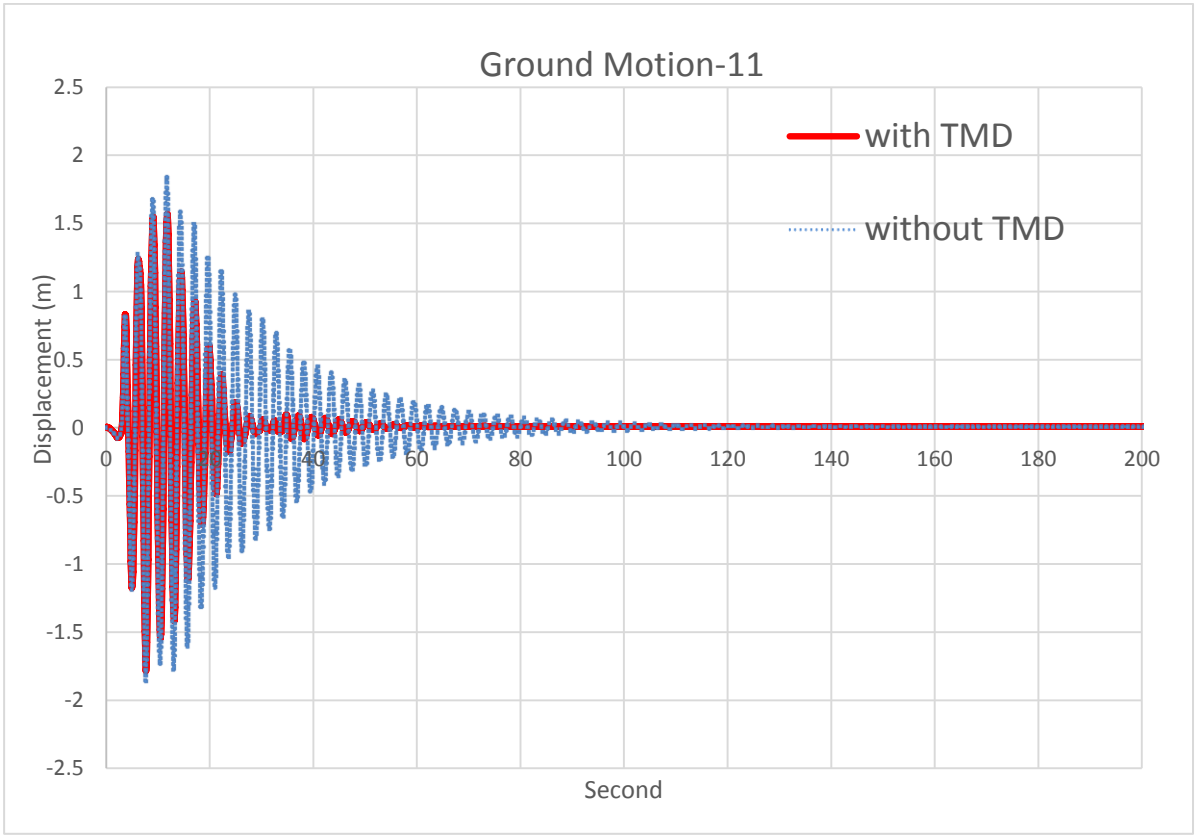
Ground Motion-11
with TMD
without TMD
Displacement (m)
Second
2.5
2
1.5
1
0.5
0
-0.5
-1
-1.5
-2
-2.5
0
20
40
60
80
100
120
140
160
180
200

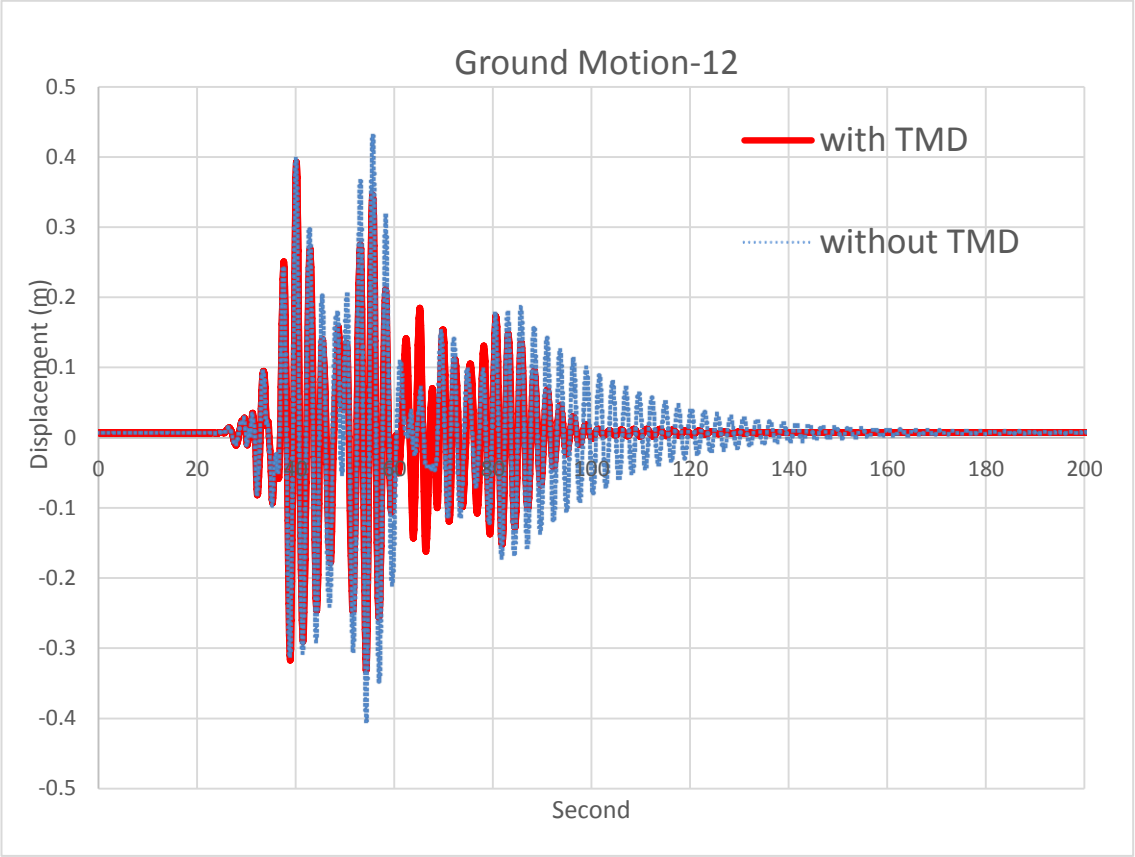


**Figure A-3:** Non-linear time history analysis graph

**APPENDIX A-3**

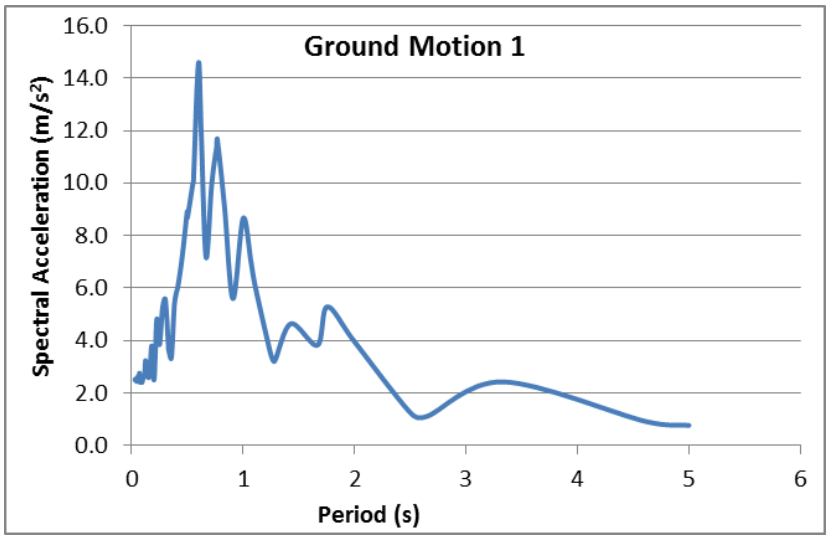
Ground Motion 1
Spectral Acceleration (m/s²)
16.0
14.0
12.0
10.0
8.0
6.0
4.0
2.0
0.0
0
1
2
3
4
5
6
Period (s)

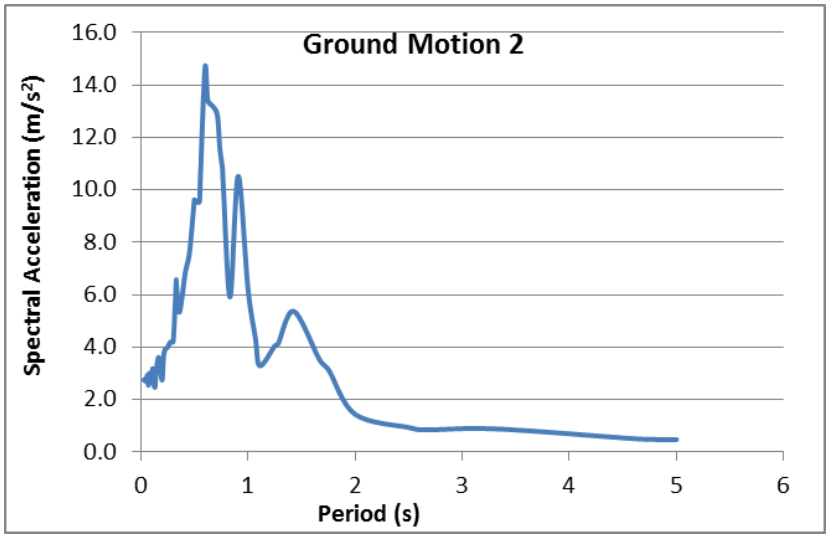
Ground Motion 2
Spectral Acceleration (m/s²)
16.0
14.0
12.0
10.0
8.0
6.0
4.0
2.0
0.0
0
1
2
3
4
5
6
Period (s)

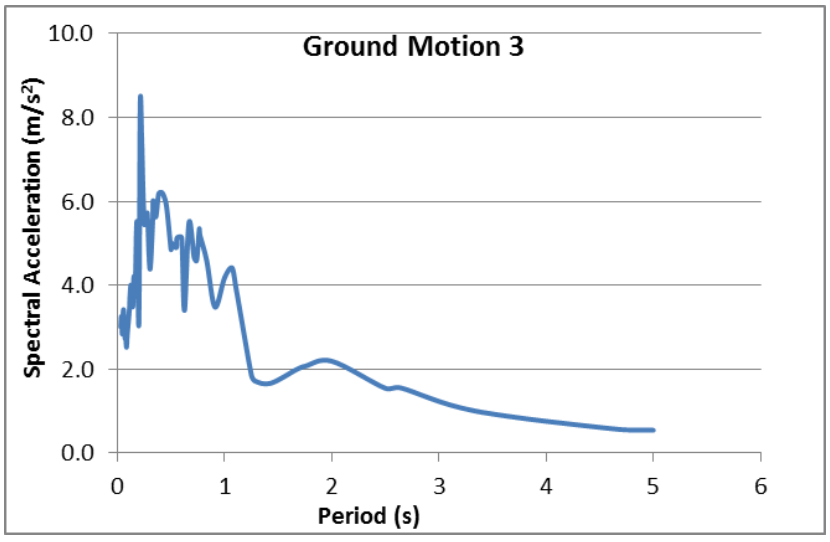
Ground Motion 3
Spectral Acceleration (m/s²)
10.0
8.0
6.0
4.0
2.0
0.0
0
1
2
3
4
5
6
Period (s)

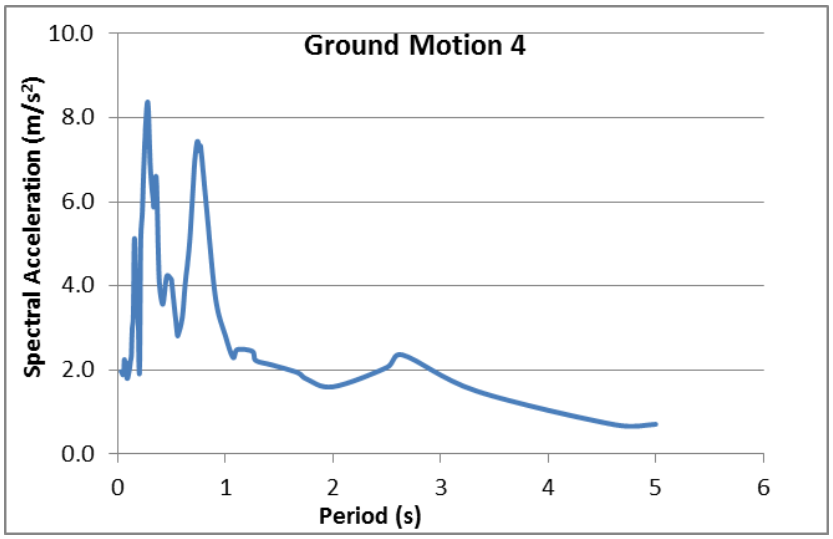
Ground Motion 4
Spectral Acceleration (m/s²)
10.0
8.0
6.0
4.0
2.0
0.0
0
1
2
3
4
5
6
Period (s)

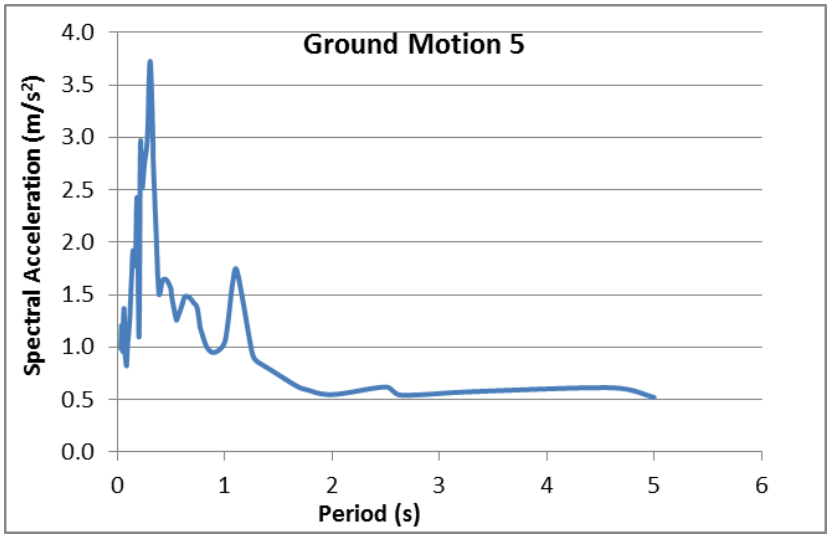
Ground Motion 5
Spectral Acceleration (m/s²)
4.0
3.5
3.0
2.5
2.0
1.5
1.0
0.5
0.0
0
1
2
3
4
5
6
Period (s)

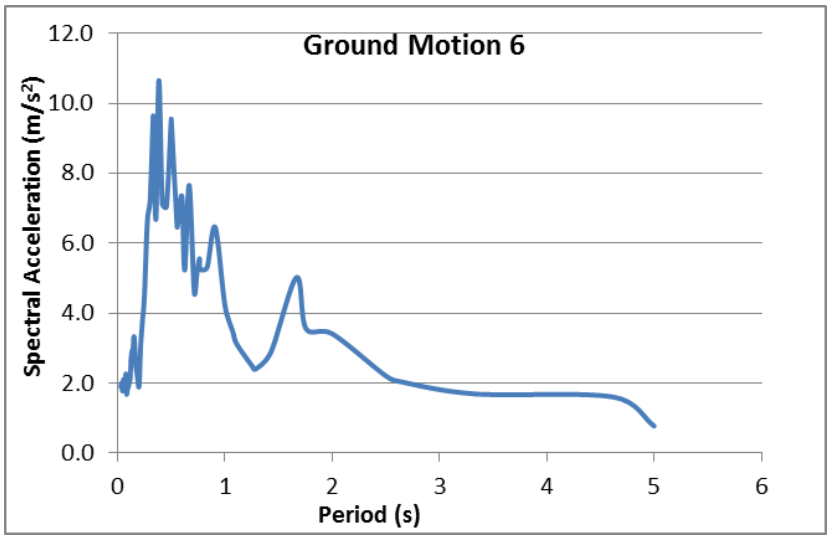
Ground Motion 6
Spectral Acceleration (m/s²)
12.0
10.0
8.0
6.0
4.0
2.0
0.0
0
1
2
3
4
5
6
Period (s)

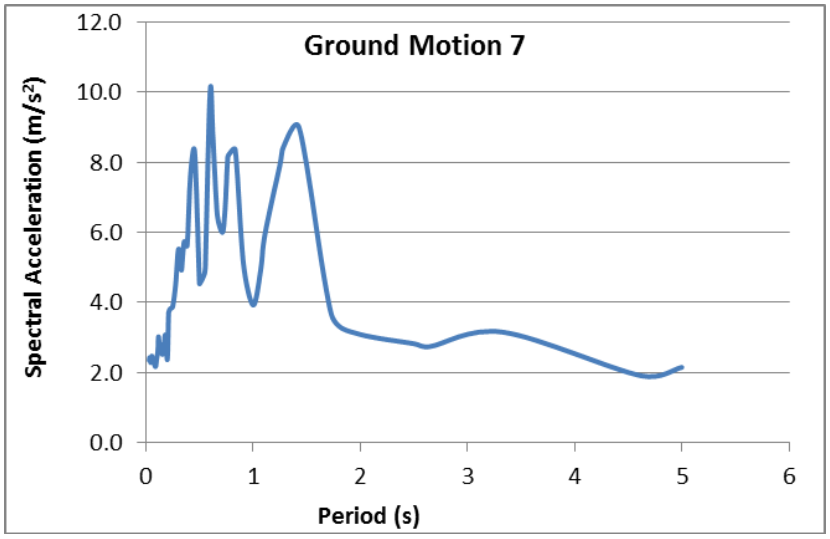
Ground Motion 7
Spectral Acceleration (m/s²)
12.0
10.0
8.0
6.0
4.0
2.0
0.0
0
1
2
3
4
5
6
Period (s)

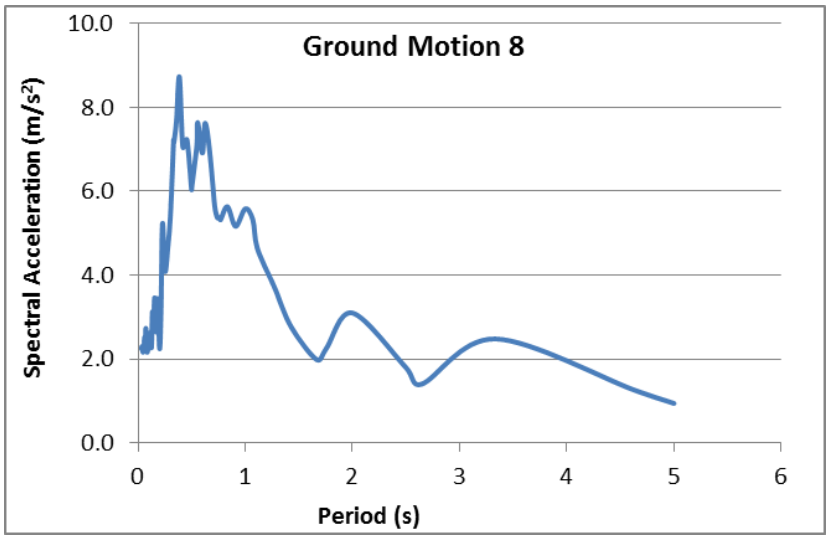
Ground Motion 8
Spectral Acceleration (m/s²)
10.0
8.0
6.0
4.0
2.0
0.0
0
1
2
3
4
5
6
Period (s)

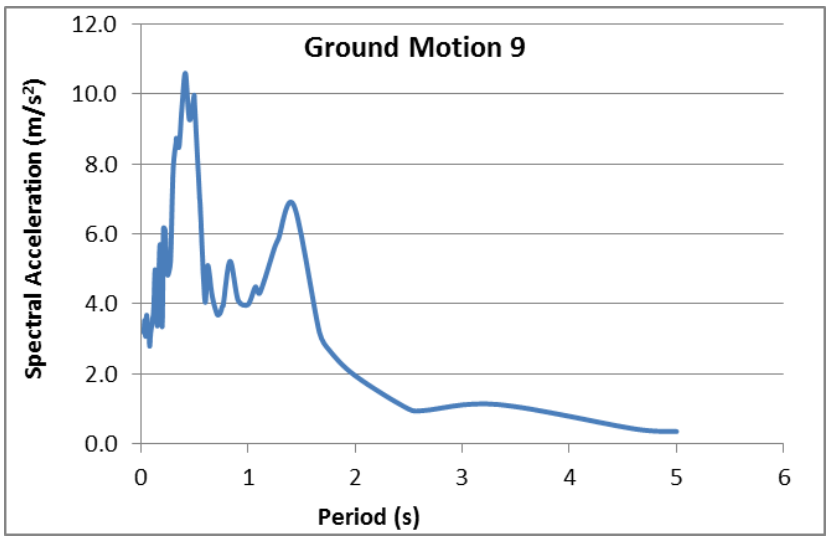
Ground Motion 9
Spectral Acceleration (m/s²)
12.0
10.0
8.0
6.0
4.0
2.0
0.0
0
1
2
3
4
5
6
Period (s)

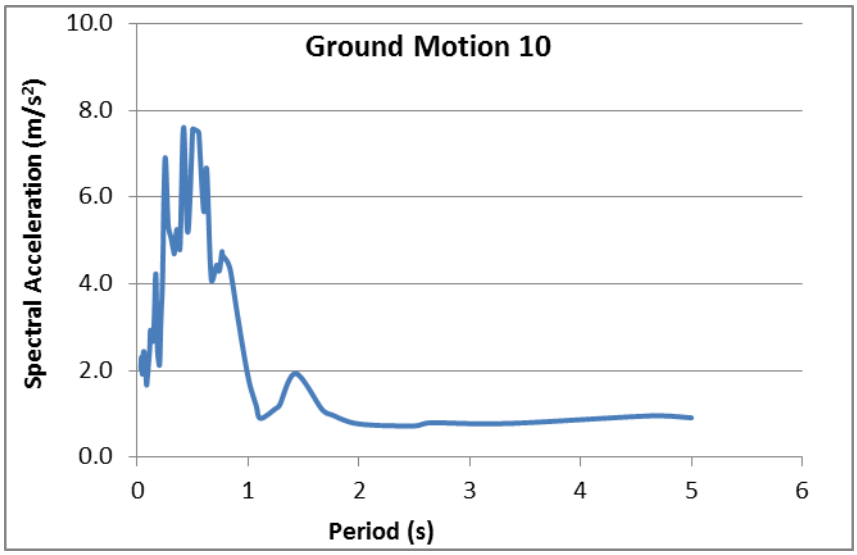
Ground Motion 10
Spectral Acceleration (m/s²)
10.0
8.0
6.0
4.0
2.0
0.0
0
1
2
3
4
5
6
Period (s)

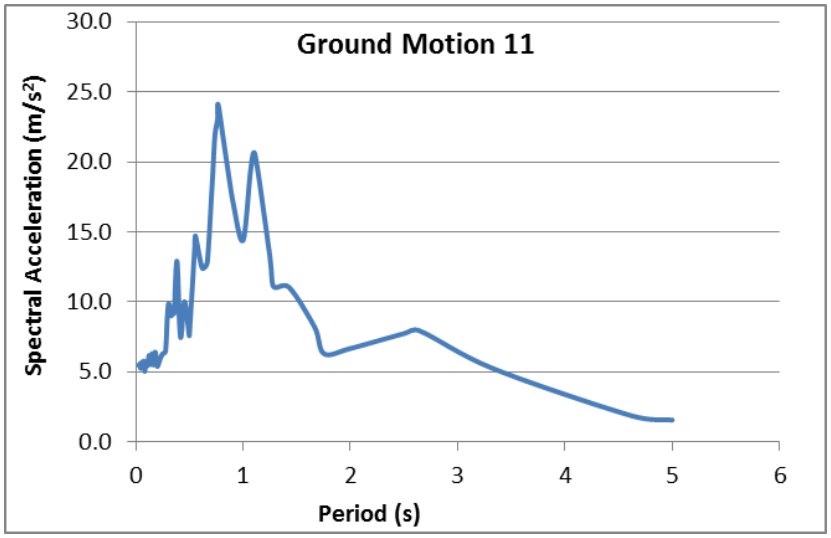
Ground Motion 11
Spectral Acceleration (m/s²)
30.0
25.0
20.0
15.0
10.0
5.0
0.0
0
1
2
3
4
5
6
Period (s)

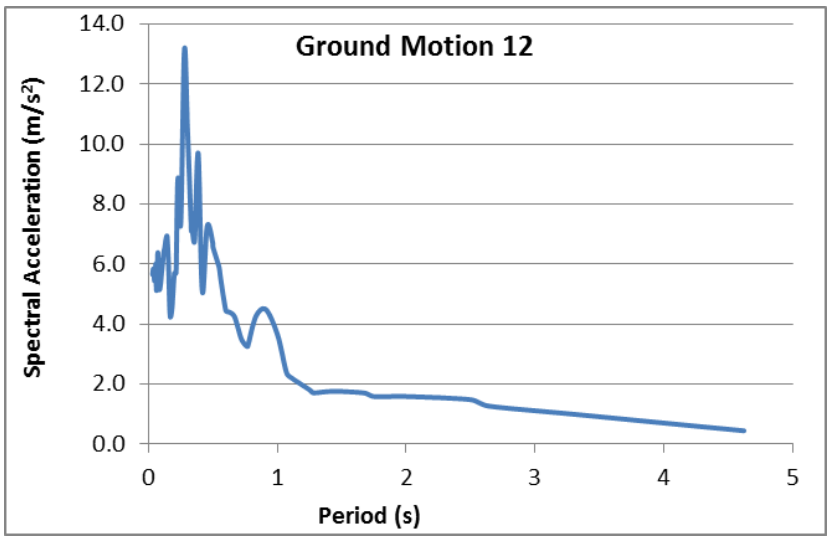
Ground Motion 12
Spectral Acceleration (m/s²)
14.0
12.0
10.0
8.0
6.0
4.0
2.0
0.0
0
1
2
3
4
5
Period (s)

**CURRICULUM VITAE**

**Name Surname: Oguz BERBER**

**Place and Date of Birth: Istanbul- 07/09/1990**

**E-Mail: oguzberber90@gmail.com**

**EDUCATION:**

**B.Sc.: 2012, Istanbul Technical University, Civil Engineering Faculty, Civil Engineering**

**PROFESSIONAL EXPERIENCE AND REWARDS:**

12.7.2010-12.8.2010, Kadikoy-Kartal Subway,Site Intern Engineer

03.06.2011-15.09.2011,As-Ya Project Eng. Company,Design Engineer

01.03.2012- 01.10.2012 Suryapi Construction Company, Planning and Procurement Engineer

01.10.2012-01.02.2013 -Suryapi Construction Company, Site Eng.

20.11.2013-....-IHI Corporation(İzmit Bay Crossing Suspension Bridge),Design Engineer